RELIABILITY EVALUATION OF MICROGRIDS BASED ON

MARKOV MODELS AND POWER FLOW ANALYSIS

BY

Abdulrahman Mohammed Safi AL-Sakkaf

A Thesis Presented to the
DEANSHIP OF GRADUATE STUDIES

KING FAHD UNIVERSITY OF PETROLEUM & MINERALS

DHAHRAN, SAUDI ARABIA

In Partial Fulfillment of the
Requirements for the Degree of

MASTER OF SCIENCE

In

ELECTRICAL ENGINEERING

December 2014

KING FAHD UNIVERSITY OF PETROLEUM & MINERALS

DHAHRAN- 31261, SAUDI ARABIA

DEANSHIP OF GRADUATE STUDIES

This thesis, written by **Abdulrahman Mohammed Safi AL-Sakkaf** under the direction

his thesis advisor and approved by his thesis committee, has been presented and accepted

by the Dean of Graduate Studies, in partial fulfillment of the requirements for the degree

of **MASTER OF SCIENCE IN ELECTRICAL ENGINEERING.**

Dr. Mohammed M. Al-Muhaini
(Advisor)

Dr. Ibrahim M. El-Amin
(Member)

Dr. Ali A. Al-Shaikhi
Department Chairman

Dr. Ibrahim O. Habiballah
(Member)

Dr. Salam A. Zummo
Dean of Graduate Studies

21/12/14

Date

© Abdulrahman Mohammed Safi AL-Sakkaf

2014

I dedicate this thesis to my late parents

It was never possible without your prayers and support

ACKNOWLEDGMENTS

First and foremost, I would like to thank Allah for blessing me with his mercy, health, strength, and good fortune. Thank you Allah for facilitating my path to knowledge and to achieve what I have achieved.

I would like also to thank (after Allah) my advisor, Dr. Mohammed, for his invaluable assistance and guidance in every step throughout the research. Thank you for your advices, support, and understanding during all this time.

I want to thank the Electrical Engineering department and my committee members for providing all the means and resources to conduct this research.

Special thanks to my late father and mother, brothers and sisters, who have always stood by my side during the good and bad times. Thank you, you are all I have.

TABLE OF CONTENTS

LIST OF TABLES

LIST OF FIGURES

LIST OF ABBREVIATIONS

A : Availability

AENS : Average Energy Not supplied

AID : Average Interruption Duration

AIF : Average Interruption Frequency

ANSI : The American National Standards Institute

ASAI : Average Service Availability Index

ASUI : Average Service Unavailability Index

BCBV : Branch Current to Bus Voltage

BIBC : Bus Injection to Branch Current

BNPF : Branch to Node Power Flow

CAIDI : Customer Average Interruption Duration Index

CB : Circuit Breaker

CC : Central Controller

DG : Distributed Generation

DLF : Distribution Load Flow

DOE	:	U.S. Department of Energy
DPF	:	Distribution Power Flow
EENS	:	Expected Energy Not supplied
ENR	:	Enhanced Newton Raphson
EPRI	:	Electric Power Research Institute
FD	:	Frequency Duration
FDG	:	Fast Decoupled G matrix
G	:	Generation
GT	:	Gas Turbine
KCL	:	Kirchhoff's Current Law
KVL	:	Kirchhoff's Voltage Law
MC	:	Microcontroller
MM	:	Markov Model
MS	:	Microsource
MTTR	:	Mean Time To Repair
MTTF	:	Mean Time To Failure
RBTS	:	Roy Billinton's Test System

RD	:	Robust Decoupled
SAIDI	:	System Average Interruption Duration Index
SAIFI	:	System Average Interruption Frequency Index
SCB	:	Sectionalizing Circuit Breaker
T	:	Transmission
U	:	Unavailability

ABSTRACT

Full Name   : Abdulrahman Mohammed Safi AL-Sakkaf

Thesis Title   : RELIABILITY EVALUATION OF MICROGRIDS BASED ON
MARKOV MODELS AND POWER FLOW ANALYSIS

Major Field   : Power System

Date of Degree   : December 2014

Reliability is a very important issue for power systems design and operation, and it has significant impact on safety and economy. Researches in this area are concerned on how to model and assess the reliability of the future power distribution systems including distributed generation. In this research, Markov model and distribution power flow analysis are utilized together to perform a practical and accurate reliability evaluation of the power distribution system including distributed generation. Three techniques of distribution power flow are presented and tested to evaluate their performance on a networked distribution system including distributed generation. These methods are the distribution load flow matrix method DLF, the enhanced Newton Raphson method ENR, and the Robust decoupled method RD. The Markov model is used to model the power distribution system. Based on the connectivity between the source and the loads, each state of the Markov model is either classified as (down state) or (up state). The power flow analysis is used to reclassify the states of the Markov model based on the system's transfer capability. Then, Markov model is used to compute the load and system reliability indices. The study is implemented on the weakly meshed RBTS-bus2 system including DG. Five case studies are conducted to investigate the effect of the location and capacity of DG on the voltage profile and the reliability of the system.

ملخص الرسالة

الاسم الكامل: عبدالرحمن محمد صافي السقاف

عنوان الرسالة: تقييم الموثوقية لنظام توزيع الطاقة الفعال باستخدام نموذج ماركوف وتحليل تدفق الطاقة

التخصص: الهندسة الكهربائية

تاريخ الدرجة العلمية: صفر، ١٤٣٦

الكهرباء أصبحت واحدة من أكثر الخدمات الأساسية والتي لا غنى عنها في حياتنا. لذا يجب على شركات الطاقة توليد كهرباء مع مستوى مناسب من الجودة والموثوقية. الموثوقية هي قضية مهمة جدا لتصميم أنظمة الطاقة والتشغيل، ولها تأثير كبير على السلامة والاقتصاد. البحوث حول الموثوقية تركز دائما على كيفية تصميم نموذج لنظام الطاقة و على كيفية حساب مؤشرات الموثوقية. في هذا البحث، سيتم دمج نموذج ماركوف مع طريقة حساب تدفق الطاقة لنظام التوزيع لإجراء تقييم عملي ودقيق للموثوقية. ايضا سيتم تقديم ثلاثة أساليب لحساب تدفق الطاقة الكهربائية واختبارهم لتقييم أدائهم على نظام التوزيع الشبكي مع اضافة التوليد الموزع DG. هذه الطرق هي طريقة DLF، طريقة ENR، و طريقة RD. يتم استخدام نموذج ماركوف لإنشاء نموذج لنظام التوزيع. وسيتم تصنيف كل حاله من حالات النموذج إما باعتبارها (حالة توقف) أو (حالة تشغيل) بناء على وجود ربط بين المصدر والأحمال. وسيتم استخدام تحليل تدفق الطاقة إلى إعادة تصنيف الحالات من جديد بناء على القدرة على نقل الجهد الى جميع الاحمال. ثم سيتم استخدام نموذج ماركوف لحساب مؤشرات الموثوقية. ويتم تنفيذ هذه الدراسة على نظام RBTS-bus2 الشبكي مضافا اليه التوليد الموزع DG. وسيتم دراسات خمس حالات لدراسة تأثير موقع وكمية الطاقة المولدة من التوليد الموزع DG على الجهد وعلى موثوقية النظام.

CHAPTER 1

INTRODUCTION

Electricity is one of the most important and Indispensable services, and because of the growing population every year, demands for this service are also growing. Due to the increasing demand, it is necessary that power systems provide satisfactory electrical energy with good and adequate reliability and quality. Reliability in general is the probability that a system would achieve its mission adequately. From a power system point of view, power reliability can be defined as the probability that power system would deliver electricity within accepted standards and amount to customers, and it relates to the absence of equipment outages and customer interruptions.

Researches about reliability concentrate on how to model the power system with different configurations and operations, and how to evaluate and calculate the reliability indices. These interruptions could be momentary interruptions or sustained interruptions [1]. Momentary interruption is defined as single operations of interruption results in zero voltage for less than 5 minutes. Sustained interruption is an interruption within a period of 5 minutes or longer [2]. Reliability indices represent average values of the reliability characteristic for the system. There are two types of indices, load point indices and system indices [3]. Load point indices are calculated for each load point in the system, and they include failure rate (λ), repair rate (μ), annual availability (A), expected energy

not supplied (*EENS*), etc. System indices are computed for the entire system and they provide overall indication for the system reliability. System indices include system average interruption frequency index (*SAIFI*), system average interruption duration index (*SAIDI*), customer average interruption duration index (*CAIDI*), etc [4]. These indices are explained with more details in chapter 2 and chapter 4.

In general, power system is composed of a generation system, transmission system, and distribution system [1]. In the past, electric utilities were paying more attention to the generation and transmission systems than the distribution system in reliability modelling and evaluation. That is because they are capital intensive, and their inadequacy can have severe economic consequences. Reliability assessment for a generation system can be performed by using one day in 10 years loss of load expectation criterion. Transmission system reliability is evaluated using sophisticated computer models [2]. Recently, the interest has been moving toward distribution systems. Statistics and analysis of customers' failures of most utilities indicate that the distribution system is the most effective element of reliability because of the radial nature of most distribution systems, the large number of components, and the sparsity of protection devices and switches. Therefore, improving distribution reliability is the key to improving customer reliability.

Failure of the distribution components causes disconnection between the load points and the utility source, which results in service interruptions and lower level of reliability. In addition to the connectivity, transfer capability is another issue that can affect the reliability of distribution systems. Because distribution systems have a large number of nodes and load points, high power losses and drop voltages could occur through the system. Therefore, delivering an acceptable level of voltage and power to each load point

during the interruptions is a challenge and concern that affects the reliability of the system. In order to mitigate the influence of these two problems, tie switches can be connected between the lines of the distribution system to improve the connectivity between the source and the loads. Furthermore, when the distribution system is integrated with DGs and advanced control systems, the voltage profile and reliability will improve and it is called a Microgrid system. Microgrid is an active distribution network with DGs, power electronic interfaces, and control system that provides electricity to local area or customers [5]. In this research, the reliability of Microgrid system is evaluated based on the connectivity and transfer capability since they have large impacts on the reliability. DGs are included with different locations and capacities to study their influence on the reliability.

1.1 Literature Review

Reliability evaluation is categorized into two main techniques, analytical and simulation [6]. In the analytical technique, the system is represented by a mathematical model and reliability is evaluated by a mathematical equations applied to this model. However, simulation method, such as Monte Carlo simulation, assesses the reliability by simulating the actual system and its random behaviour [7]. Analytical technique is the most common because it is efficient and it provides the needed results whereas simulation technique requires a large amount of computing time. Huge efforts have been done in the area of assessing and evaluating the reliability of distribution system, and there are several methods for computing the reliability indices.

A direct method for reliability evaluation in transmission and distribution system was proposed in [8]. Three indices have been widely used to assess the reliability, frequency of failure, average duration of outage, and average total hours of outage in a year. The technique employed in [8] was the minimal cut set. After determining all minimal cut sets, the system was represented in a series-parallel configuration. Then, reliability indices were calculated easily by the series and parallel equations. This approach uses simple and general equations that do not involve complex conditions in practical systems. On the other hand, it considers only the failure rates without including successful states, which saves effort and time.

An educational test system (RBTS) has been developed with overall power system reliability assessment in [9]. Main reliability indices in [9] were the failure rate, the average duration of failure, and the annual unavailability, which we called earlier the load point indices. System indices were also calculated for each bus in the system. Overall system evaluation incorporated the three functional zones of generation, transmission and distribution in the analysis. By using the approach in the literature, load point indices and system indices for the RBTS were obtained. The results of the evaluation showed that failures at distribution affect the overall system reliability. The RBTS system has been widely used in reliability studies ever since.

In reference [10], a technique for evaluating a distribution system depending on a simplified network model and network-equivalent has been presented. The distribution system is divided into different parts or zones based on components' reliability characteristics. The decomposition technique used in [10] provides an equivalent and simple system to the original that can be used in the reliability analysis. Since the

components in each zone have the same reliability characteristics, the number of components and calculations will be considerably reduced. The algorithm was applied in a RBTS-Bus 6 system. Compared to the conventional method, this has a fewer number of calculations and is as accurate as the conventional method.

Reference [11] suggested a new method to analyze and assess the current reliability of an operating power system with an equivalent model based on the Markov chain. The Markov chain is a method used to evaluate reliability based on the probability of system states. The power system here is divided into three states, normal state, fault state, and risk state. The RBTS-Bus 6 system was used to test this approach. The calculation is done by the Monte Carlo simulation program. Calculations and results indicate that the proposed algorithm is efficient and practical. However, in large systems, the number of Markov states is huge and this is why simulation program is used instead of analytical method.

Reduction and truncation techniques were proposed in [12] to overcome the problem of large number of components and states in Markov matrices. Number of components and states were considerably reduced without affecting the reliability evaluation. The Markov model was represented by system states and the transition probabilities between those states and then, it was used to evaluate the reliability of RBTS distribution system.

In [13] a new approach of evaluating the reliability of a networked distribution system was developed. The evaluation was based on the connection between source and loads of the system by determining the minimal tie sets. Markov model was utilized with the reduction techniques to compute the reliability indices of the system. The study was

implemented on the RBTS system. The proposed method was effective and suitable for future distribution networks. One drawback in this approach, that reliability evaluation is depending on only one factor, which is the connectivity.

In this thesis, Reliability of a Microgrid will be evaluated using Markov model and power flow analysis. Literature survey shows that Markov model is an effective tool for the reliability evaluation. All possible states of the system such as normal state and fault state can be described in Markov model. Another factor will be included in the reliability analysis in addition to the connectivity, which is the transfer capability. This will improve the accuracy of the reliability calculation. The states of Markov model will be classified as an (up state) or (down state) based on the connectivity between the source and loads. Then, power flow analysis will be used to reclassify the states based on the transfer capability of the voltage from the source to loads.

1.2 Thesis Motivations

Reliability is a very important issue for power systems design and operation, and it has significant impact on safety and economy. Life-saving services in hospitals, heating and cooling systems, emergency communications, certain transportations, and so many other essential services need electricity with high level of reliability. Any interruption in the electric power could result in sever safety and economic losses to utilities and customers. The Electric Power Research Institute (EPRI) and the U.S. Department of Energy (DOE) have conducted research about the cost of electricity outages, which is estimated to be 30 to 400 billion dollars per year [14].

The basic function of the power system is to deliver reliable electricity to the customers. Since the distribution system has high influence on the reliability and it is connected directly to the end users, the reliability of the distribution side must be assessed to monitor the service and assure adequate level of reliability. For this reason, studying and analyzing the reliability of distribution system is considered as one of the most important areas in electrical power system.

Because distribution system has a large number of nodes and load points, delivering an acceptable level of voltage and power to each load point is a concern that affects the reliability of the system. Microgrid can improve the voltage profile and hence, the reliability of the system because of the contribution of DGs.

Therefore, due to the significance of the power reliability and its impacts on design, operation, economy, and safety of power system and customers, this thesis focuses on evaluating the reliability of Microgrid power system. Moreover, since the reliability has direct relation with the voltage profile of the system, the voltage profile and its impact on the reliability will be investigated in this thesis. Reliability indices for each load points and for the entire system will be computed to assess the reliability of the Microgrid.

1.3 Thesis Objectives

Power system reliability is an essential factor that affects service quality, economy, and safety for electric utilities and their planning and operation. The objectives of this thesis are as follows:

- Investigating several power flow techniques that designated for distribution systems, and testing them to evaluate their performance on a networked distribution system including distributed generation. Technique with the best performance will be used in reliability evaluation.

- Modeling and evaluating the reliability of the Microgrid power system using Markov models. The study will be implemented on the RBTS-bus2 system [3]. MATLAB is used as the implementation platform.

- Computing the load and system reliability indices based on the connectivity between the source and the loads, and based on the transfer capability between the main feeders. Power flow calculation will be involved to analyze the voltage profile of the system and its influence on the reliability.

- Studying the impacts of distributed generators on the voltage profile and reliability. Different locations and capacities of distributed generators will be considered.

1.4 Thesis Outline

Chapter 1 starts with an introduction about the reliability and literaure review about reliability evaluation. Motivations and objectives of the thesis are also presented. In chapter 2 the concept of Markov model and how it can be used in reliability evaluation is explained. The equations to calculate load point indices and system indices are also stated. In chapter 3 distribution power flow techniques are presented and tested to be used in reliability evaluation. In chapter 4 Markov model and distribution power flow are used

to evaluate the reliability of the RBTS-bus2 system. Five case studies are conducted, and the results with comparisons among the cases are presented. In chapter 5 the conclusion of the thesis with some recommendations for future work are presented.

CHAPTER 2

RELIABILITY ANALYSIS USING MARKOV MODEL

Markov chains are used to model a sequence of discrete or continuous random variables that correspond to a set of system states. Markov approach can be applicable for a system with two features to simplify the process, a lack of memory and being stationary (homogeneous). Lack of memory means that the future states of a system depend only on the preceding state and are independent from all others in the past. Stationary means the probability of the transition from one state to another is constant at all times in the past and future. In order to satisfy these two conditions, exponential distribution must be used to describe the system behaviour since it has constant hazard rate. Markov with discrete space and time is known as a Markov chain, but when space is discrete and time is continuous it is known as a Markov process [15].

Markov model (MM) can be defined as a number of states (S) and a set of transition probabilities (p) that travel from one state to another in one step or in a specified time interval. The probabilities p can be arranged to form a (P) matrix as following

$$P = \begin{bmatrix} p_{11} & p_{12} & \cdots & p_{1n} \\ p_{21} & p_{22} & \cdots & p_{2n} \\ : & : & \cdots & : \\ p_{n1} & p_{n2} & \cdots & p_{nn} \end{bmatrix} \qquad (2.1)$$

P is a matrix of probabilities that have values lie between 0 and 1, and the summation of each row in the matrix is equal 1 since each row represents a probability vector. The

diagonal p_{ii} is the probability that the system will stay in state *i* during a specified time or one transition. *P*-matrix is also known as stochastic transitional probability matrix.

2.1 Discrete Markov Chains

Assuming that we have a system with three discrete states, S1, S2 and S3, and p_{ii} is the probability of the transition from one state S_i to another S_j.

$$P = \begin{bmatrix} p_{11} & p_{12} & p_{13} \\ p_{21} & p_{22} & p_{23} \\ p_{31} & p_{32} & p_{33} \end{bmatrix} \tag{2.2}$$

The states and probabilities for this system can be represented by a state space diagram or state transition diagram as shown in figure 2.1.
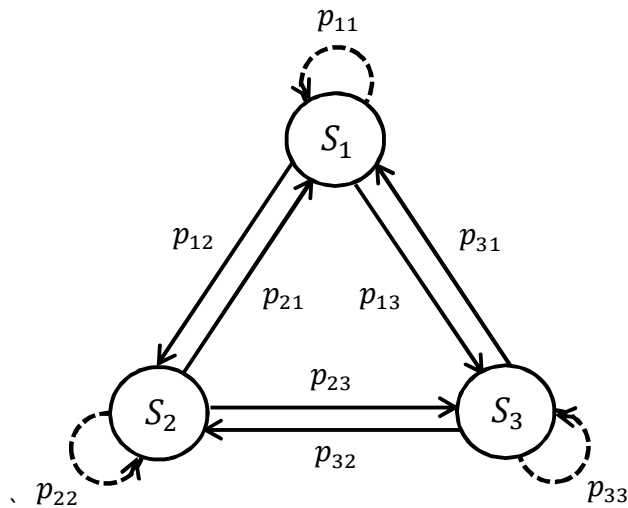
Figure 2.1 State transition diagram for a three states model

The initial probability distribution vector can be calculated as

$$p(0) = [p_1(0) \quad p_2(0) \quad p_3(0) \dots p_n(0)] \tag{2.3}$$

Then after one step, $p(1)$ is calculated as

$$p(1) = p(0)P = [p_1(0) \quad p_2(0) \quad p_3(0) \dots p_n(0)] \, P \tag{2.4}$$

After k steps

$$p(k) = p(0)P^k \tag{2.5}$$

where P^k is the K_{th} step transition matrix, $P^k = PPP \dots . P \,(k \; times)$.

After infinite number of steps and when the probability of being in any state is independent of the initial probabilities, the system is called *ergodic* and has a limiting state probability vector (α). The limiting state vector is the probability of being in state i after infinite number of steps and it can be calculated by

$$\alpha P = \alpha \tag{2.6}$$

where α is a row of vectors as

$$\alpha = [\alpha_1 \quad \alpha_2 \quad \alpha_3 \dots . \alpha_n] \tag{2.7}$$

and the summation of all vectors is equal one.

$$\sum_{j=1}^n \alpha_j = 1 \tag{2.8}$$

2.2 Continuous Markov Processes

If we have a system with n discrete state, $S_1, S_2, \dots , S_n$ and ρ_{ij} determines the transition from one state to another (rate of departure).

$$
\begin{array}{cccc}
& S_1 & S_2 & \;\;.... & S_n \\
\begin{array}{c} S_1 \\ S_2 \\ \vdots \\ S_n \end{array} &
\left[\begin{array}{cccc}
\rho_{11} & \rho_{12} & \cdots & \rho_{1n} \\
\rho_{21} & \rho_{22} & \cdots & \rho_{2n} \\
\vdots & \vdots & \cdots & \vdots \\
\rho_{n1} & \rho_{n2} & \cdots & \rho_{nn}
\end{array}\right]
\end{array}
\tag{2.9}
$$

Then, the probability P of transition from one state S_i to another S_j in the time interval Δt

is given by

$$
P_{ij} = \rho_{ij}\, \Delta t \tag{2.10}
$$

And the probability of finding the system in S_i at time $(t + \Delta t)$ is

$$
P_i(t + \Delta t) = \sum_{\substack{j=1 \\ j \neq i}}^{n} \rho_{ji}\Delta t P_j(t) + \left[1 - \sum_{\substack{j=1 \\ j \neq i}}^{n} \rho_{ij}\Delta t\right]P_i(t) \tag{2.11}
$$

By simplifying this equation, we get

$$
\frac{P_i(t + \Delta t) - P_i(t)}{\Delta t} = \sum_{\substack{j=1 \\ j \neq i}}^{n} \rho_{ji}P_j(t) - [P_i(t)]\sum_{\substack{j=1 \\ j \neq i}}^{n} \rho_{ji} \tag{2.12}
$$

By taking the limit as Δt goes to 0, (2.12) will be a first order differential equation.

$$
P_i' = \sum_{\substack{j=1 \\ j \neq i}}^{n} \rho_{ji}P_j(t) - [P_i(t)]\sum_{\substack{j=1 \\ j \neq i}}^{n} \rho_{ji} \tag{2.14}
$$

This general equation can be written in matrix form with (i = 1, 2, … , n) as

$$
\begin{bmatrix} p_1'(t) \\ p_2'(t) \\ \vdots \\ p_n'(t) \end{bmatrix} =
\begin{bmatrix}
-\displaystyle\sum_{j=2}^{n}\rho_{1j} & \rho_{21} & \cdots & \rho_{n1} \\
\rho_{12} & -\displaystyle\sum_{\substack{j=1 \\ j\neq 2}}^{n}\rho_{2j} & \cdots & \rho_{n2} \\
\vdots & \vdots & \cdots & \vdots \\
\rho_{1n} & \rho_{2n} & \cdots & -\displaystyle\sum_{j=1}^{n-1}\rho_{nj}
\end{bmatrix}
\begin{bmatrix} p_1(t) \\ p_2(t) \\ \vdots \\ p_n(t) \end{bmatrix}
\tag{2.15}
$$

Solving this differential equation with appropriate initial condition obtains the time dependent system state probabilities.

P matrix can be obtained from the corresponding rates of departures matrix (2.9) as:

$$P = \begin{bmatrix} 1 - \sum_{j=2}^{n} \rho_{1j}\Delta t & \rho_{12}\Delta t & ... & \rho_{1n}\Delta t \\ \rho_{21}\Delta t & 1 - \sum_{\substack{j=1 \\ j \neq 2}}^{n} \rho_{2j}\Delta t & ... & \rho_{2n}\Delta t \\ \vdots & \vdots & ... & \vdots \\ \rho_{n1}\Delta t & \rho_{n2}\Delta t & ... & 1 - \sum_{j=1}^{n-1} \rho_{nj}\Delta t \end{bmatrix} \qquad (2.16)$$

Δt can be removed from the P matrix and hence it is not a stochastic matrix anymore because the matrix elements are transition rates but not probabilities.

$$P = \begin{bmatrix} 1 - \sum_{j=2}^{n} \rho_{1j} & \rho_{12} & ... & \rho_{1n} \\ \rho_{21} & 1 - \sum_{\substack{j=1 \\ j \neq 2}}^{n} \rho_{2j} & ... & \rho_{2n} \\ \vdots & \vdots & ... & \vdots \\ \rho_{n1} & \rho_{n2} & ... & 1 - \sum_{j=1}^{n-1} \rho_{nj} \end{bmatrix} \qquad (2.17)$$

2.3 Markov Model in Reliability Evaluation

In power system, most components have only two possible states; up or down. The transition from the (up) state to (down) state is called the failure rate (λ), whereas the transition from the (down) state to (up) state is called the repair rate (μ). Figure 2.2 shows the two states model diagram or the binary model for repairable components.
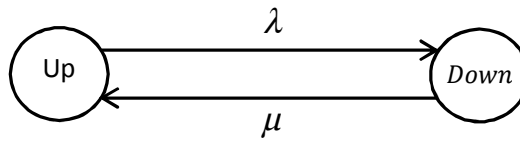
Figure 2.2 Two states binary model

where,

$$failure\ rate\ \lambda\ =\ \frac{Number\ of\ failures}{Total\ operation\ time} \qquad (2.18)$$

$$repair\ rate\ \mu\ =\ \frac{Number\ of\ repairs}{Total\ duration\ of\ all\ repairs} \qquad (2.19)$$

Let us consider a system with two components that are connected once in series and another in parallel as they are shown in figure 2.3 and 2.4 respectively. λ_1 and μ_1 are the failure and repair rates of the first component and λ_2 and μ_2 are the same for the second.
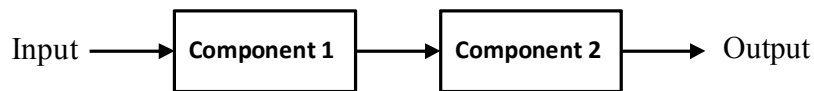
Figure 2.3 Simple system with two components connected in series
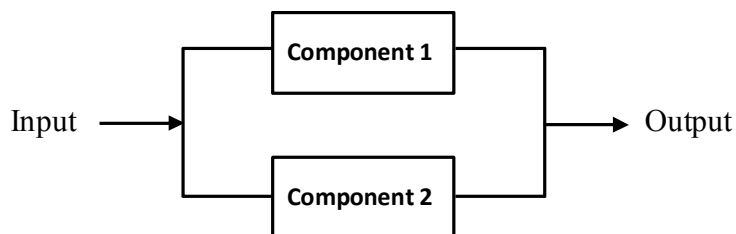
Figure 2.4 Simple system with two components connected in parallel

15

The number of possible states for a binary system can be obtained by (2^n), where n is the number of components. In this case, the total number of states for the system is $2^2=4$. In the series system, if a failure occurred in one of the components or both of them, the system will be down. The system will be up only when both components are up. On the other hand, parallel system is always up except for one case when both components are down. Table 2.1 shows the status and the output of both systems.

Table 2.1 Possible states for both series and parallel systems

State Number	Binary Representation	Component 1	Component 2	Series Output	Parallel Output
S1	11	up	Up	up	up
S2	10	up	Down	down	up
S3	01	down	Up	down	up
S4	00	down	Down	down	down

The departure rates (ρ) matrix for both systems is given by

$$\rho = \begin{bmatrix} 0 & \rho_{12} & \rho_{13} & 0 \\ \rho_{21} & 0 & 0 & \rho_{24} \\ \rho_{31} & 0 & 0 & \rho_{34} \\ 0 & \rho_{42} & \rho_{43} & 0 \end{bmatrix} \qquad (2.20)$$

By substituting failure and repair rates in the ρ-matrix we get

$$\rho = \begin{bmatrix} 0 & \lambda_2 & \lambda_1 & 0 \\ \mu_2 & 0 & 0 & \lambda_1 \\ \mu_1 & 0 & 0 & \lambda_2 \\ 0 & \mu_1 & \mu_2 & 0 \end{bmatrix} \qquad (2.21)$$

The state space diagram for the two systems in terms of transition rates is shown in figure 2.5.

16
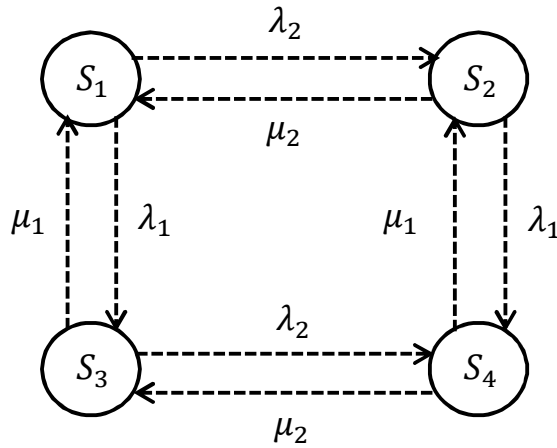
Figure 2.5 State space diagram in terms of transition rates

And the P matrix can be obtained by

$$
P = \begin{bmatrix}
1 - (\lambda_2 + \lambda_1) & \lambda_2 & \lambda_1 & 0 \\
\mu_2 & 1 - (\mu_2 + \lambda_1) & 0 & \lambda_1 \\
\mu_1 & 0 & 1 - (\mu_1 + \lambda_2) & \lambda_2 \\
0 & \mu_1 & \mu_2 & 1 - (\mu_1 + \mu_2)
\end{bmatrix} \quad (2.22)
$$

The state transition diagram in terms of the transition probabilities is shown in figure 2.6. By multiplying all elements in the P matrix by Δt, we get the probabilities of the transition from one state to another. However, Diagonal elements in the P matrix represent the probability of being at the same state.
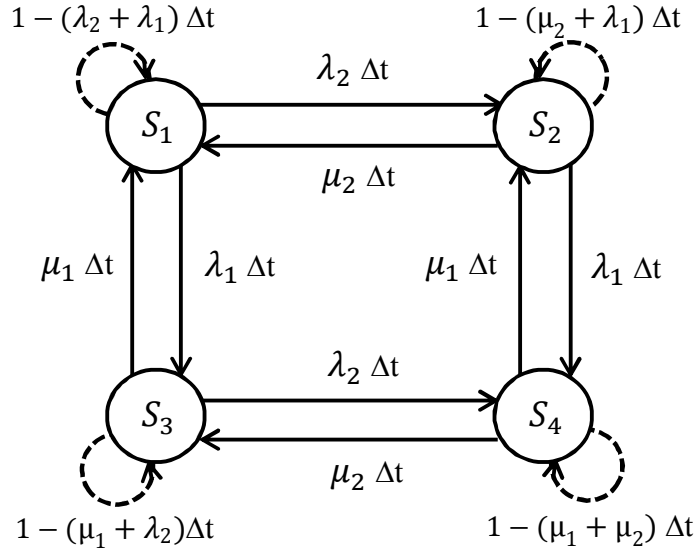
Figure 2.6 State space diagram in terms of transition

From equation (2.15), the differential equations for the system state probabilities are given by

$$
\begin{bmatrix} p_1'(t) \\ p_2'(t) \\ p_3'(t) \\ p_4'(t) \end{bmatrix} = \begin{bmatrix} -(\lambda_2 + \lambda_1) & \mu_2 & \mu_1 & 0 \\ \lambda_2 & -(\mu_2 + \lambda_1) & 0 & \mu_1 \\ \lambda_1 & 0 & -(\mu_1 + \lambda_2) & \mu_2 \\ 0 & \lambda_1 & \lambda_2 & -(\mu_1 + \mu_2) \end{bmatrix} \begin{bmatrix} p_1(t) \\ p_2(t) \\ p_3(t) \\ p_4(t) \end{bmatrix} \quad (2.23)
$$

The coefficient matrix of the Markov differential equations is called Q-matrix, and hence the differential equations can be rewritten as

$$
\begin{bmatrix} p_1'(t) \\ p_2'(t) \\ p_3'(t) \\ p_4'(t) \end{bmatrix} = Q \begin{bmatrix} p_1(t) \\ p_2(t) \\ p_3(t) \\ p_4(t) \end{bmatrix} \quad (2.24)
$$

Power system reliability can be evaluated using continuous Markov process. This can be done by solving the Markov differential equations for the system. After solving the differential equations, steady state probabilities can be calculated under the steady state condition,

18

$$p_i'(t) = 0 \text{ for } i = 1, 2, \dots, n \tag{2.25}$$

And with $\sum\limits_{i=1}^{n} P_i = 1$, the Markov differential equations become

$$
\begin{bmatrix} 0 \\ 0 \\ \vdots \\ 1 \end{bmatrix} =
\begin{bmatrix}
-\sum\limits_{j=2}^{n} \rho_{1j} & \rho_{21} & \cdots & \rho_{n1} \\
\rho_{12} & -\sum\limits_{\substack{j=1 \\ j \neq 2}}^{n} \rho_{2j} & \cdots & \rho_{n2} \\
\vdots & \vdots & \cdots & \vdots \\
1 & 1 & \cdots & 1
\end{bmatrix}
\begin{bmatrix} P_1 \\ P_2 \\ \vdots \\ P_n \end{bmatrix}
\tag{2.26}
$$

The steady-state probabilities can be found by solving these algebraic equations.

After finding the steady-state probabilities, load point reliability indices and system reliability indices can be calculated.

2.4 Availability and Unavailability

Availability of a system is the probability of this system to work, and unavailability is completely the opposite. Consider we have the system that represented by table 1. Then, steady state Markov equation can be formed as

$$
\begin{bmatrix}
-(\lambda_2 + \lambda_1) & \mu_2 & \mu_1 & 0 \\
\lambda_2 & -(\mu_2 + \lambda_1) & 0 & \mu_1 \\
\lambda_1 & 0 & -(\mu_1 + \lambda_2) & \mu_2 \\
1 & 1 & 1 & 1
\end{bmatrix}
\begin{bmatrix} P_1 \\ P_2 \\ P_3 \\ P_4 \end{bmatrix}
=
\begin{bmatrix} 0 \\ 0 \\ 0 \\ 1 \end{bmatrix}
\tag{2.27}
$$

By solving equation (2.27), system probabilities can be given by

$$
P_1 = \frac{\mu_1 \mu_2}{(\lambda_1 + \mu_1)(\lambda_2 + \mu_2)} \qquad P_2 = \frac{\mu_1 \lambda_2}{(\lambda_1 + \mu_1)(\lambda_2 + \mu_2)}
$$

$$\tag{2.28}$$

$$
P_3 = \frac{\mu_2 \lambda_1}{(\lambda_1 + \mu_1)(\lambda_2 + \mu_2)} \qquad P_4 = \frac{\lambda_1 \lambda_2}{(\lambda_1 + \mu_1)(\lambda_2 + \mu_2)}
$$

If the two components of the system are connected in series, the system will work or be

up when both components are up as in the first state in table 1. However, it will be down

when any of them or both are down as in states 2, 3, and 4. Therefore, availability and

unavailability are computed as

$$\text{Availability } A = P_1 \qquad \text{Unavailability } U = P_2 + P_3 + P_4 \qquad (2.29)$$

Generally, availability and unavailability can be calculated by summing the steady state

probabilities of the system

$$A = P_{UP} = \sum_{i=1}^{U} P_{up\,i} \qquad U = P_{DOWN} = \sum_{i=1}^{D} P_{down\,i} \qquad (2.30)$$

2.5 Mean Time to Failure MTTF and Mean Time to Repair MTTR

MTTF is the average time of operation before the system fails, whereas MTTR is the

average time of failure before repairing the system. MTTF and MTTR can be found by

calculating the fundamental matrix N as

$$N = [I - S]^{-1} \qquad (2.31)$$

where N generally represents the expected number of steps or time intervals to leave the

transient states and enter the absorbing states, I is the identity matrix, and S is called the

truncated or transition matrix. In transient state it is possible for the state to communicate

with other states in both directions. However, in absorbing state there is only one way to

communicate with that state and once the system enter that state it stays until a new

process is started. To calculate the MTTF, the failure states are considered as absorbing states and it can be given by

$$MTTF = [I - S_u]^{-1} \tag{2.32}$$

S_u is the transition matrix of the system after deleting all the failure or down states. If we have the system that represented by table 1, the transition matrix will be formed as

$$P = \begin{bmatrix} 1 - (\lambda_2 + \lambda_1) & \lambda_2 & \lambda_1 & 0 \\ \mu_2 & 1 - (\mu_2 + \lambda_1) & 0 & \lambda_1 \\ \mu_1 & 0 & 1 - (\mu_1 + \lambda_2) & \lambda_2 \\ 0 & \mu_1 & \mu_2 & 1 - (\mu_1 + \mu_2) \end{bmatrix} \tag{2.33}$$

In the case of series components, state 1 represents the up state, while states 2, 3, and 4 represent the down states. To calculate MTTF, S_u is found by deleting all the rows and coloumns of the down states from the P-matrix. S_u is given by

$$S_u = [1 - (\lambda_2 + \lambda_1)] \tag{2.34}$$

By substituting (2.34) in (2.32), MTTF can be found as

$$MTTF = [[1] - [1 - (\lambda_1 + \lambda_2)]]^{-1} \tag{2.35}$$

and after mathematical simplification,

$$MTTF = \frac{1}{\lambda_1 + \lambda_2} \tag{2.36}$$

To find the MTTR, the up states are assumed to be the absorbing states,

$$MTTR = [I - S_d]^{-1} \tag{2.37}$$

21

where S_d is the transition matrix after deleting all the up states. At the preceding example, S_d is found by deleting all the rows and columns of the up states from the P-matrix. S_d is given by

$$S_d = \begin{bmatrix} 1-(\mu_2+\lambda_1) & 0 & \lambda_1 \\ 0 & 1-(\mu_1+\lambda_2) & \lambda_2 \\ \mu_1 & \mu_2 & 1-(\mu_1+\mu_2) \end{bmatrix} \quad (2.38)$$

and by substituting (2.38) in (2.37), the MTTR becomes

$$MTTR = \begin{bmatrix} \mu_2+\lambda_1 & 0 & -\lambda_1 \\ 0 & \mu_1+\lambda_2 & -\lambda_2 \\ -\mu_1 & -\mu_2 & \mu_1+\mu_2 \end{bmatrix}^{-1} \quad (2.39)$$

The inverse of the matrix is given as

$$MTTR = \frac{1}{det} \begin{bmatrix} (\mu_1+\mu_2)(\mu_1+\lambda_2)-\lambda_2\mu_2 & \lambda_1\mu_2 & \lambda_1(\mu_1+\lambda_2) \\ \mu_1\lambda_2 & (\mu_1+\mu_2)(\mu_2+\lambda_1)-\lambda_1\mu_1 & \lambda_2(\mu_2+\lambda_1) \\ \mu_1(\mu_1+\lambda_2) & \mu_2(\mu_2+\lambda_1) & (\mu_2+\lambda_1)(\mu_1+\lambda_2) \end{bmatrix} \quad (2.40)$$

where $det = (\lambda_1+\mu_2)(\lambda_2+\mu_1)(\mu_1+\mu_2)-\lambda_2\mu_2(\lambda_1+\mu_2)-\lambda_1\mu_1(\lambda_2+\mu_1)$.

The MTTR for the system is the sum of one of the rows that represent the current state divided by the determination. The MTTR for the system to move from S_2 to S_1 is

$$MTTR = \frac{sum\ of\ first\ row = (\mu_1+\mu_2)(\mu_1+\lambda_2)-\lambda_2\mu_2+\lambda_1\mu_2+\lambda_1(\mu_1+\lambda_2)}{det = (\lambda_1+\mu_2)(\lambda_2+\mu_1)(\mu_1+\mu_2)-\lambda_2\mu_2(\lambda_1+\mu_2)-\lambda_1\mu_1(\lambda_2+\mu_1)} \quad (2.41)$$

2.6 Frequency and Duration Interruptions

There are other parameters or variables that it is important to compute in addition to the steady-state probabilities, such as passage time, residence time, and cycle time. The time

that would the system takes to transit from one state to another is called passage time. Residence time is the passage time from a current state to any other state. Cycle time is the time required to complete an (in) and a (not-in) cycle for a state. These three variables are continuous random variables and have expected values.

The expected cycle time is equal to the sum of the residence time and the time between the residences.

$$E[T_c] = E[T_r] + E[T_{br}] \tag{2.42}$$

In different words, it is also equal to the sum of the MTTF and MTTR.

$$E[T_c] = MTTF + MTTR \tag{2.43}$$

The expected frequency for occurrence of any state is equal to the reciprocal of the cycle time for that state.

$$f_i = \frac{1}{E[T_c]} \tag{2.44}$$

after substituting (2.42) in (2.44), f_i is given as

$$f_i = \frac{1}{E[T_r] + E[T_{br}]} \tag{2.45}$$

In term of $MTTF$ and $MTTR$,

$$f_i = \frac{1}{MTTF + MTTR} \tag{2.46}$$

By multiplying the frequency with

$$\frac{E[T_r]}{E[T_r]}$$

the frequency becomes

$$f_i = \frac{E[T_r]}{E[T_c]} \frac{1}{E[T_r]} \tag{2.47}$$

Frequency of occurrence can be found in term of probability by

$$f_i = \frac{P_i}{E[T_r]} \tag{2.48}$$

Where P_i is the probability of being in state i. Since the expected residence time is equal to the MTTF, it can be given by

$$E[T_r] = [I - S_u]^{-1} \tag{2.49}$$

And by deleting all the rows and columns of the absorbing states, S_u becomes

$$S_u = \left[1 - \sum_{j=2}^{n} \rho_{ij}\right] \tag{2.50}$$

where ρ_{ij} is the rate departure from state i to state j. After substituting (2.50) in (2.49), the expected residence time is

$$E[T_r] = \left[[1] - \left[1 - \sum_{j=2}^{n} \rho_{ij}\right]\right]^{-1} \tag{2.51}$$

and with mathematical simplification we get

$$E[T_r] = \left[\sum_{j=2}^{n} \rho_{ij}\right]^{-1} \tag{2.52}$$

By substituting (2.52) in (2.48), the expected frequency can be computed as

$$f_i = P_i \sum_{j=2}^{n} \rho_{ij} \tag{2.53}$$

Equation (2.53) shows that the expected frequency of state i is equal to the probability of that state multiplied by the rates departure from the same state. In the previous example

of two components in series, the frequency of occurrence for state 1 can be calculated using (2.53),

$$f_1 = P_1 \sum_{j=2}^{4} \rho_{1j} \tag{2.54}$$

By substituting P_1 from (2.28) and $\sum_{j=2}^{4} \rho_{1j}$ from (2.33) in (2.54), we get

$$f_1 = \frac{\mu_1 \mu_2}{(\lambda_1 + \mu_1)(\lambda_2 + \mu_2)} (\lambda_1 + \lambda_2) \tag{2.55}$$

And by the same way, the frequency of occurrence for states 2, 3, and 4 are

$$f_2 = \frac{\mu_1 \lambda_2}{(\lambda_1 + \mu_1)(\lambda_2 + \mu_2)} (\mu_2 + \lambda_1) \tag{2.56}$$

$$f_3 = \frac{\mu_2 \lambda_1}{(\lambda_1 + \mu_1)(\lambda_2 + \mu_2)} (\mu_1 + \lambda_2) \tag{2.57}$$

$$f_4 = \frac{\lambda_1 \lambda_2}{(\lambda_1 + \mu_1)(\lambda_2 + \mu_2)} (\mu_1 + \mu_2) \tag{2.58}$$

In power system, the theory of frequency of occurrence is used to find failure frequency of the system. Failure frequency is the frequency of occurrence from up state to down state and it is equal to the frequency of occurrence for the down states of the system.

If the system has multiple down states, the rate departures for the down states need to be modified by excluding all the mutual transition between the failure states in order to calculate the failure frequencies.

$$f_i = P_i \sum_{j=2}^{n} \rho'_{ij} \tag{2.59}$$

Where ρ'_{ij} are the modified rates of departure. Then, the system failure frequency is given by summing the failure frequencies for all down states.

$$f_{system} = \sum_{i=1}^{d} f_i \tag{2.60}$$

Where $\boldsymbol{d}$ is the number of down states. The modified transition rates matrix for the same example of two components in series is given by removing all the mutual rates of departure between the down states (S_2, S_3, and S_4).

$$\rho'_d = \begin{bmatrix} 0 & \lambda_2 & \lambda_1 & 0 \\ \mu_2 & 0 & 0 & 0 \\ \mu_1 & 0 & 0 & 0 \\ 0 & 0 & 0 & 0 \end{bmatrix} \tag{2.61}$$

Using equation (2.60) the failure frequencies for the down states are

$$f_2 = \frac{\mu_1 \lambda_2}{(\lambda_1 + \mu_1)(\lambda_2 + \mu_2)} (\mu_2) \tag{2.62}$$

$$f_3 = \frac{\mu_2 \lambda_1}{(\lambda_1 + \mu_1)(\lambda_2 + \mu_2)} (\mu_1) \tag{2.63}$$

$$f_4 = \frac{\lambda_1 \lambda_2}{(\lambda_1 + \mu_1)(\lambda_2 + \mu_2)} (0) \tag{2.64}$$

Then, the system failure frequency becomes

$$f_{system} = f_2 + f_3 + f_4 = \frac{\mu_1 \mu_2 (\lambda_1 + \lambda_2)}{(\lambda_1 + \mu_1)(\lambda_2 + \mu_2)} \tag{2.65}$$

2.7 Main Equations of Reliability Indices

Availability, *MTTF*, and failure frequency are used to calculate the load point reliability indices and system reliability indices. Load point indices are computed for each load point in the system and they are as such: Average Interruption Duration (*AID*), Average Interruption Frequency (*AIF*), Frequency Duration (*FD*), and Energy Not Supplied (*ENS*). System indices are calculated for a group of load points or an entire system [1][4]. The most common system indices are:

- System Average Interruption Frequency Index (*SAIFI*):

  SAIFI measures the probability that average customer will experience an interruption during a year.

- System Average Interruption Duration Index (*SAIDI*):

  SAIDI measures the total duration of interruption for average customer during a year.

- Customer Average Interruption Duration Index (*CAIDI*):

  CAIDI measures the time to restore the service after an outage, or the duration for average interruption.

- Average Service Availability Index (*ASAI*) and Average Service Unavailability Index (*ASUI*):

  ASAI is a measure of the overall reliability of the system. It measures the percent of time that the average customer has a service during a year, whereas *ASUI* is exactly the opposite.

- Energy Not Supply (*ENS*) and Average Energy Not Supply (*AENS*):

ENS measures the energy not supplied to the system due to the interruption, and *AENS* measures the average energy not supplied to the average customer.

Equations that required for calculation of all reliability indices are summarized in table 2.2.

Table 2.2 Main equations of reliability indices

Index	Equation	Unit
Load point indices		
Availability	$A = \sum_{i=1}^{U} P_{(up)\,i}$	-
Unavailability	$U = 1 - A$	-
MTTF	$MTTF\ (S1)$	Y
AIF	$AIF = f$	f/y
AID	$AID = U \times 8760$	h/y
FD	$FD = \dfrac{AID}{AIF}$	h/f
ENS	$ENS = AID \times P_{avg}$	MWh
System indices		
SAIFI	$SAIFI = \dfrac{\sum_{i=1}^{B} AIF_i N_i}{N_T}$	f/c.y
SAIDI	$SAIDI = \dfrac{\sum_{i=1}^{B} AID_i N_i}{N_T}$	h/c.y
CAIDI	$CAIDI = \dfrac{SAIDI}{SAIFI}$	h/f
ASAI	$ASAI = \dfrac{\sum_{i=1}^{B} 8760 N_i - \sum_{i=1}^{B} AID_i N_i}{\sum_{i=1}^{B} 8760 N_i}$	-
ASUI	$ASUI = 1 - ASAI$	-
ENS	$ENS = \sum_{i=1}^{B} AID_i P_{avgi}$	MWh/y
AENS	$AENS = \dfrac{ENS}{N_T}$	MWh/c.y

Where, B is the number of load point, N_i is the number of interrupted customers, N_T is the total number of customers, and P_{avg} is the average load power for each load point.

CHAPTER 3

DISTRIBUTION POWER FLOW ANALYSIS

Power flow analysis, also known as load flow, is one of the most important analyses in the power system. This analysis determines the steady state conditions of a power system for a set of specified power generations and load demand. Power flow analysis is essential for power planning, operation, economic scheduling, and exchange of power between utilities. Furthermore, it is necessary for other analyses such as fault analysis and stability.

In power flow analysis each bus has four parameters, real power (P), reactive power (Q), voltage magnitude (V), and voltage angle (δ). Two of the parameters must be specified to calculate the others. There are three types of buses: a slack bus has two specified parameters, V and $\angle \delta$; a generator bus has two specified parameters, P and V; and a load bus has two specified parameters, P and Q. Because of that, the generator bus is called P-V bus, and the load bus is called P-Q bus.

Load flow calculation is usually carried out using the node voltage method. First, an admittance matrix for the system is formed. Then, linear algebraic equations in terms of node currents are derived. If node currents are known, node voltages can be calculated by the linear algebraic equation. However, in the power system this is not always the case. Powers are specified instead of currents, which results in complex nonlinear equations in

terms of system powers, called power flow equations. To calculate node voltages and the other parameters, power flow equations must be solved. The most common techniques used for load flow calculation are the iterative techniques, Gauss-Seidel, Newton-Raphson, and Fast Decoupled [16].

The preceding methods were developed to solve the power flow for transmission systems. However, in distribution systems, they may not work appropriately due to the special features of distribution systems [17]. These features can be summarized as followings:

- Radial with sometimes weakly meshed structure.

- High resistance to reactance (r/x) ratios.

- Multiphase and unbalanced oriented.

- Extremely large number of branches and nodes.

Figure 3.1 shows a sample of small distribution system.
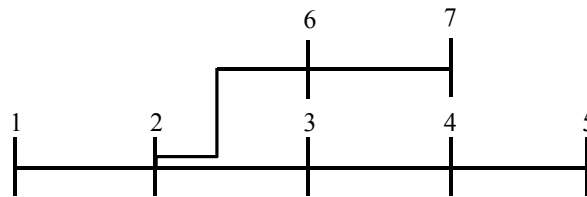
Figure 3.1 Small distribution system

3.1 Power Flow Techniques for Distribution System

Many power flow algorithms especially suited for distribution systems have been developed. A compensation-based method (forward/backward method) using a multi-port compensation technique and basic formulations of Kirchhoff's laws has been proposed in [18]. This method solves power flow for weakly meshed distribution systems. At the beginning, a meshed system was converted into a radial system by breaking the interconnected points, also known as break points. Then, the radial system was directly solved by Kirchhoff's voltage and current laws (KVL and KCL). Finally, the multi-port compensation method was used to calculate the breakpoint currents. The number of iteration is high due to calculation of breakpoint currents. As mentioned before, the forward/backward algorithm has two main steps. First, the backward sweep calculates branch currents starting from the last node toward the source. Second, the forward sweep calculates node voltages starting from the source toward the last node. In each iteration, voltages are updated in backward steps to calculate the branch current, and currents are updated in forward steps to calculate node voltages. The number of iterations here are high due to the calculation of breakpoint currents.

A fast decoupled method using G-matrix (FDG) for the power flow of distribution systems, based on equivalent current injections with the first time to use the fast decoupled technique in distribution systems has been outlined in [19]. This method uses the Newton Raphson technique but with rectangular coordinates. The Jacobian matrix here is called G matrix. It is formed in terms of currents instead of powers. After deriving current equations, real and imaginary parts are separated into conductance (G) and

susceptance (B). The G matrix will be formed by the values of G and B of the distribution system, and it can be decoupled with certain assumptions. After several iterations, the power flow will be solved. The FDG method is sensitive to the r/x ratio. The r/x ratio must be multiplied by a factor between 0.5 and 1.5 to meet the technique requirement. However, the G matrix is constant and formed only once and hence consumes less time.

A simple and efficient branch-to-node matrix based power flow (BNPF) for radial distribution systems has been presented in [20]. Key features for this method are that voltages for all nodes are calculated from the source voltage. A branch-to-node matrix is used to define the relation between branch current and node currents with no inversion of any matrices. This matrix is formed based on the topology and configuration of the system. Loads can be represented by any kind of models, constant power, constant impedance, constant admittance, or constant current. Load flow is carried out by calculating branch currents then computing branch voltages, and finally calculating bus voltages in terms of source voltage and branch voltages.

A distribution power flow (DPF) technique with the objective to enhance the convergence rate by partially linearizing the power flow equations has been developed in [21]. Power equations here are linearized by eliminating the trigonometric part. Trigonometric terms are replaced with adopted variables (a) and (b). Power equations are linearized around operating points (a) and (b). The Jacobian matrix of linearization process will be formed and bus voltage will be solved. This method is insensitive to the resistance to reactance (r/x) ratio and applicable for large-scale distribution systems. On the other hand, forming, calculating, and inverting the Jacobian matrix provides complexity and is more time consuming.

A direct approach of DPF using bus injection to branch current matrix (BIBC) and branch current to bus voltage matrix (BCBV) has been obtained in [22]. The two matrices are obtained from the topological characteristics of distribution systems, and they represent the relationship among bus current injections, branch currents, and bus voltages. BIBC is used to calculate branch currents. BCBV is used to obtained difference voltages or drop voltages. Eventually, bus voltages are calculated in terms of difference voltages and source voltage. LU factorization, forming a Jacobian matrix, and matrix inversion are not needed in this method. It is applicable for large distribution systems and high r/x ratios. Therefore, this method is efficient, fast, and robust.

A robust decoupled power flow technique has been presented in [23]. This method is based on line current flow in rectangular coordinates with elimination of the off-diagonal blocks of the Jacobian matrix. This elimination makes perfect decoupling of the problem, unlike FDG which is based on unrealistic assumptions. The algorithm of this method is the same as the FDG method. However, this technique proposes a constant transformation matrix. This transformation matrix is composed of two-sub diagonal matrices of cosine and sine of system admittance angles. By multiplying mismatched equations of the power system by the transformation matrices, the equation will be decoupled into two-sub equations for solving the power flow. This method is unaffected by the range of r/x ratio and provides a solution for large distribution systems. It is efficient, accurate, and robust.

In this research, three techniques of DPF will be presented and tested in order to apply them in the reliability evaluation for RBTS system. These methods are distribution load

flow matrix method DLF, enhanced Newton Raphson method ENR, and Robust decoupled method RD.

3.2 Distribution Load Flow Matrix Method (DLF)

This method solves the DPF directly by using two matrices—bus injection to branch current matrix (BIBC) and branch current to bus voltage matrix (BCBV) [24]. BIBC and BCBV are formed based on the configuration of the system. BIBC and BCBV are utilized for branch currents and drop voltages calculation respectively. Multiplying those two matrices results in one matrix called distribution load flow matrix DLF. DLF is used in one step to compute bus voltages.
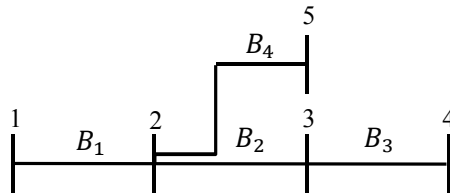
Figure 3.2 Sample distribution system

The power distribution system in figure 3.2 is used as an example. At the beginning, we assume that all bus or node voltages are equal to the source node. Specified data in the distribution system are load active power (P) and reactive power (Q) for each bus. Node currents can be computed in terms of specified P and Q as

$$I_{node} = \frac{(P + Q)^*}{V^*} \tag{3.1}$$

By applying Kirchhoff's current law (KCL) to the distribution system, branch currents can be obtained in terms of node currents by the following equations:

34

$$I_{branch1} = I_{node2} + I_{node3} + I_{node4} + I_{node5} \qquad (3.2)$$

$$I_{branch2} = I_{node3} + I_{node4}$$

$$I_{branch3} = I_{node4}$$

$$I_{branch4} = I_{node5}$$

The relation between branch currents and node currents in equation (3.2) can be expressed with the BIBC matrix as:

$$
\begin{bmatrix} I_{branch1} \\ I_{branch2} \\ I_{branch3} \\ I_{branch4} \end{bmatrix} = \begin{bmatrix} 1 & 1 & 1 & 1 \\ 0 & 1 & 1 & 0 \\ 0 & 0 & 1 & 0 \\ 0 & 0 & 0 & 1 \end{bmatrix} \begin{bmatrix} I_{node2} \\ I_{node3} \\ I_{node4} \\ I_{node5} \end{bmatrix} \qquad (3.3)
$$

By rewriting equation (3.3) in general expression as:

$$I_{branch} = [BIBC] * I_{node} \qquad (3.4)$$

The bus voltages can be calculated in terms of drop voltages by:

$$V_2 = V_1 - (I_{branch1} * Z_{B1}) = V_1 - V_{D1} \qquad (3.5)$$

$$V_3 = V_2 - (I_{branch2} * Z_{B2}) = V_2 - V_{D2}$$

$$V_4 = V_3 - (I_{branch1} * Z_{B3}) = V_3 - V_{D3}$$

$$V_5 = V_2 - (I_{branch1} * Z_{B4}) = V_2 - V_{D4}$$

The relation between branch currents and bus voltages in equations (3.5) can be expressed with the BCBV matrix as:

$$
\begin{bmatrix} V_{D1} \\ V_{D2} \\ V_{D3} \\ V_{D4} \end{bmatrix} = \begin{bmatrix} Z_{B1} & 0 & 0 & 0 \\ Z_{B1} & Z_{B2} & 0 & 0 \\ Z_{B1} & Z_{B2} & Z_{B3} & 0 \\ Z_{B1} & 0 & 0 & Z_{B4} \end{bmatrix} \begin{bmatrix} I_{branch1} \\ I_{branch2} \\ I_{branch3} \\ I_{branch4} \end{bmatrix} \qquad (3.6)
$$

By rewriting equation (3.6) in general expression, we get:

$$V_D = [BCBV] * I_{branch} \qquad (3.7)$$

By substituting equation (3.4) in (3.7), we get:

$$V_D = [\ DLF\ ] * I_{node} \qquad\qquad (3.8)$$

where DLF is the distribution load flow matrix and equals $[\ DLF\ ] = [BCBV] * [BIBC]$.

$$DLF = \begin{bmatrix} Z_{B1} & Z_{B1} & Z_{B1} & Z_{B1} \\ Z_{B1} & Z_{B1} + Z_{B2} & Z_{B1} + Z_{B2} & Z_{B1} \\ Z_{B1} & Z_{B1} + Z_{B2} & Z_{B1} + Z_{B2} + Z_{B3} & Z_{B1} \\ Z_{B1} & Z_{B1} & Z_{B1} & Z_{B1} + Z_{B4} \end{bmatrix}$$

At the end, bus voltages are computed by:

$$V_{Bus} = V_{Source} - V_{drop} \qquad\qquad (3.9)$$

After solving the voltages for all buses by equation (3.9), we check for convergence. If the solution is converged, we stop. Otherwise, we start the algorithm again iteratively until reaching the convergence. Figure 3.3 shows the algorithm for the DLF method.
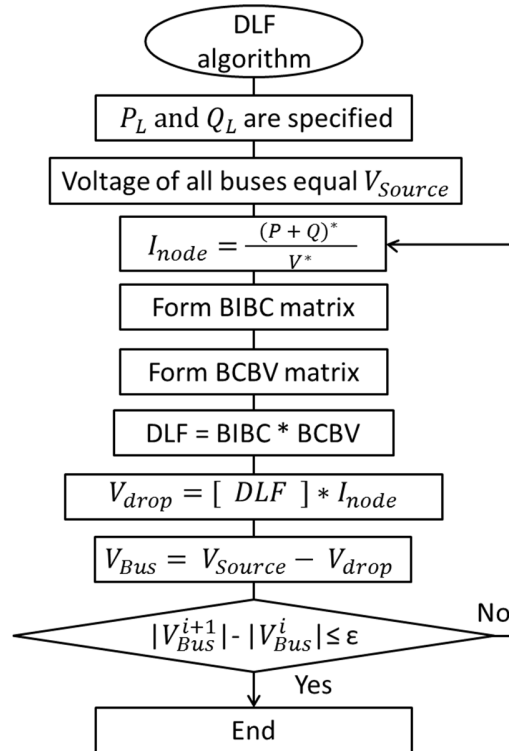
Figure 3.3 DLF method algorithm

3.3 Enhanced Newton Raphson Method (ENR)

This method provides a solution for distribution load flow using the current-injection technique based on the Newton-Rapson method and rectangular coordinates [19]. The Jacobian matrix in ENR is called "G matrix," and it is constant and formed for once unlike with the conventional Newton Raphson method. For the first time, decoupling can be applied to the DPF by assuming off-diagonal blocks of the G matrix to be zeros.

For a distribution system with (n) number of buses, the specified node current can be calculated in terms of specified active power (P) and reactive power (Q) as:

$$I_{node} = \frac{(P + Q)^*}{V^*} \qquad (3.10)$$

Specified branch currents can be calculated as:

$$I_{branch}^{sp} = [C] * I_{node} \qquad (3.11)$$

where C is a branch to bus matrix.

Bus voltage will be represented in rectangular coordinates as:

$$V = e + j\,f \qquad (3.12)$$

By substitute (3.10) and (3.12) in (3.11), equation (3.11) will be:

$$I_{branch}^{sp} = [C] * \frac{(P + Q)^*}{(e + j\,f)^*} \qquad (3.13)$$

Branch current can also be calculated in terms of branch admittance in rectangular coordinates.

$$I_{branch} = [(e_i - e_{i+1}) + j(f_i - f_{i+1})]\,[G_j - B_j] \qquad (3.14)$$

where i represents the buses in the system $i=1,2,3,\ldots$, n. and j represents the branches, $j=1,2,3,\ldots$, n-1. By separating the real and imaginary parts of equations (3.13) and (3.14), the Newton-Raphson solution for the load flow can be formulated as:

$$\begin{bmatrix} J_1 & J_2 \\ J_3 & J_4 \end{bmatrix} \begin{bmatrix} \Delta e \\ \Delta f \end{bmatrix} = \begin{bmatrix} \Delta I^r_{branch} \\ \Delta I^i_{branch} \end{bmatrix} \tag{3.15}$$

Jacobians are calculated for once as:

$$J_1 = \frac{\partial I^r_{branch}\ (e,f)}{\partial e} = G \qquad J_2 = \frac{\partial I^r_{branch}\ (e,f)}{\partial f} = -B$$

$$J_3 = \frac{\partial I^i_{branch}\ (e,f)}{\partial e} = G \qquad J_4 = \frac{\partial I^i_{branch}\ (e,f)}{\partial f} = B$$

Current mismatches ΔI^r_{branch} and ΔI^i_{branch} are calculated using:

$$\Delta I^r_{branch} = Re(\ I^{sp}_{branch}\ ) - Re(\ I_{branch}\ ) \tag{3.16}$$

$$\Delta I^i_{branch} = Im(\ I^{sp}_{branch}\ ) - Im(\ I_{branch}) $$

Correction values Δe and Δf can be given by factorizing equation (3.15):

$$\begin{bmatrix} \Delta e \\ \Delta f \end{bmatrix} = \begin{bmatrix} G & -B \\ B & G \end{bmatrix}^{-1} \begin{bmatrix} \Delta I^r_{branch} \\ \Delta I^i_{branch} \end{bmatrix} \tag{3.17}$$

Finally, voltage magnitudes and angles, are computed and updated by:

$$e_{new} = e_{old} + \Delta e \tag{3.18}$$

$$f_{new} = f_{old} + \Delta f$$

After computing e and f by equation (3.18), we check for convergence. If the solution is converged, we stop. Otherwise, we start the algorithm iteratively, except for the one-time calculation equation, until reaching the convergence. Figure 3.4 shows the algorithm for the ENR method.

The G matrix can be decoupled by assuming the off-diagonal blocks of G matrix to be zeros:

$$\begin{bmatrix} \Delta e \\ \Delta f \end{bmatrix} = \begin{bmatrix} G & 0 \\ 0 & G \end{bmatrix}^{-1} \begin{bmatrix} \Delta I^r_{branch} \\ \Delta I^i_{branch} \end{bmatrix} \tag{3.19}$$

Then Δe and Δf can be calculated as

$$\Delta e = G \, \Delta I^r_{branch} \tag{3.20}$$

$$\Delta f = G \, \Delta I^i_{branch}$$

A draw back for this assumption is that in large systems the solution may not converge.
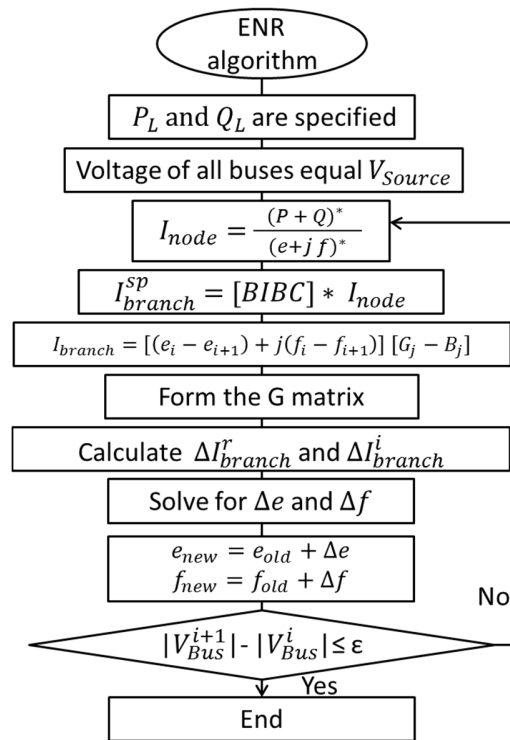
Figure 3.4 ENR method algorithm

3.4 Robust Decoupled Method (RD)

The main idea in the robust decoupled method is to decouple the Newton Raphson equation into two sub-equations by a constant transformation matrix [23]. Multiplying the Jacobian matrix by the transformation matrix will result in zero off-diagonal blocks of Jacobian. Equation (3.15) is multiplied by the transformation matrix in order to decouple the equation.

$$\begin{bmatrix} T_1 & T_2 \\ -T_2 & T_1 \end{bmatrix} \begin{bmatrix} J_1 & J_2 \\ J_3 & J_4 \end{bmatrix} \begin{bmatrix} \Delta e \\ \Delta f \end{bmatrix} = \begin{bmatrix} T_1 & T_2 \\ -T_2 & T_1 \end{bmatrix} \begin{bmatrix} \Delta I^r_{branch} \\ \Delta I^i_{branch} \end{bmatrix} \tag{3.28}$$

T_1 and T_2 are diagonal matrices of cosine and sine admittance angles, respectively. Equation (3.21) after decoupling will be represented as

$$[T][\Delta e] = [\Delta I^{r\_T}_{branch}] \tag{3.22}$$

$$[T][\Delta f] = [\Delta I^{i\_T}_{branch}]$$

Sub-Jacobian matrix T is computed by

$$[T] = [T_1] \frac{\partial I^r_{branch}(e,f)}{\partial e} + [T_2] \frac{\partial I^i_{branch}(e,f)}{\partial e} \tag{3.23}$$

$$= [-T_2] \frac{\partial I^r_{branch}(e,f)}{\partial f} + [T_1] \frac{\partial I^i_{branch}(e,f)}{\partial f}$$

$\Delta I^{r\_T}_{branch}$, and $\Delta I^{i\_T}_{branch}$ are calculated by

$$[\Delta I^{rT}_{branch}] = [T_1] [\Delta I^r_{branch}] + [T_2] [\Delta I^i_{branch}] \tag{3.24}$$

$$[\Delta I^{iT}_{branch}] = [-T_2] [\Delta I^r_{branch}] + [T_1] [\Delta I^i_{branch}]$$

Equation (3.23) is calculated for once as the Jacobian. Correction values Δe and Δf can be given by dividing equation (3.22) by $[T]$.

$$[\Delta e] = [T]^{-1} [\Delta I^{r\_T}_{branch}] \tag{3.25}$$

$$[\Delta f] = [T]^{-1} [\Delta I^{i\_T}_{branch}]$$

And finally, voltage magnitudes and angles, are computed and updated by

$$e_{new} = e_{old} + \Delta e \qquad (3.26)$$

$$f_{new} = f_{old} + \Delta f$$

After computing e and f by equation (3.26), check for convergence, we keep updating the voltage magnitude and angles until reaching the convergence as can be shown in Figure 3.5.
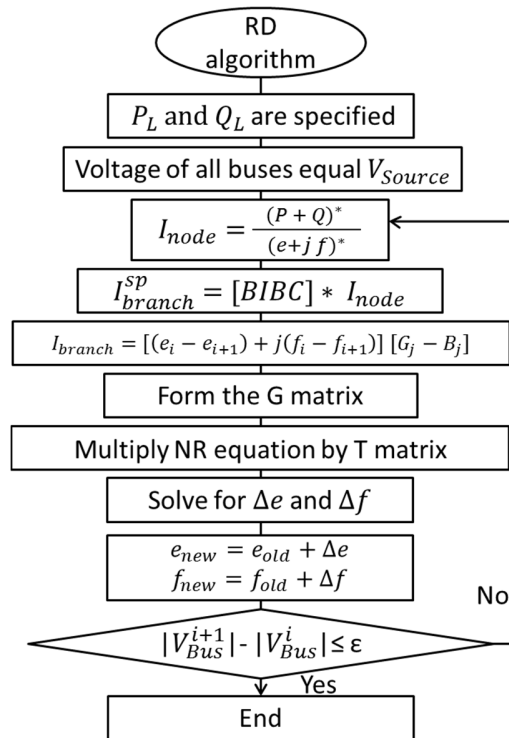
Figure 3.5 RD method algorithm

3.5 Weakly Meshed Distribution Load Flow

A distribution system has large number of feeders, load points connected to these feeders, and normally open tie switches. Tie switches are closed in contingency or when serving high-density loads. When some of the tie switches are closed, it leads to some loops in

the distribution system, and it will be in weakly mesh configuration rather than radial. This new configuration leads to losses reduction, voltage profile improvement, reliability and power quality enhancement. A simple weakly meshed distribution system is shown in Figure 3.6.

The DLF method can be utilized here with few modifications.
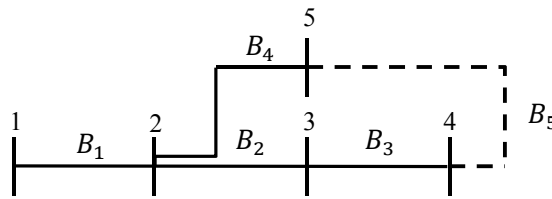
Figure 3.6 Small weakly meshed distribution system

Figure 3.6 shows that a new branch (B_5) is added to the system. The branch current $I_{branch5}$ is flowing through B_5 from node 4 to node 5. I_{node4} and I_{node5} will be calculated as [25]:

$$I'_{node4} = I_{node4} + I_{branch5} \tag{3.27}$$

$$I'_{node5} = I_{node5} - I_{branch5} \tag{3.28}$$

The DLF matrix will be modified as well. If a new branch is added from a bus i to a bus j, elements in the j_{th} column are subtracted from the elements in the i_{th} column in the existing DLF matrix and the results are filled in the new k_{th} column and k_{th} row of the DLF matrix. The diagonal element of the k_{th} row and column is found by summing all the impedances of the branches which involved in forming the loop or 'weakly mesh'.

$$DLF = \begin{bmatrix} Z_{11} & Z_{12} & Z_{13} & Z_{14} & Z_{13-14} \\ Z_{21} & Z_{22} & Z_{23} & Z_{24} & Z_{23-24} \\ Z_{31} & Z_{32} & Z_{33} & Z_{34} & Z_{33-34} \\ Z_{41} & Z_{42} & Z_{43} & Z_{44} & Z_{43-44} \\ Z_{13-14} & Z_{23-24} & Z_{33-34} & Z_{43-44} & Z_{55} \end{bmatrix}$$

After modifying the DLF matrix, Kron's reduction is applied to the new DLF matrix to make it the same dimension as before [11]:

$$Z_{new} = Z_{old} - \frac{corresponding(Z_{i-j(column)} * Z_{i-j(row)})}{Z_{i-j(diagonal)}} \qquad (3.29)$$

This technique is only applicable to DLF method because it depends on modifying the DLF matrix.

3.6 Distribution Load Flow including Distribution Generation (DG)

Distribution generation DG is a generation system that spreads through the distribution system for improving the service and the reliability. DG could be photovoltaic system, wind turbines, fuel cells, micro turbines, etc. The DG units have different operational modes [26]. They could supply a power with a predetermined amount of reactive power (fixed power factor). In this case, DG units are not controlling the voltage at the connection point. On the other hand, DG units could supply a power by controlling and regulating the voltage at the connection points.
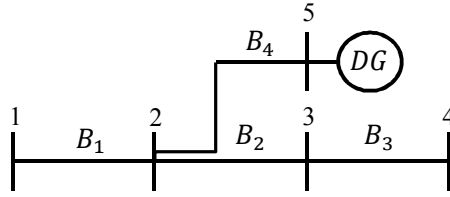
Figure 3.7 Small distribution system with distributed generation

If a DG unit generates a predetermined amount of power, the DG is modelled as a PQ bus and treated as a load bus with negative values for P and Q. However, when a DG unit regulates and controls the voltage at the connection point, the DG is modelled as a PV bus.

In the case of PV, active DG power P_{DG} is specified, reactive DG power Q_{DG} is initially set to zero, and the voltage at the P-V node is set to the desirable value. The DLF, ENR, or RD method can be utilized here with some adjustments. Branch currents will be calculated with:

$$I_{branch} = [BIBC] * (I_{node} + I_{DG}) \tag{3.30}$$

After computing the bus voltages, if $|V_i - V_{i\,set}| \leq$ error tolerance, the solution is converged. Otherwise, Q_{DG} will be generated by PV node to maintain the voltage at the specified value. Q_{DG} can be computed as:

$$Q_{DG\,new} = Q_{DG\,old} + Im(V_i \frac{V_i^*}{Z}) \tag{3.31}$$

where i is the number of the DG bus, $V_{i\,set}$ is the set voltage at the DG bus, and V_i is the calculated voltage at the DG bus. The algorithm for solving a DPF with the inclusion of the DG is the same as the three methods with considering equations (3.30) and (3.31).

3.7 Tests and Results

Tests and simulations for the presented methods are conducted. Three methods, DLF, ENR, and RD, are tested on a radial 33-bus distribution system. Then, the DLF method is tested on weakly meshed 33-bus distribution system. Lastly, the DLF method is tested on weakly meshed 33-bus distribution system including a DG. Line and load data for the system are mentioned in [27]. The base data is 12.66 KV and 10 MW, and the convergence tolerance is 0.0001. MATLAB is used as the implementation platform.

3.7.1 Radial Distribution System

The preceding distribution load flow methods, DLF, ENR, and RD, were tested on radial 33-bus [27] in order to assess their performance, accuracy, speed of calculation, robustness, and computational efficiency. Figure 3.8 shows the IEEE radial 33-bus system.

Solution of the three methods, DLF, ENR, and RD for the radial 33-bus are shown in Table 3.1. The results in Table 3 show that all three methods provide the same solution. These results are identical to those of previous studies of DPF [28][29]. For DLF, ENR, and RD, the solution is converged after the same number of iterations, 4, so all the three methods have a good convergence. In terms of computational time, DLF comes first with 46 ms, then ENR with 70 ms, and lastly RD with 80 ms. All three methods are accurate and efficient. However, DLF is simpler and faster than ENR and RD. Table 3.2 shows a comparison among all three methods.
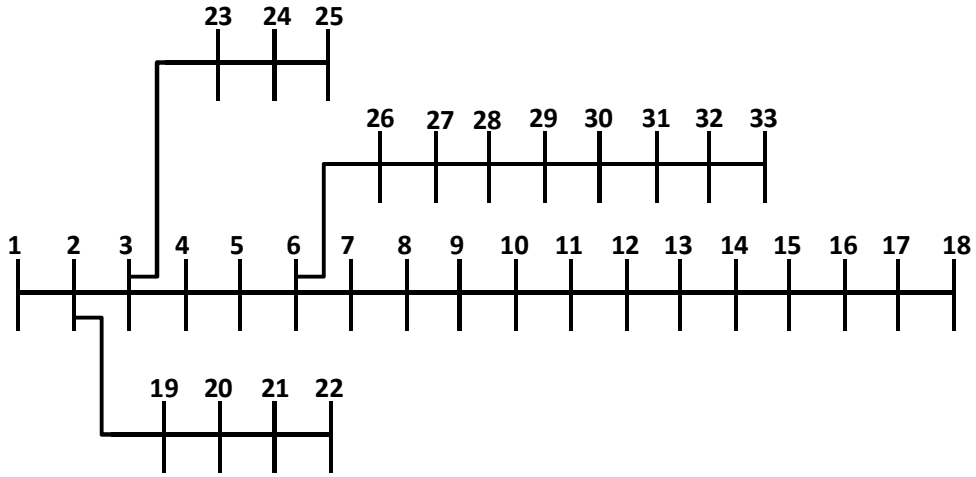
Figure 3.8 33-Bus distribution system

Table 3.1 PF solution for 33-Bus system

Bus no.	DLF, ENR, and RD		Bus no.	DLF, ENR, and RD	
	V_{pu}	δ_{deg}		V_{pu}	δ_{deg}
1	1	0	18	0.9131	-0.4950
2	0.9970	0.0145	19	0.9965	0.0037
3	0.9829	0.0960	20	0.9929	-0.0633
4	0.9755	0.1616	21	0.9922	-0.0827
5	0.9681	0.2283	22	0.9916	-0.1030
6	0.9497	0.1338	23	0.9794	0.0651
7	0.9462	-0.0965	24	0.9727	-0.0237
8	0.9413	-0.0604	25	0.9694	-0.0674
9	0.9351	-0.1335	26	0.9477	0.1733
10	0.9292	-0.1960	27	0.9452	0.2295
11	0.9284	-0.1888	28	0.9337	0.3124
12	0.9269	-0.1773	29	0.9255	0.3903
13	0.9208	-0.2686	30	0.9220	0.4956
14	0.9185	-0.3473	31	0.9178	0.4112
15	0.9171	-0.3849	32	0.9169	0.3881
16	0.9157	-0.4082	33	0.9166	0.3804
17	0.9137	-0.4855			

Table 3.2 Comparison of the three DPF methods

DPF methods	DLF	ENR	RD
Accuracy	accurate	accurate	Accurate
Number of iterations	4	4	4
Computational time	46 ms	70 ms	80 ms
Flexibility	flexible	inflexible	Inflexible
Complexity	simple	complex	Complex
Sensitivity to r/x ratio	insensitive	insensitive	Insensitive

3.7.2 Weakly Meshed Distribution System

The DLF method with the presented modification for a weakly meshed distribution system was tested on the 33-bus system having five loops [25] shown in Figure 3.9. The new mesh connections cause a reduction to the branch current values. This reduces the voltage drop and power losses, and improves the voltage profile. The obtained results from the power flow solution are identical to the results in [25] as shown in table 3.3. Convergence was reached after 3 iterations and 69 ms.
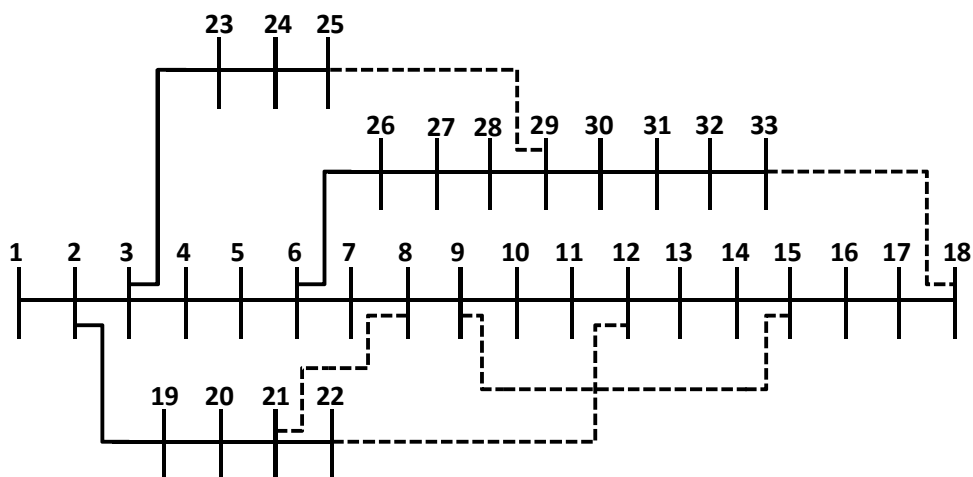
Figure 3.9 33-Bus distribution system with 5 closed tie lines

47

Table 3.3 PF solution for weakly meshed 33-Bus system

Bus no.	DLF method		Bus no.	DLF method	
	V_{pu}	δ_{deg}		V_{pu}	δ_{deg}
1	1	0	18	0.9521	-0.2327
2	0.9971	0.0143	19	0.9954	-0.0003
3	0.9861	0.0555	20	0.9813	-0.0845
4	0.9822	0.0640	21	0.9774	-0.1340
5	0.9785	0.0702	22	0.9749	-0.1863
6	0.9698	-0.0387	23	0.9807	0.0464
7	0.9689	-0.1416	24	0.9703	-0.0115
8	0.9676	-0.1653	25	0.9632	-0.0233
9	0.9633	-0.1955	26	0.9688	-0.0241
10	0.9620	-0.2166	27	0.9674	-0.0031
11	0.9618	-0.2161	28	0.9616	0.0077
12	0.9617	-0.2173	29	0.9576	0.0275
13	0.9588	-0.2314	30	0.9543	0.1408
14	0.9579	-0.2494	31	0.9509	-0.0155
15	0.9578	-0.2494	32	0.9502	-0.0504
16	0.9561	-0.2396	33	0.9503	-0.0727
17	0.9531	-0.2548			

The voltage profile is improved due to closing the tie lines and all bus voltages become within the limit of ± 5% of base voltage as shown in table 3.3. The improvement has a range of (-1.68%) to (+4.44%). Although voltages at bus 19-22 and 24-25 decrease with small percentage, they remain within the acceptable voltage limit. Figure 3.10 shows the improvement of voltage profile in percentage, due to the mesh connections. Red points in figure 3.10 indicate the voltage deterioration.
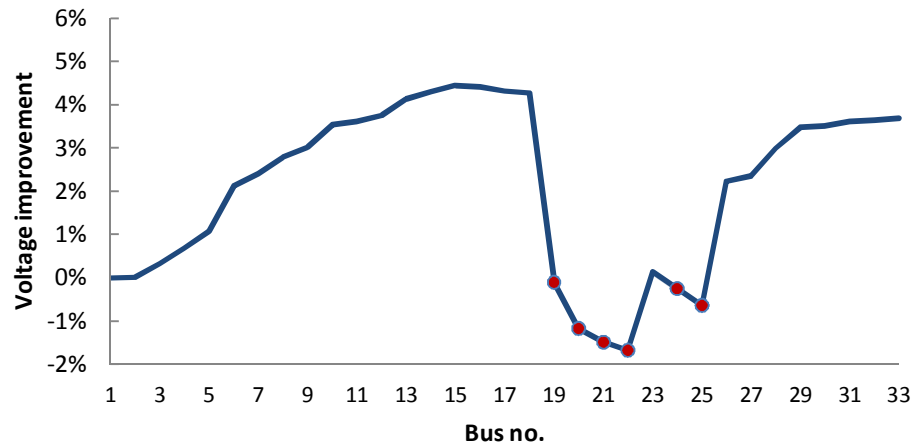
Figure 3.10 Voltage profile improvement due to mesh connections

3.7.3 Weakly Meshed Distribution System with DGs

The DLF method with the additional equations to include the distribution generation DG unit in the distribution system was tested on the 33-bus weakly meshed distribution system. Figure 3.11 shows a DG installed at bus 22 and generates 1000 KW. The DG is modelled as a PV bus with controlling the voltage at the connection point. The voltage at bus 22 is set at 1 pu. Table 3.4 shows the results of the DPF calculation.
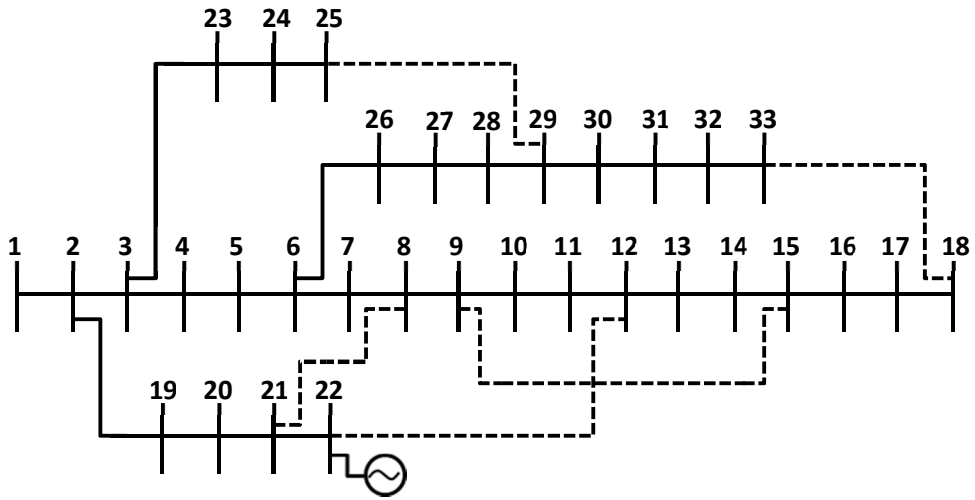
Figure 3.11 33-Bus distribution system with DG

Table 3.4 DPF solution for weakly meshed system and DG

Bus no.	DLF method		Bus no.	DLF method	
	V_{pu}	δ_{deg}		V_{pu}	δ_{deg}
1	1	0	18	0.9627	-0.2897
2	0.9980	-0.0011	19	0.9975	-0.0189
3	0.9888	0.0147	20	0.9945	-0.1493
4	0.9860	0.0095	21	0.9940	-0.1871
5	0.9834	0.0014	22	1.0000	-0.1783
6	0.9775	-0.1039	23	0.9839	0.0019
7	0.9781	-0.1468	24	0.9745	-0.0596
8	0.9789	-0.2174	25	0.9684	-0.0755
9	0.9758	-0.2415	26	0.9763	-0.0882
10	0.9756	-0.2561	27	0.9749	-0.0655
11	0.9757	-0.2581	28	0.9686	-0.0532
12	0.9759	-0.2639	29	0.9643	-0.0322
13	0.9722	-0.2738	30	0.9613	0.0400
14	0.9708	-0.2962	31	0.9586	-0.0758
15	0.9703	-0.2960	32	0.9582	-0.1080
16	0.9682	-0.2841	33	0.9586	-0.1246
17	0.9641	-0.3126			

The voltage profile is improved because of the mesh connections and DG connected to the system, where the DG generates 970 Kvar. This improvement extends from (-0.1%) to (+5.80%), and has only one bus voltage decreases by 0.1% at bus 25 as shown in figure 3.12.
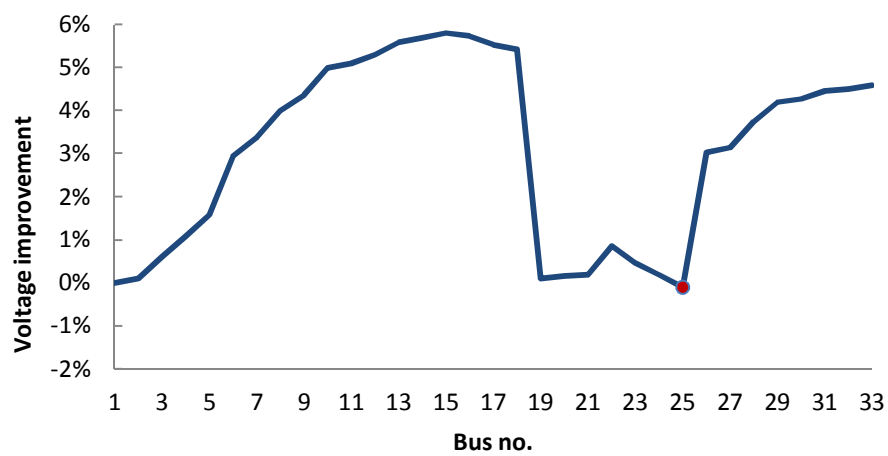
Figure 3.12 Voltage profile improvement due to 1000 KW DG

CHAPTER 4

RELIABILITY EVALUATION USING MM & DPF

In this research, the reliability of an active distribution system or Microgrid is evaluated using MM and DPF analysis. The reliability can be assessed by investigating the availability of the service at each load point of the system. To study the probability of the the availability of the system, two principles are utilized. First, examining the connections between the source and the loads. This can be achieved by considering all the scenarios or states of outages or faults in MM states. Second, using DPF to study the transfer capability and verify the quality of the voltage at each load points. Then, MM of the system will be used to calculate all the reliability indices. In order to proceed with the study, several procedures must be performed during the process. First, system reduction. Then, states classification using cut and tie sets. After that, prime numbers encoding to simplify the classification process.

4.1 System Reduction

In power system, most of components have only two possible states; up or down. The number of possible states for a binary system can be obtained by (2^n), where n is the number of components. Therefore, in large systems number of states can be extremely

large and difficult to deal with. To overcome this problem, several reductions are applied in this study [12]. These reductions are removing irrelevant load points, combining series and parallel components, removing irrelevant sections, and considering only the states of two possible failures at a time.

After the reduction process, there will be a number of states that represent the MM of the power system. The states will be determined as either up or down based on the connectivity and transfer capability. Connectivity is investigated by finding tie and cut sets [4]. Tie sets represent the up states, and cut sets represent the down states.

4.2 Cut and Tie Sets

Networks connection is series, parallel, combination of both, or complex connection. The reliability of series and parallel systems can be evaluated using the approximate method, and network reduction method is used for the systems with the combination of series and parallel. However, the future power system is expected to have a complex connection network, and one of the techniques that can solve this type of networks, is to decompose the network into a group of subsystems or a set of components (line sets) and then determine the system reliability. These components sets are tie set, minimal tie set, cut set, and minimal cut set. They can be defined as follows [4]:

1. Tie set: is any set of components that create a path between the source and the load.
2. Minimal tie set: is a set of minimum components that create a path between the source and the load.

3. Cut set: is a set of components that have to fail to cut the path between the source and the load.

4. Minimal cut set: is a set of minimum components that have to fail to cut the path between the source and the load.

Figure 4.1 shows a sample of a complex system, which is called the bridge system, and figures 4.2 and 4.3 show the minimal tie sets and cut sets for the same system respectively.
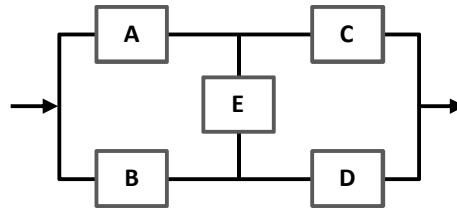
Figure 4.1 Complex system
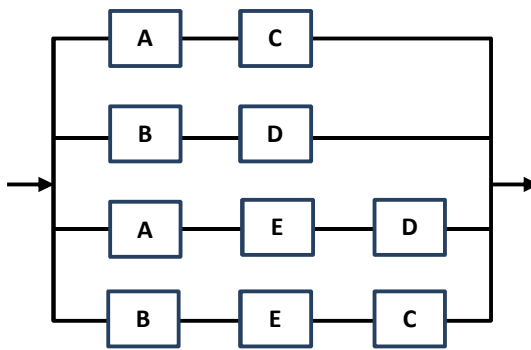
Figure 4.2 Minimal tie sets
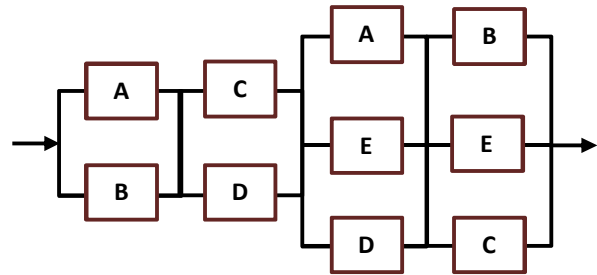
Figure 4.3 Minimal cut sets

In small systems, these sets of components can be determined by logical inspection. However, in large and complex systems the process is more difficult and complicated. Two methods will be used in this research to determine the tie and cut sets for large

systems, the petri nets and prime encoding method [30]. The petri nets method is used to find the minimal tie sets by the following steps:

1. Find A matrix and ΔM matrix in the the following equation,

$$AP=\Delta M \tag{4.1}$$

where A is a connection matrix, P is a column vector for the firing count, M is a column vector of input – output vector (the change in marking). $A = [a_{ij}]$ and a_{ij} = 1 if there is a connection between i and j, and a_{ij} = 0 if there is not. $M=m_i$ and m_i= 1 for $i = source\ or\ destination$ and $m_i = 0$ otherwise. $P=p_i$ and $p_i = 0$ if the bus is not included in the path.

2. If any column of A equals to ΔM, it represents an Lth success path (L= 1).

3. Mod-2 addition is used to add L columns starting from $L = 2$. If the addition equals ΔM, the corresponding indices is a successful path of length L. This process is repeated for all possible L combinations.

4. L is increased by 1, and steps 2 and 3 are repeated until L becomes equal to N-1. where N = total number of columns in A or total number of sections in the system.

4.3 Prime Number Encoding

Another method used to determine the components sets are the prime encoding [30]. Each component or line in the system will have a prime number. Then, each set of lines that represents a tie or cut set will be identified by a unique ID number equals to the product of the prime numbers of those lines. The ID number can be decoded to restore the prime numbers of the lines. If a system consists of 14 lines, then the prime coding

number and ID numbers can be as shown in table 4.1 [30]. The 14 lines of the system are divided into two groups to avoid the extremely large ID numbers.

After determining the minimal tie sets using the petri nets, and find all possible sets using prime numbers and ID numbers, the remaining sets can be found by dividing the ID numbers of the unknown sets by the ID numbers of the minimal tie sets. If the remaining of the division is equal zero, this means that this set is a tie set. After finding all the tie sets, the rest will be either a cut set or minimal cut set and they can be determined by the same process.

Table 4.1 Prime and ID numbers for 14 lines system

Line	Prime Number	Line	Prime Number	Possible Set	ID Number
1	2	8	2	1	[2,0]
2	3	9	3	1,2	[6,0]
3	5	10	5	1,..,7	[510510, 0]
4	7	11	7	8	[0,2]
5	11	12	11	8,9	[0,6]
6	13	13	13	8,..,14	[0, 510510]
7	17	14	17	1,..,14	[510510,510510]

4.4 Reliability Evaluation of RBTS-Bus 2

This study will be implemented on the RBTS-bus 2 system shown in figure 4.4 [31]. Base voltage of this distribution system is 11 KV, and it has 22 load points and 36 feeders of three different types as shown in table 4.2. Customer type, number of customers, and average and peak load at each load point are shown in table 4.3. Failure rate, repair rate, and repair time for each component are shown in table 4.4. Table 4.5 shows transformers data.

Table 4.2 Feeder types of RBTS-bus 2

Feeder type	Length	Feeder section number	Impedance
1	0.60 km	2 6 10 14 17 21 25 28 30 34	
2	0.75 km	1 4 7 9 12 16 19 22 24 27 29 32 35	0.14+j0.412 Ω/Km
3	0.80 km	3 5 8 11 13 15 18 20 23 26 31 33 36	

Table 4.3 Customers data of RBTS-bus 2

Number of load point	Load points	Customer type	Average load (MW)	Peak load (MW)	Number of customers
5	1-3 10 11	Residential	0.535	0.8668	210
4	12 17-19	Residential	0.450	0.7291	200
1	8	Small user	1.00	1.6279	1
1	9	Small user	1.15	1.8721	1
6	4 5 13 14 20 21	Gov. inst.	0.566	0.9167	1
5	6 7 15 16 22	Commercial	0.454	0.7500	10
Totals			12.291	20.00	1908

Table 4.4 Component reliability data of RBTS-bus 2

Component number	Overhead Lines			Underground Cables		
	Failure rate (f/y)	Repair rate (r/y)	Repair Time (h)	Failure rate (f/y)	Repair rate (r/y)	Repair Time (h)
2 6 10 14 17 21 25 28 30 34	0.03900	1752	5	0.024	292	30
1 4 7 9 12 16 19 22 24 27 29 32 35	0.04875	1752	5	0.030	292	30
3 5 8 11 13 15 18 20 23 26 31 33 36	0.05200	1752	5	0.032	292	30

Table 4.5 Transformers reliability data of RBTS-bus 2

Component number	Type	Failure Rate (f/y)	Repair Rate (r/y)	Repair time (h)	Replacing Rate (r/y)	Replacing time (h)
37-56	Trans. 11/0.415	0.015	43.8	200	876	10
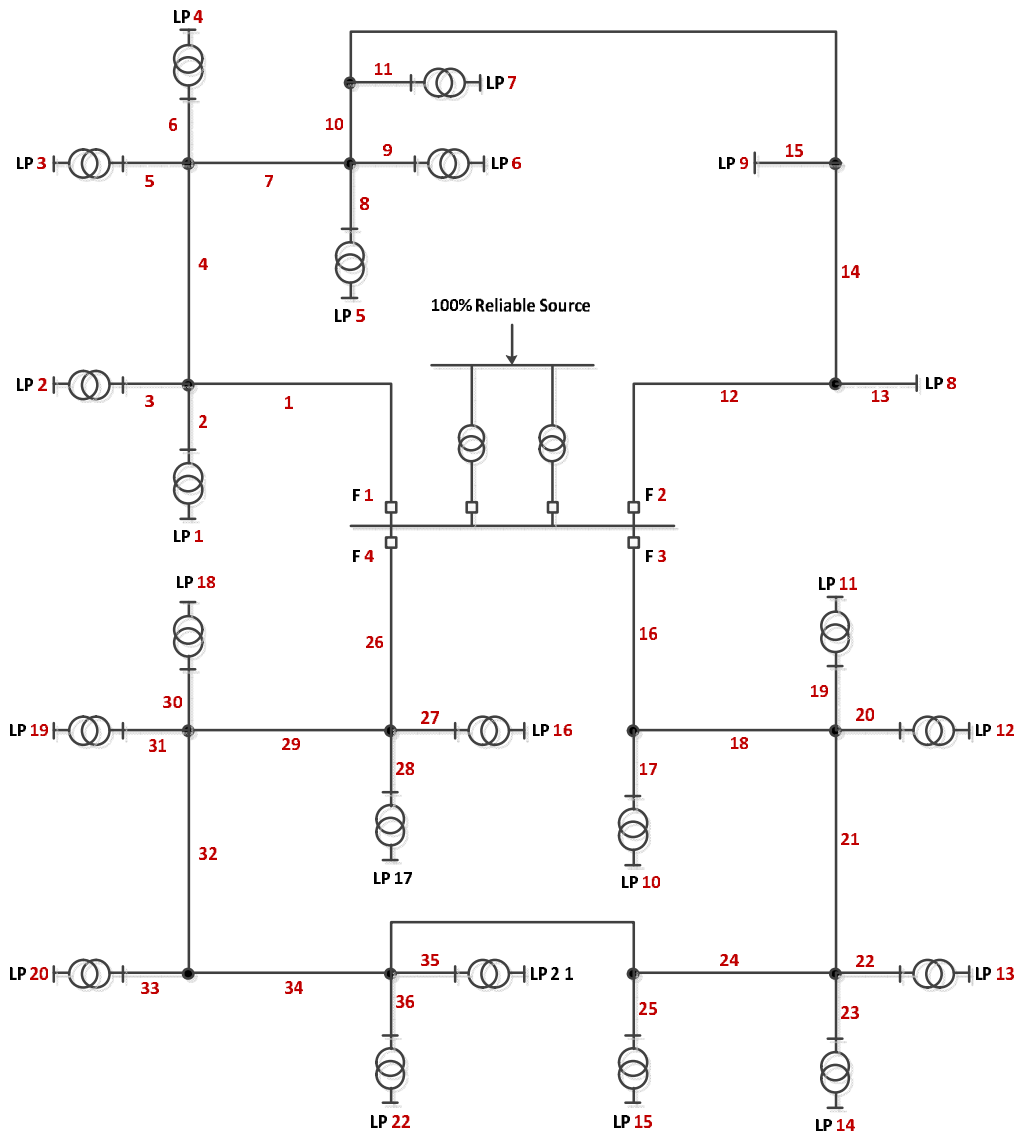
Figure 4.4 Single line diagram for RBTS-BUS2 [31]

In this study, the peak load will be considered in the power flow analysis with power factor of 0.9. The lines or components of the system will be assumed to be overhead lines. The reliability evaluation is going to be performed through the following steps:

1. Reducing the number of components and states of the system by the reduction techniques.

2. Classifying the states of the system as an (up state) or (down state) by the cut and tie set method based on the connectivity between the source and the load.

3. Reclassifying the states using the DPF analysis based on the transfer capacity and voltage profile.

4. Using MM to calculate the reliability indices of the system.

The steps are summarized in the flow chart shown in figure 4.5.

Five case studies are conducted in this chapter. First, the weakly meshed RBTS-bus 2 distribution system without DGs. The remaining four cases integrate DGs to the RBTS-bus2 system with different capacities and locations. DGs are used to improve the voltage profile of the system, and therefore improve the reliability. Capacity and location of DGs are considered to study their influence on the voltage profile, and therefore on the reliability.

4.5 Case Study 1: Weakly Meshed RBTS-Bus2

In case study 1, the preceding steps are used to evaluate the reliability of the weakly mesh RBTS-bus 2 with closing the two tie links in the system. Main substation is supplying the system without any inclusion of DG.

```
                    ╭─────────────────────╮
                    │ Reliability evaluation │
                    │          of          │
                    │      RBTS-BUS2       │
                    ╰─────────────────────╯
                              │
                              ▼
        ┌─────────────────────────────────────────┐
        │            Reduction Process            │
        │                                         │
        │  1) Remove irrelevant load points       │
        │  2) Remove irrelevant lines             │
        │  3) Remove irrelevant sections          │
        │  4) Consider only two simultanous failures │
        └─────────────────────────────────────────┘
                              │
                              ▼
        ┌─────────────────────────────────────────┐
        │         Classifying System's States     │
        │                                         │
        │   (Based on the connectivity between the │
        │            source and loads)            │
        └─────────────────────────────────────────┘
                              │
                              ▼
        ┌─────────────────────────────────────────┐
        │        Reclassifying System's States    │
        │                                         │
        │  (Based on transfer capability of the system) │
        └─────────────────────────────────────────┘
                              │
                              ▼
        ┌─────────────────────────────────────────┐
        │        Reliability Indices Calculation  │
        │                                         │
        │   (Using MM to calculate load point indices │
        │            and system indices)          │
        └─────────────────────────────────────────┘
                              │
                              ▼
        ╭─────────────────────────────────────────╮
        │            Reliability Indices          │
        │                                         │
        │  1) Load point indices:                 │
        │       A, U, AIF, MTTF, AID, FD,ENS.     │
        │  2) System indices:                     │
        │       SAIFI, SAIDI, CAIDI, ASAI, ENS.   │
        ╰─────────────────────────────────────────╯
```
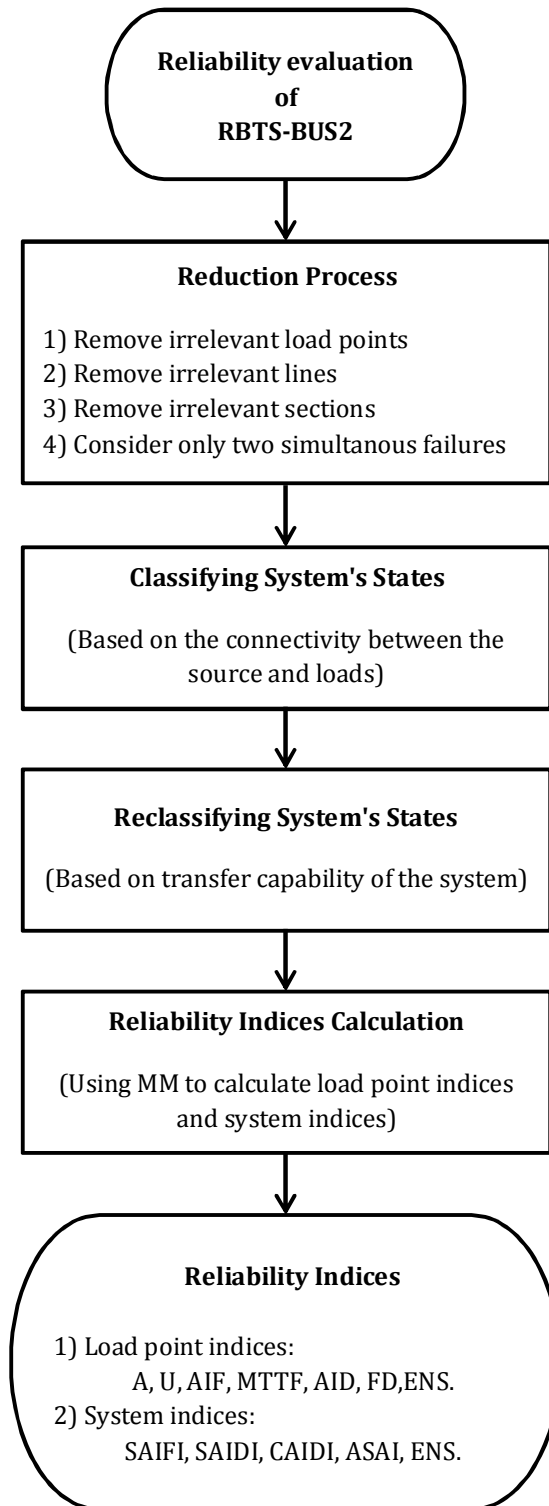
Figure 4.5 Flow chart for the process of reliability evaluation

4.5.1 Reduction Process

Figure 4.4 shows the line diagram of RBTS-bus2. It consists of two main sections, first one has the load points from 1-to-9, and the second one has the load points from 10-to-22. The system has 56 components including the lines and transformers. Number of states before the reduction is $2^{56} = 7.2058 \times 10^{16}$, which is extremely large and difficult to deal with.

Four levels of reduction can be applied to the RBTS-bus2 as mentioned in 4.1:

1. Removing the irrelevant load points. If we considering the first load point (LP1), then all other load points are irrelevant and removed.

2. Removing all lines that connected to the irrelevant load points except for the main line that connected directly to the source.

3. Removing the irrelevant section. Since LP1 belongs to the first section, the entire second section is irrelevant and removed.

4. After applying the preceding reductions, there will be 7 components instead of 56 with respect to the LP1, and the number of states will be $2^7 = 128$. This number of states is still large and it can be reduced by neglecting the states of more than two simultaneous failures since it is very unlikely to happen in power systems. Final number of states for LP1 after these four reductions is 29. This will be the case for all load points at section one, whereas in section two number of components will be 9 and number of states will be 46. Figure 4.6 and 4.7 shows the reduced system with respect to LP10 and LP1.
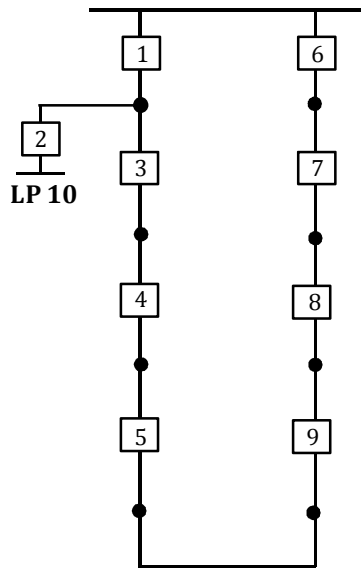
**Figure 4.6 RBTS-bus 2 Section-2
after reduction**
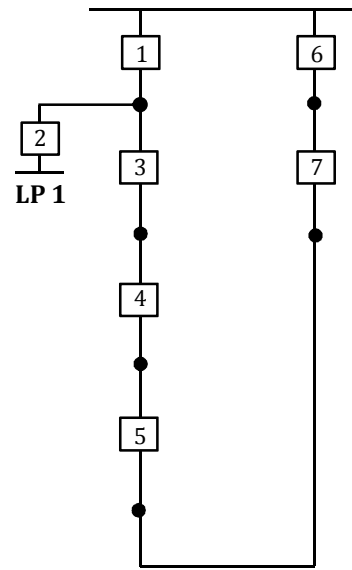
**Figure 4.7 RBTS-bus 2 Section-1
after reduction**

4.5.2 Classifying Process Based on Connectivity

The states of the system are classified as an (up state) or (down state) according to the connectivity between the source and the load, using cut and tie set method. Tie sets represent the up states and cut sets represent the down states. First, each component is encoded with a prime number. In the case of LP1, the prime numbers for component 1-7 are (2, 3, 5, 7, 11, 2, 3). Then, minimal tie sets are determined by the petri nets method, and every set is given an ID number. For instance, two minimal tie sets can be found for LP1. First set contains only components 1 and 2. However, it is not considered since the remaining five components are down and we assumed only 2 simultaneous failures can occur. The other minimal tie set contains components (6, 7, 5, 4, 3, 2). After that, the remaining sets are classified as tie set, cut set, and minimal cut set using the prime

number encoding method as explained in (4.2). The states for LP1 are shown in table 4.6, and the states for the remaining load points are found by the same method. All possible states or scenarios of two failures maximum are stated in table 12. At each state, components that have ones are up, and components that have zeros are down. The states are classified as (up) if they compose MTSs or TSs. On the other hand, if they form a MCSs or CSs, they are considered as (down states).

Table 4.6 States classification of LP1

State number	Component number							State classification
	1	2	3	4	5	6	7	
1	0	0	1	1	1	1	1	CS
2	0	1	0	1	1	1	1	MCS
3	0	1	1	0	1	1	1	MCS
4	0	1	1	1	0	1	1	MCS
5	0	1	1	1	1	0	1	MCS
6	0	1	1	1	1	1	0	MCS
7	0	1	1	1	1	1	1	MTS
8	1	0	0	1	1	1	1	CS
9	1	0	1	0	1	1	1	CS
10	1	0	1	1	0	1	1	CS
11	1	0	1	1	1	0	1	CS
12	1	0	1	1	1	1	0	CS
13	1	0	1	1	1	1	1	MCS
14	1	1	0	0	1	1	1	TS
15	1	1	0	1	0	1	1	TS
16	1	1	0	1	1	0	1	TS
17	1	1	0	1	1	1	0	TS
18	1	1	0	1	1	1	1	TS
19	1	1	1	0	0	1	1	TS
20	1	1	1	0	1	0	1	TS
21	1	1	1	0	1	1	0	TS
22	1	1	1	0	1	1	1	TS
23	1	1	1	1	0	0	1	TS
24	1	1	1	1	0	1	0	TS
25	1	1	1	1	0	1	1	TS
26	1	1	1	1	1	0	0	TS
27	1	1	1	1	1	0	1	TS
28	1	1	1	1	1	1	0	TS
29	1	1	1	1	1	1	1	TS

4.5.3 Reclassifying Process Based on Transfer Capability

System states of the RBTS-bus2 were determined depending on active paths between the source and the loads. In addition to the connectivity, voltage profile of the system at each scenario is considered in finding the system states in order to achieve a comprehensive and practical analysis of power reliability. DLF method that explained in chapter 3, is utilized here to investigate the voltage profile of the system. Figure 4.8 shows RBTS-bus2 one-line diagram that used for power flow analysis.
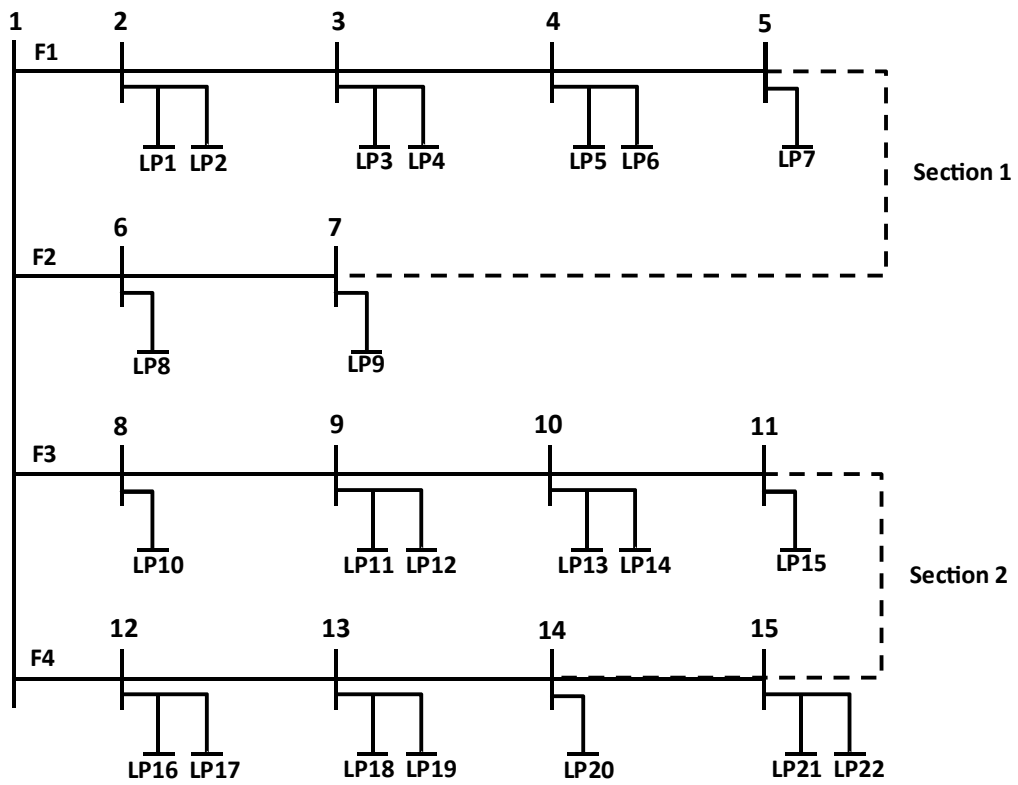

Figure 4.8 One line diagram RBTS-bus 2

DLF method finds the voltage at the distributed buses. However, to find the voltage at load point ends, additional equations are necessary. Current divider rule can provide a solution to find the voltage at each load point as shown in figure 4.9.
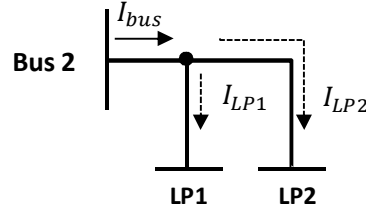

Figure 4.9 Schematic of a current divider circuit

I_{LP1} and I_{LP2} are calculated by the current divider rule as:

$$I_{LP1} = I_{bus} \frac{Z_{LP2}}{Z_{LP1} + Z_{LP2}} \tag{4.2}$$

$$I_{LP2} = I_{bus} \frac{Z_{LP1}}{Z_{LP1} + Z_{LP2}} \tag{4.3}$$

Then, the voltage at each load point is calculated by:

$$V_{LP1} = V_{bus} - (I_{LP2} * Z_{LP2}) \tag{4.4}$$

$$V_{LP2} = V_{bus} - (I_{LP1} * Z_{LP1}) \tag{4.5}$$

The preceding equations and DLF method are used to study the voltage profile of the system for the states of which the system is up to determine whether the system at those states has a voltage within the limit or not. If the voltage is under 0.95 pu or above 1.05 pu according to (ANSI C84.1), the state of the system will change from up to down. This study is applied to all load points in the RBTS-bus2. Result of DPF for LP1 is shown in table 4.7.

Table 4.7 DPF results for LP1 – case study 1

State number	State classification	Voltage at LP1	State after PF
7	MTS	0.9302 ↓	Down ↓
14	TS	0.9947	Up
15	TS	0.9947	Up
16	TS	0.9947	Up
17	TS	0.9947	Up
18	TS	0.9947	Up
19	TS	0.9908	Up
20	TS	0.9908	Up
21	TS	0.9908	Up
22	TS	0.9908	Up
23	TS	0.9871	Up
24	TS	0.9871	Up
25	TS	0.9871	Up
26	TS	0.9808	Up
27	TS	0.9766	Up
28	TS	0.9808	Up
29	TS	0.9883	Up

All the tested states in table 4.7 have a voltage within the limit at the connection point of LP 1, except for state number 7. It has a voltage less than the required standard, and so its state changed from up to down. At state 7, component 1 fails and it is isolated from the system as shown in figure 4.10. Only one main feeder (feeder 2) feeds the system after the isolation. This results in weak voltage at the end of the feeder. Voltage profile of the system for all load points in section one at state number 7 is illustrated in figure 4.11.

At this scenario, LP1 – to – LP6 have a voltage below 0.95 pu due to the weak voltage at the end of the line. The red points in figure 4.11 indicate the voltages under the limit. On the other hand, the remained load points have a voltage within the limit.
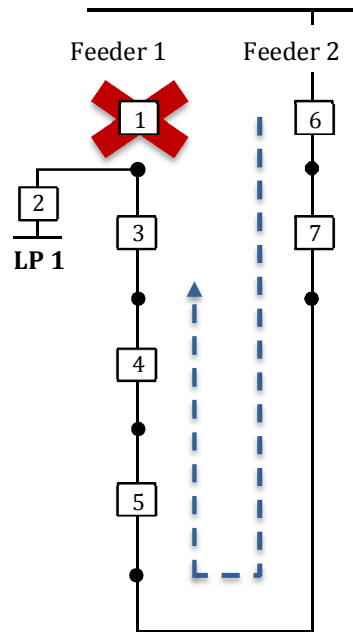
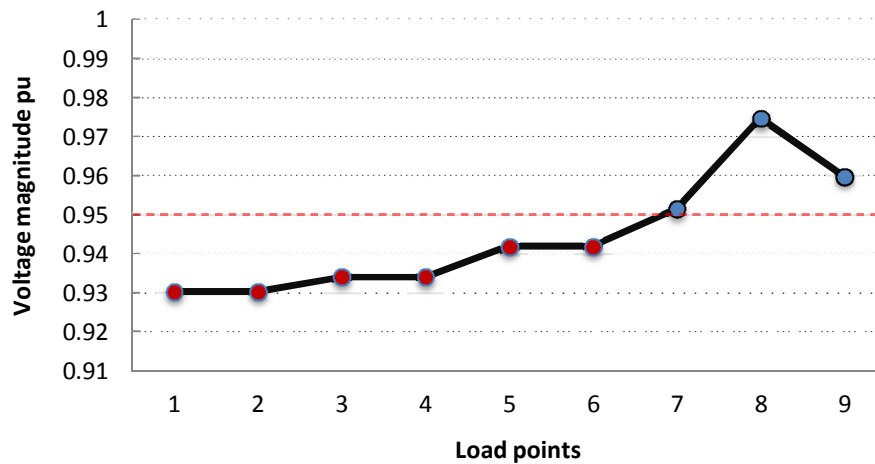**Figure 4.10 RBTS-bus 2 Section-1 state 7 after isolation**

Figure 4.11 Voltage profile of RBTS-bus2 section 1 at state 7

Each load point has different number of up states based on load point's location and connectivity to the source. The DPF is applied to all load point to reclassify those up states of the system. Table 4.8 shows the results of the DPF for load points at section one.

Shaded slots in the table represent the under voltages conditions. Based on the results of all load point, number of changed states from up to down at each load point is illustrated in figure 4.12.

Table 4.8 DPF results for all load poits at section 1 – case study 1

Up states	Voltage (pu) LP1 LP2	Voltage (pu) LP3 LP4	Voltage (pu) LP5 LP6	Voltage (pu) LP7	Voltage (pu) LP8	Voltage (pu) LP9
1	0.9302 ↓	0.9528	0.9566	0.9629	0.9791	0.9678
2	0.9947	0.9340 ↓	0.9707	0.9738	0.9834	0.9754
3	0.9947	0.9528	0.9419 ↓	0.9835	0.9872	0.9822
4	0.9947	0.9870	0.9707	0.9515	0.9929	0.9598
5	0.9947	0.9870	0.9566	0.9738	0.9746	0.9754
6	0.9947	0.9870	0.9707	0.9835	0.9834	0.9822
7	0.9908	0.9870	0.9759	0.9629	0.9872	0.9678
8	0.9908	0.9796	0.9759	0.9835	0.9929	0.9822
9	0.9908	0.9796	0.9759	0.9738	0.9791	0.9754
10	0.9908	0.9796	0.9576	0.9835	0.9872	0.9822
11	0.9871	0.9673	0.9452 ↓	0.9531	0.9929	0.9472 ↓
12	0.9871	0.9588	0.9576	0.9376 ↓	0.9834	0.9285 ↓
13	0.9871	0.9673	0.9794	0.9531	0.9929	0.9472 ↓
14	0.9808	0.9819		0.9804	0.9872	0.9801
15	0.9766				0.9261 ↓	
16	0.9808				0.9929	
17	0.9883				0.9860	

It is noticed from figure 4.12 that the further the load point located from the source, the more voltage violation occurs and the more state changes. When a fault takes place, the section that directly connected to the fault is isolated. This isolation could weaken the supplied voltage, especially when the network has high load rating and loads far from the source. In case study 2-5, this problem is overcome by installing DGs at different locations.
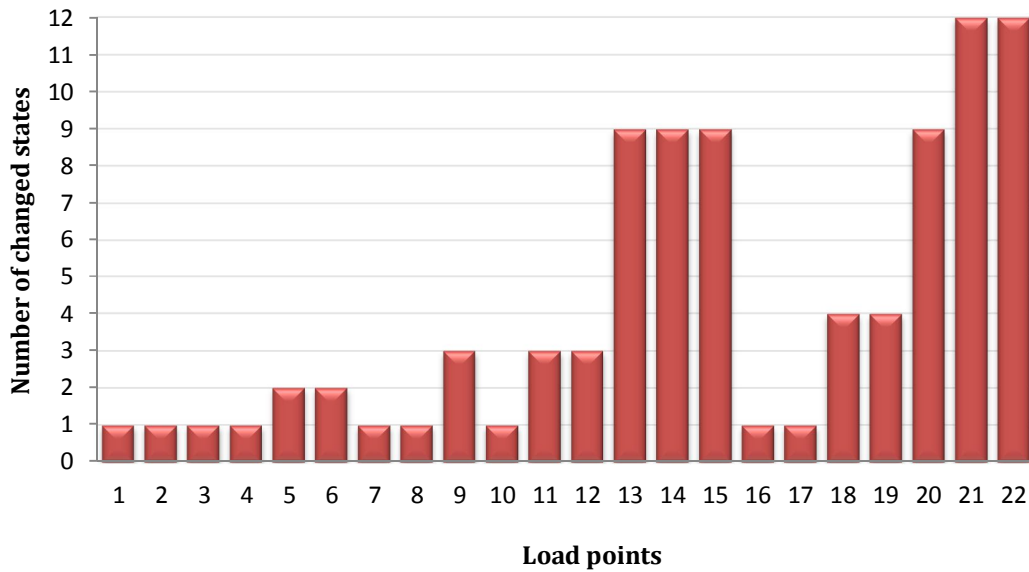
Figure 4.12 Changed states from up to down after the DPF

4.5.4 Reliability calculation using MM

After finding all the states for the system based on connectivity and transfer capability, MM is used to calculate reliability indices. As explained in chapter 2, transition matrix of the system is formed. Then, the Q matrix is found. After that, the Markov differential equation is solved to find all up and down probabilities. Lastly, load point indices and system reliability indices are computed by the equations in (2.7). Tables 4.9 and 4.10 show the load point indices and system indices respectively.

Figure 4.13 shows the availability and the unavailability. LP20 and LP21 have the lowest availability since they have the largest number of voltage violations and down states, as shown in figures 4.12. On the other hand, highest availability is at LP8 and LP9. These load points have small users and connected directly to the main substation without any

transformers, which makes them have lower interruption duration and frequency duration. Figure 4.14 shows the AID and FD for all load points. AID measures the duration that the system is unavailable and it is directly related to the unavailability. AIF and MTTF are shown in figure 4.15. AIF measures the frequency of failing and it is related to the number of down states of the system. MTTF is approximately the reciprocal of the AIF. The ENS is also shown in figure 4.16. ENS is equal to the load power multiplied by the AID at each load point. Higher availability and MTTF indicate higher reliability. Higher unavailability, AID, FD, AIF, and ENS reflect lower reliability.

Table 4.9 Load point reliability indices for all load points – case study 1

Load Points	A	U	MTTF (y)	AIF (f/y)	AID (h/y)	FD (h/f)	ENS (MWh/y)
1	0.999608	0.000392	9.732646	0.102710	3.437556	33.468668	1.839093
2	0.999600	0.000400	8.639594	0.115704	3.502529	30.271531	1.873852
3	0.999600	0.000400	4.319228	0.115713	3.502546	30.269130	1.873862
4	0.999608	0.000392	4.865616	0.102719	3.437574	33.465659	1.945667
5	0.999572	0.000428	3.039591	0.164438	3.746172	22.781622	2.120333
6	0.999574	0.000426	3.100846	0.161190	3.729929	23.139951	1.693388
7	0.999600	0.000400	8.638827	0.15712	3.502544	30.269506	1.590155
8	0.999942	0.000058	9.925844	0.100744	0.503728	5.000072	0.503728
9	0.999920	0.000080	7.155921	0.139734	0.698713	5.000132	0.803520
10	0.999608	0.000393	9.732646	0.102710	3.437556	33.468668	1.839093
11	0.999572	0.000428	6.079313	0.164430	3.746174	22.782840	2.004203
12	0.999571	0.000429	5.961537	0.167678	3.762417	22.438353	1.693088
13	0.999520	0.000480	1.957277	0.255377	4.200942	16.449931	2.377733
14	0.999519	0.000481	1.932696	0.258625	4.217184	16.306144	2.386926
15	0.999498	0.000502	1.698059	0.294357	4.395832	14.933670	1.995708
16	0.999600	0.000400	8.639594	0.115704	3.502529	30.271531	1.590148
17	0.999606	0.000394	9.434248	0.105958	3.453799	32.595864	1.554210
18	0.999550	0.000450	2.457360	0.203408	3.941055	19.375081	1.773475
19	0.999543	0.000457	2.309820	0.216401	4.006024	18.512041	1.802711
20	0.999485	0.000515	1.576393	0.317087	4.509517	14.221717	2.552387
21	0.999465	0.000535	1.416747	0.352813	4.688177	13.287985	2.653508
22	0.999463	0.000537	1.403825	0.356061	4.704418	13.212399	2.135806

Table 4.10 System reliability indices – case study 1

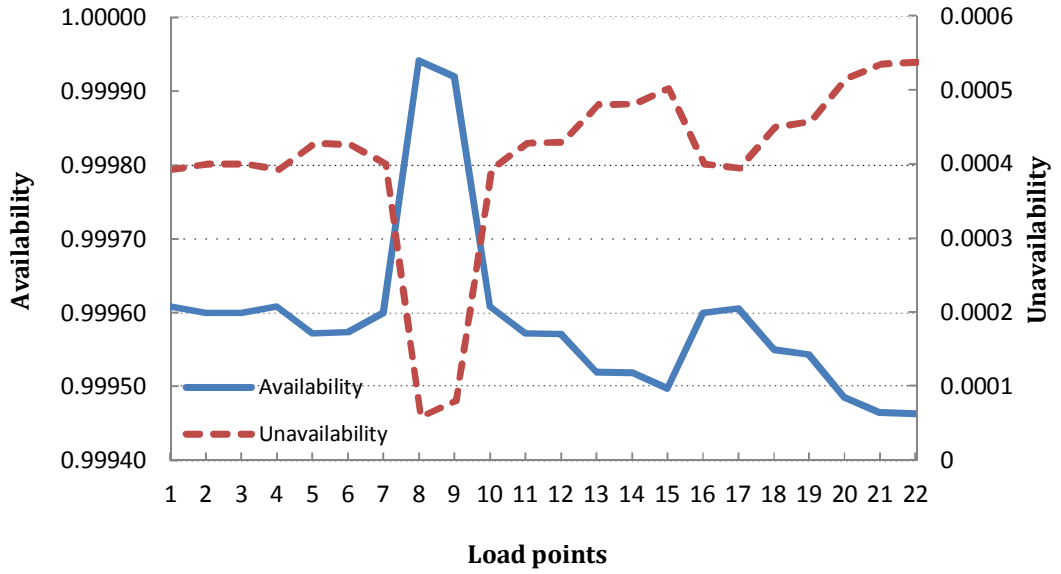| SAIFI (f/c.y)	SAIDI (h/c.y)	CAIDI (h/f)	ASAI	ASUI	ENS (MWh/y)	AENS (MWh/c.y)
0.145218	3.647039	25.114154	0.999584	0.000416	40.602592	0.021280

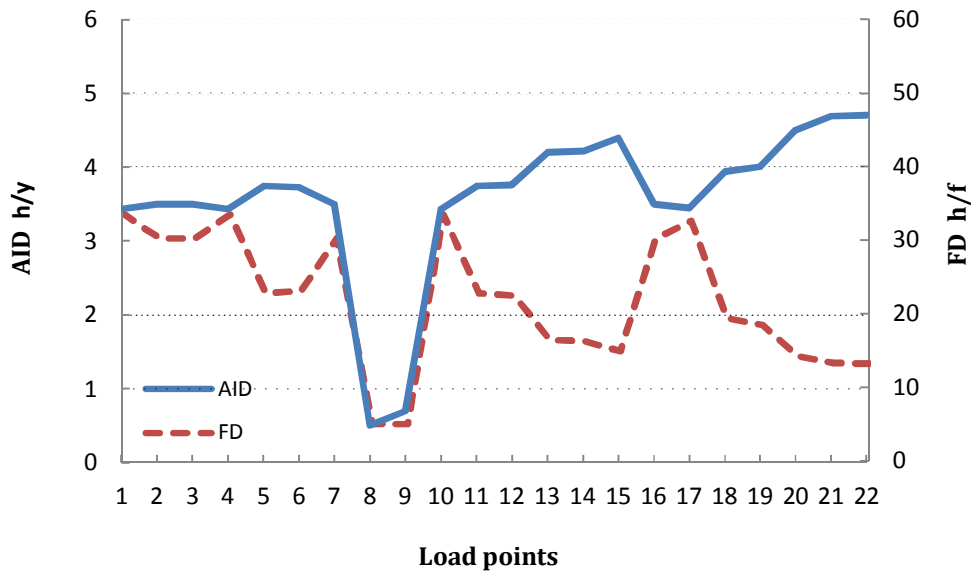Figure 4.13 Availability and unavailability - case study 1

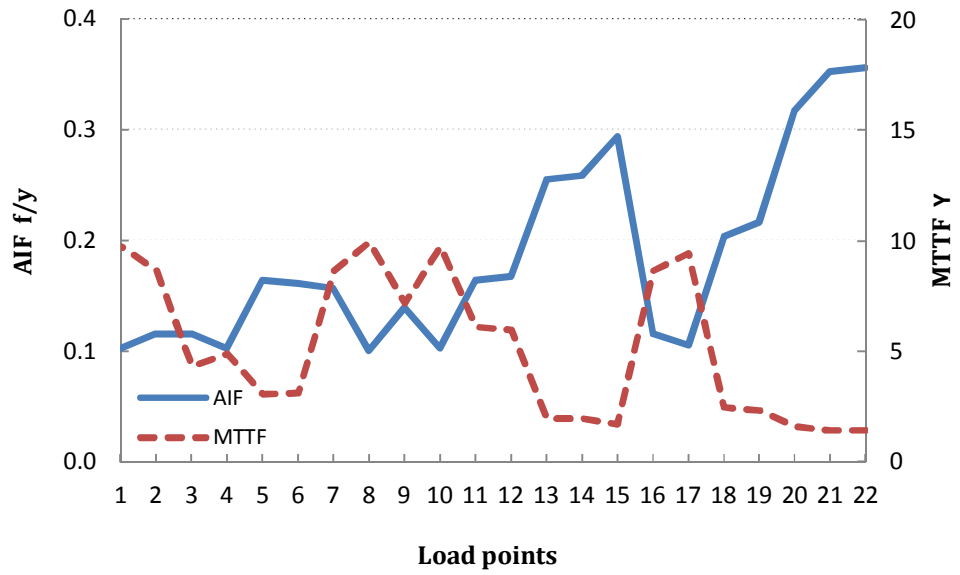Figure 4.14 AID and FD - case study 1

71

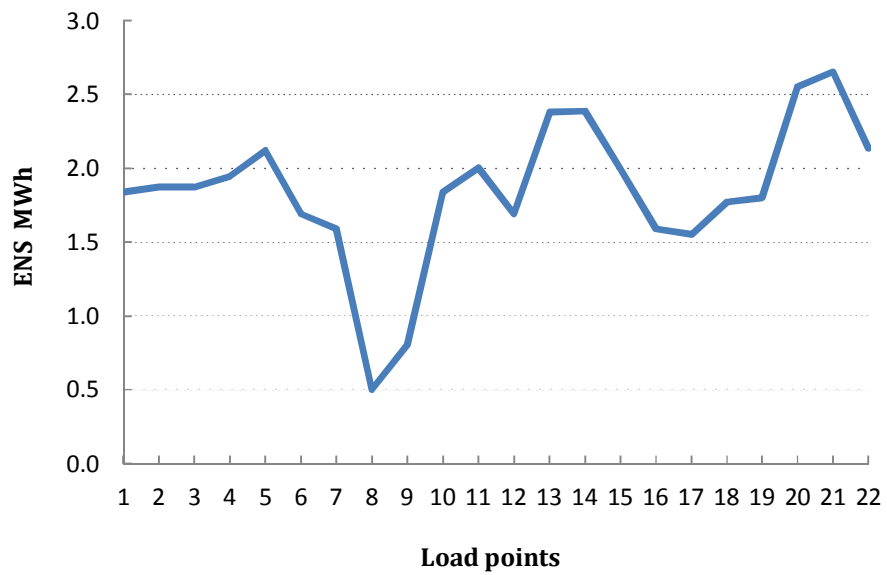**Figure 4.15 AIF and MTTF - case study 1**

Figure 4.16 ENS - case study 1

4.5.5 Accuracy Improvement of Reliability Calculation

In reference [31], reliability of the RBTS-bus2 was evaluated using MM. The number of components and states of the system were reduced by the same techniques used in this thesis. The states were identified based on the connectivity between the source and loads of the system. Then, the reliability indices were computed. The transfer capability of the voltage was not considered in [31]. Figure 4.17 shows a comparison between the availability of case study 1 and reference [31]. AIF of case study 1 and reference [31] is shown in figure 4.18. Table 4.11 shows a comparison between system reliability indices of case study 1 and reference [31].
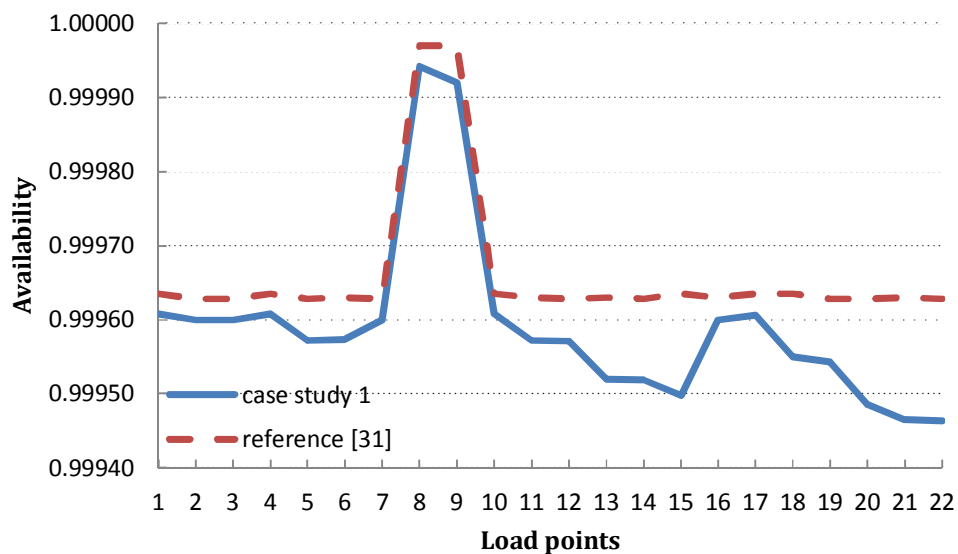

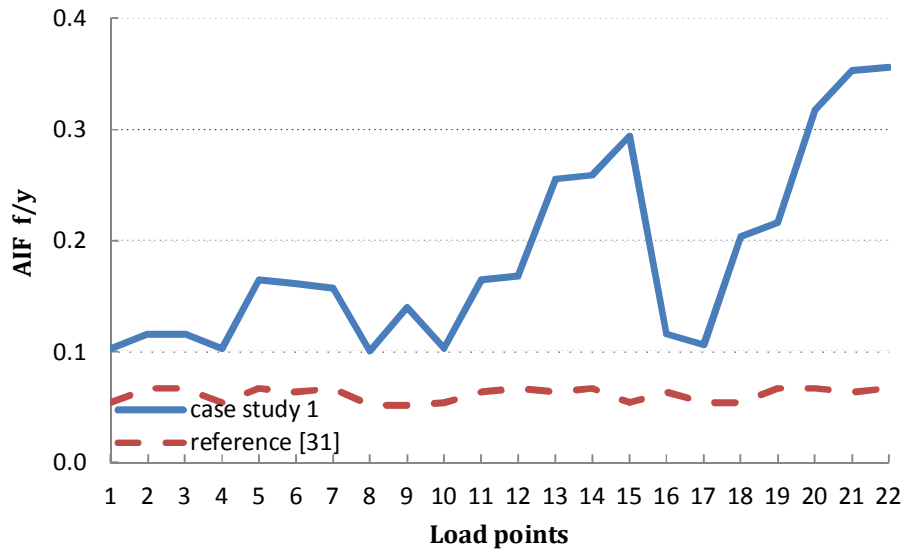**Figure 4.17 Availability of case study 1 and reference [31]**

Figure 4.18 AIF of case study 1 and reference [31]

Table 4.11 System reliability indices of case study 1 and reference [31]

	SAIFI (f/c.y)	SAIDI (h/c.y)	ASAI	ENS (MWh/y)
Case study 1	0.145218	3.647039	0.999584	40.602592
Reference [31]	0.060928	3.225517	0.999632	33.371922
Accuracy improvement of case study 1	58.04%	11.56%	0.005%	17.81%

Figures 4.17 and 4.18 show that reference [31] provides higher values of availability and lower values of AIF than case study 1. Furthermore, computed ASAI in [31] is higher and computed SAIFI, SAIDI, and ENS are lower than case study 1. This indicates that reference [31] provides results of higher level of reliability. However, these calculations are not very accurate since they are based only on the factor of connectivity, without considering the impact of voltage violations on the reliability. Case study 1 has more accurate results due to the inclusion of transfer capability of the system in addition to the connectivity. The reliability in case study 1 is lower because of voltage violations.

4.6 Case Study 2: RBTS-Bus2 with PQ-DG at Bus 3 and 9

After applying the DPF to the RBTS-bus2 system, a considerable number of states change from up to down as a result of weak supplied voltage as shown in figure 4.12. These changes affect the reliability of the system undesirably. DGs are used to improve the voltage profile of the system, and therefore improve the reliability.

In case study 2, two DGs are used at the middle of the feeder 1 (bus 3) and feeder 3 (bus 9) as shown in figure 4.19. DGs at this case are modeled as a PQ bus with fixed amount of power. They provide an active power of 200 KW and reactive power of 150 Kvar.

4.6.1 Reclassifying Process Based on Transfer Capability

The reduction and classification based on connectivity processes are the same as case study 1 because there is no any change in the topology of the system. However, after including two DGs, the DPF must be run again. The two DGs are modelled as P-Q units with producing power of 200 KW and 0.8 power factor. The DLF method with the equations for DG in chapter 3 is applied to the RBTS-bus 2 for all load points. Result of DPF for LP1 is shown in table 4.12.
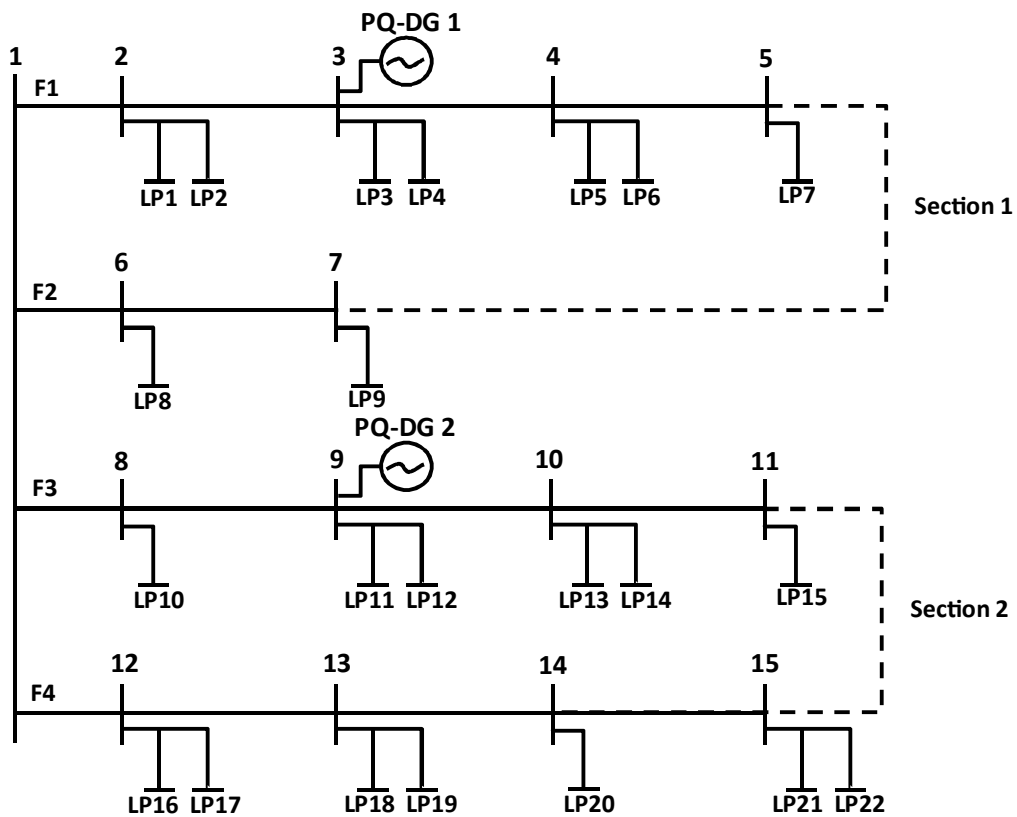
Figure 4.19 One line diagram RBTS-bus 2 with two PQ-DGs – case study 2

Table 4.12 shows that the voltage profile noticeably gets improved by the contribution of the DGs. Voltage at LP1 in state number 7 gets raised from 0.9302 pu to 0.9580 pu, and so its state changes from down to up. States number 19-29 also get enhanced, but they already are up states.

Table 4.12 DPF results for LP1 – case study 2

| State number	State classification	Voltage at LP1 before DG	Voltage at LP1 after DG	State after PF
7	MTS	0.9302	0.9580 ⬆	UP ⬆
14	TS	0.9947	0.9947	Up
15	TS	0.9947	0.9947	Up
16	TS	0.9947	0.9947	Up
17	TS	0.9947	0.9947	Up
18	TS	0.9947	0.9947	Up
19	TS	0.9908	0.9965 ⬆	Up
20	TS	0.9908	0.9965 ⬆	Up
21	TS	0.9908	0.9965 ⬆	Up
22	TS	0.9908	0.9965 ⬆	Up
23	TS	0.9871	0.9929 ⬆	Up
24	TS	0.9871	0.9929 ⬆	Up
25	TS	0.9871	0.9929 ⬆	Up
26	TS	0.9808	0.9869 ⬆	Up
27	TS	0.9766	0.9828 ⬆	Up
28	TS	0.9808	0.9869 ⬆	Up
29	TS	0.9883	0.9922 ⬆	Up
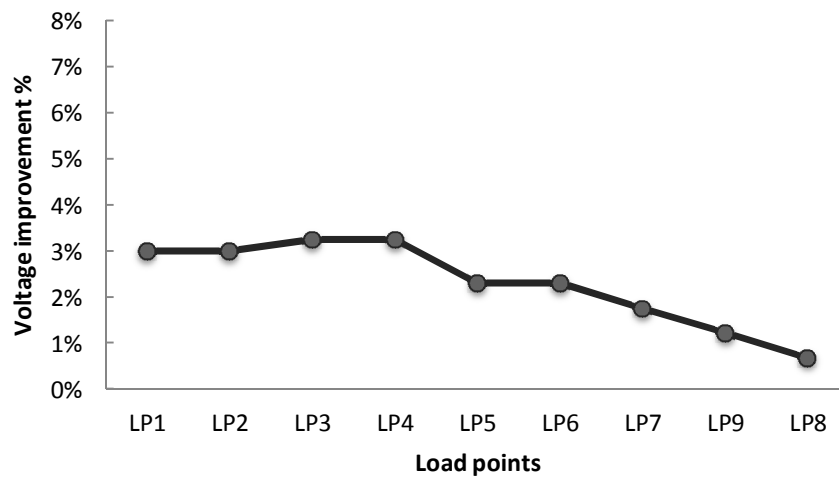
Figure 4.20 Voltage improvement at state 7 due to DGs – case study 2

DPF is applied to all load point at case study 2 to obtain the system's voltages with the DGs. Figure 4.20 shows the improvement of voltage profile at state 7 in section 1. The

improvement has a range between 0.67% and 3.25%. The maximum improvement is at LP3 and LP4 since they are connected to bus 3 where the DG installed at section 1. Some states that were down as a result of weak voltage change now to up states due to the voltage enhancement. On the other hand, all other down states that based on connectivity remain down since the network structure has no modifications. Numbers of states that change from down to up due to the contribution of the DGs at case study 2 are given in figure 4.21.
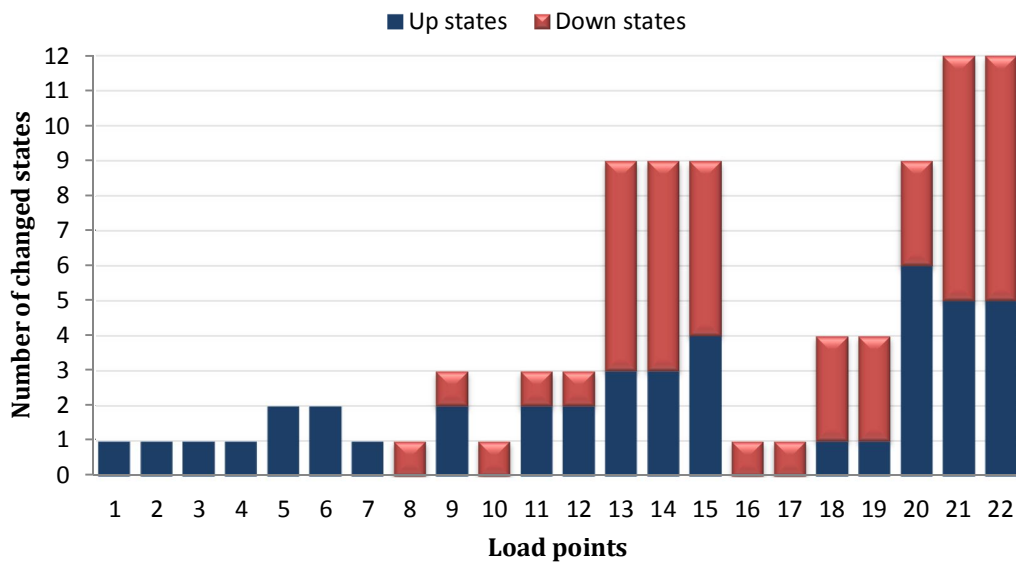

Figure 4.21 Changed states from down to up after DGs – case study 2

4.6.2 Reliability calculation using MM

Installing the DGs increases the number of up states for the system. Subsequently, the reliability of the system gets improved. MM is used again to calculate the load point indices and reliability system indices after updating the states of the system. Tables 4.13 and 4.14 show the load point indices and system indices respectively.

Table 4.13 Load point reliability indices for all load points – case study 2

Load Points	A	U	MTTF (y)	AIF (f/y)	AID (h/y)	FD (h/f)	ENS (MWh/y)
1	0.999635	0.000365	18.511872	0.053993	3.193933	59.154812	1.708754
2	0.999628	0.000372	14.920685	0.066988	3.258907	48.649451	1.743515
3	0.999628	0.000372	14.919815	0.066995	3.258925	48.644594	1.743525
4	0.999635	0.000365	18.510256	0.054000	3.193951	59.147416	1.807776
5	0.999628	0.000372	14.919868	0.066996	3.258929	48.643473	1.844554
6	0.999630	0.000370	15.680222	0.063748	3.242686	50.867610	1.472179
7	0.999628	0.000372	14.920780	0.066994	3.258923	48.645267	1.479551
8	0.999942	0.000058	9.925844	0.100744	0.503728	5.000072	0.503728
9	0.999942	0.000058	9.924864	0.100752	0.503743	4.999813	0.579305
10	0.999608	0.000392	9.732646	0.102710	3.437556	33.468668	1.839093
11	0.999602	0.000398	4.443472	0.112472	3.486319	30.997327	1.865181
12	0.999600	0.000400	4.318734	0.115720	3.502562	30.267536	1.576153
13	0.999550	0.000450	4.914290	0.203408	3.941087	19.375237	2.230655
14	0.999548	0.000452	4.837045	0.206657	3.957329	19.149299	2.239848
15	0.999556	0.000444	2.580609	0.193680	3.892359	20.096899	1.767131
16	0.999600	0.000400	8.639594	0.115704	3.502529	30.271531	1.590148
17	0.999606	0.000394	9.434248	0.105958	3.453799	32.595864	1.554210
18	0.999578	0.000422	6.462321	0.154685	3.697446	23.903119	1.663851
19	0.999571	0.000429	5.961537	0.167678	3.762417	22.438353	1.693088
20	0.999570	0.000430	5.960972	0.167691	3.762435	22.436765	2.129538
21	0.999522	0.000478	1.982330	0.252140	4.184701	16.596763	2.368541
22	0.999520	0.000480	1.957119	0.255388	4.200943	16.449285	1.907228

Table 4.14 System reliability indices – case study 2

SAIFI	SAIDI	CAIDI	ASAI	ASUI	ENS (MWh/y)	AENS (MWh/y)
0.105649	3.449167	32.647380	0.999606	0.000394	37.307552	0.019553

The availability and unavailability are shown in figure 4.22. The DGs improve the voltage profile of the system. As a result, the number of down states gets reduced and the reliability gets enhanced. Figure 4.23 shows the AID and FD. The AIF and MTTF are shown in figure 4.24. ENS is also shown in figure 4.25.
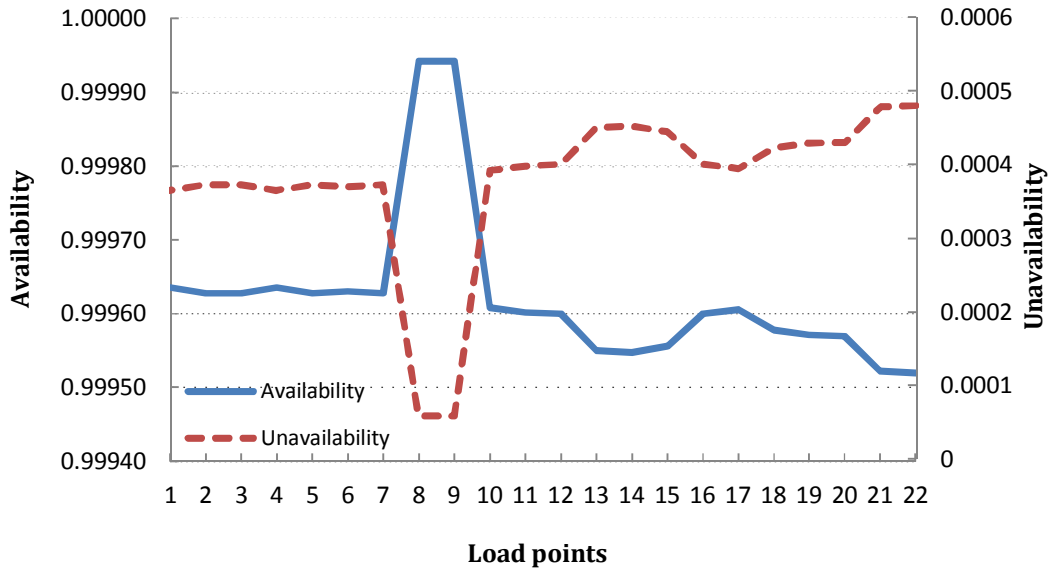
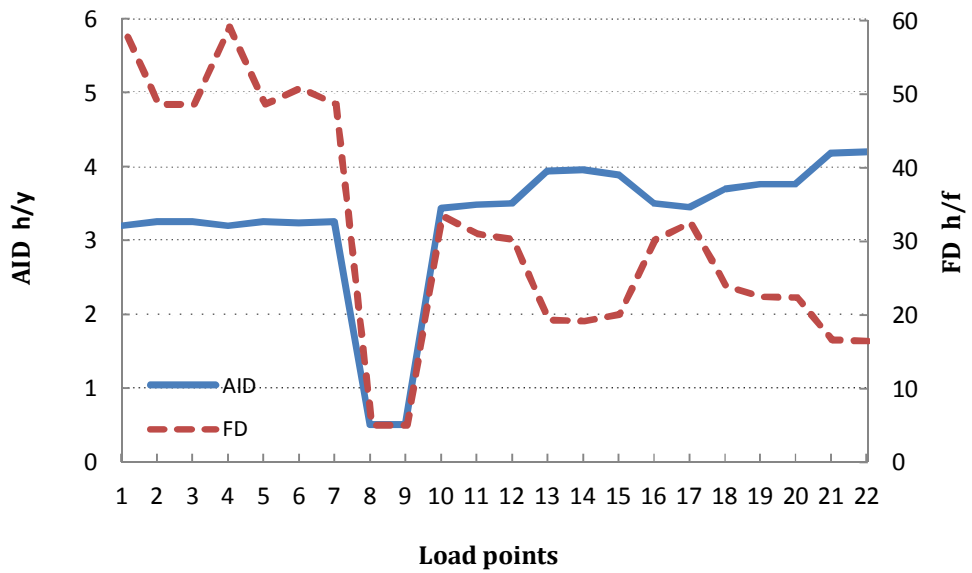**Figure 4.22 Availability and unavailability - case study 2**
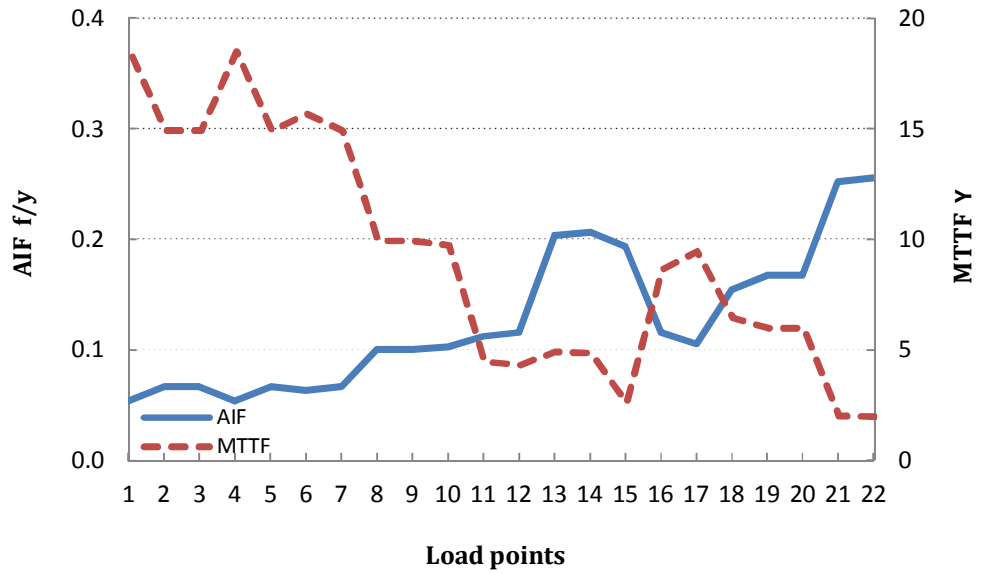

Figure 4.23 AID and FD - case study 2

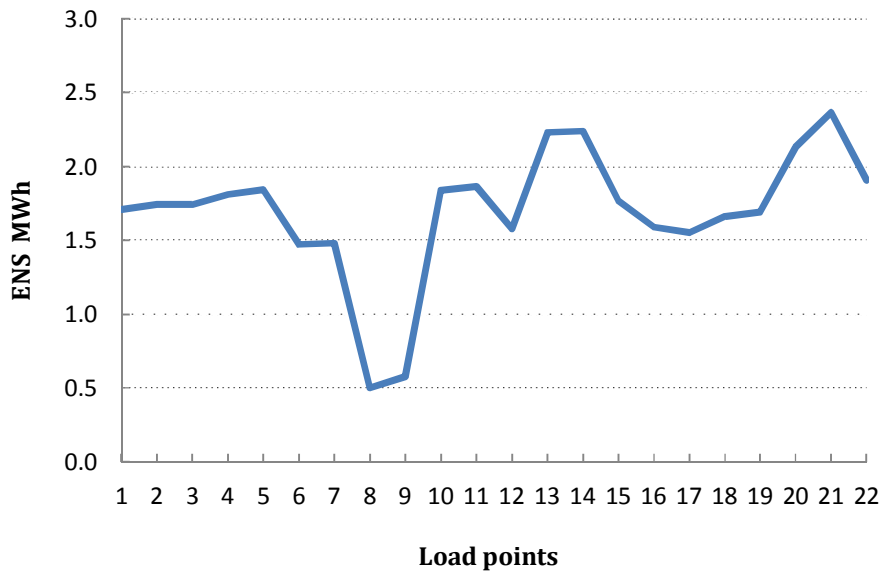**Figure 4.24 AIF and MTTF - case study 2**

Figure 4.25 ENS - case study 2

4.7 Case Study 3: RBTS-Bus2 with PQ-DG at Bus 5 and 15

In this case, two PQ-DGs with the same size as case study 2, are installed at different buses in order to study the effect of the location of DG on voltage profile and reliability. The DGs are located at the end of the feeder 1 (bus 5) and feeder 4 (bus 15) as shown in figure 4.26.
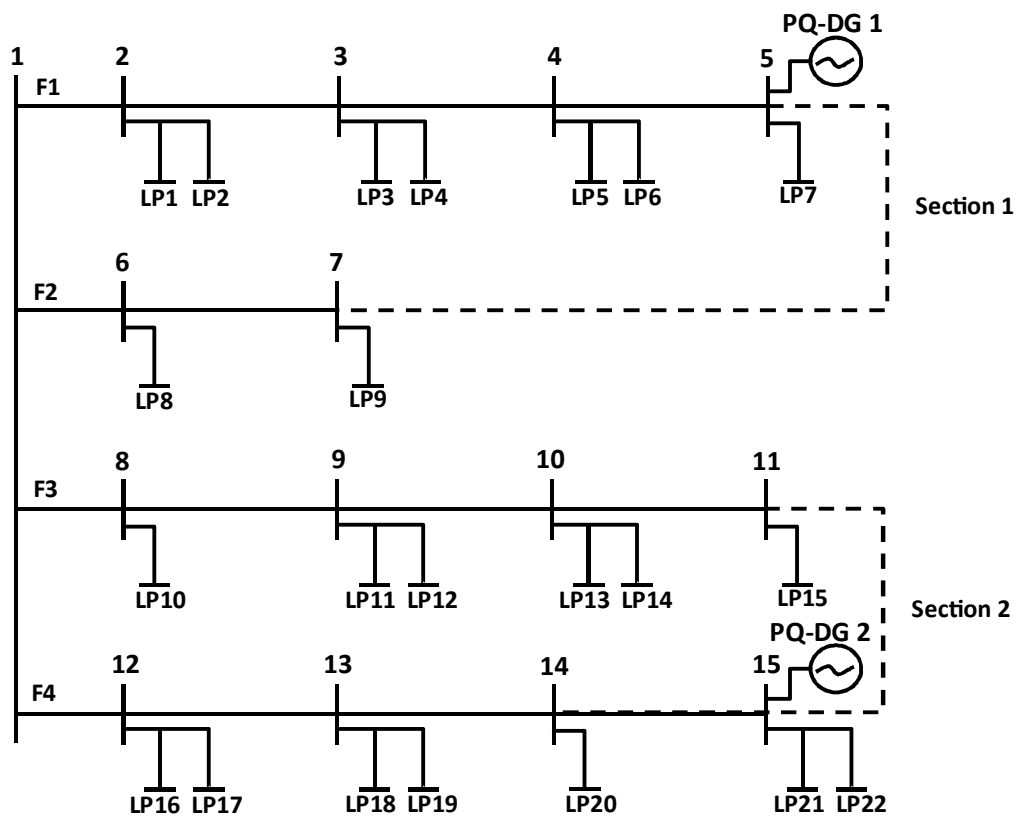

Figure 4.26 One line diagram RBTS-bus 2 with two DGs – case study 3

4.7.1 Reclassifying Process Based on Transfer Capability

Installing the DGs at the end of the line changes the shape of the voltage improvement. Table 4.15 shows the voltage magnitudes of LP1 before and after installing the DGs at bus 5 and 9. Although voltage profile gets improved at states 7 and 26-29, state 7 still down since the voltage remains below 0.95 pu. Figure 4.27 shows the voltage improvement at state 7 for all load points at section 1. The improvement extends from 0.64% to 2.33%, which is less than case study 2 at this particular scenario. Maximum improvement occurs at LP7 since it is connected to bus 5.

Table 4.15 DPF results for LP1 – case study 3

| State number	State classification	Voltage at LP1 before DG	Voltage at LP1 after DG	State after PF
7	MTS	0.9302	0.9466	Down
14	TS	0.9947	0.9947	Up
15	TS	0.9947	0.9947	Up
16	TS	0.9947	0.9947	Up
17	TS	0.9947	0.9947	Up
18	TS	0.9947	0.9947	Up
19	TS	0.9908	0.9908	Up
20	TS	0.9908	0.9908	Up
21	TS	0.9908	0.9908	Up
22	TS	0.9908	0.9908	Up
23	TS	0.9871	0.9871	Up
24	TS	0.9871	0.9871	Up
25	TS	0.9871	0.9871	Up
26	TS	0.9808	0.9871 ⬆	Up
27	TS	0.9766	0.9831 ⬆	Up
28	TS	0.9808	0.9871 ⬆	Up
29	TS	0.9883	0.9907 ⬆	Up
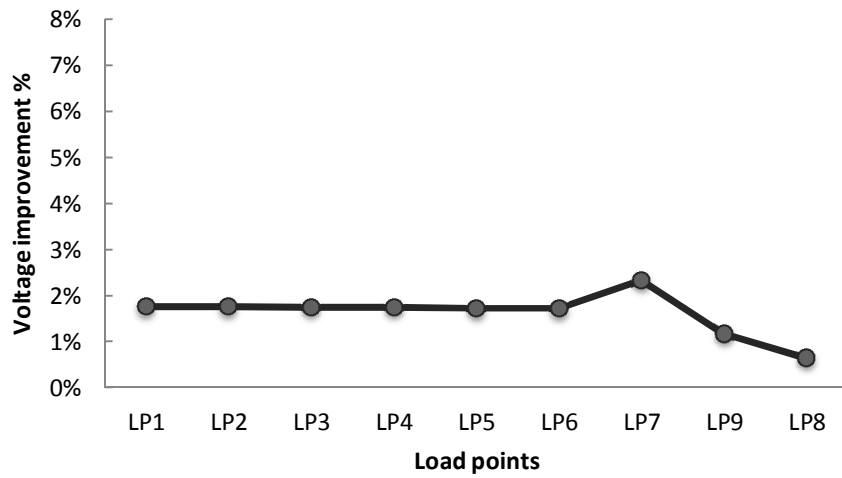
Figure 4.27 Voltage improvement at state 7 due to DGs – case study 3

At case study 3, DPF is applied to all load point to obtain the system's voltages, which leads to more accurate reliability assessment. The states of the system are updated after the DPF calculation. All states that have voltages within the limit are up. Otherwise, they are considered as down state. Figure 4.28 shows how many states change from down to up due to the integration with DGs.
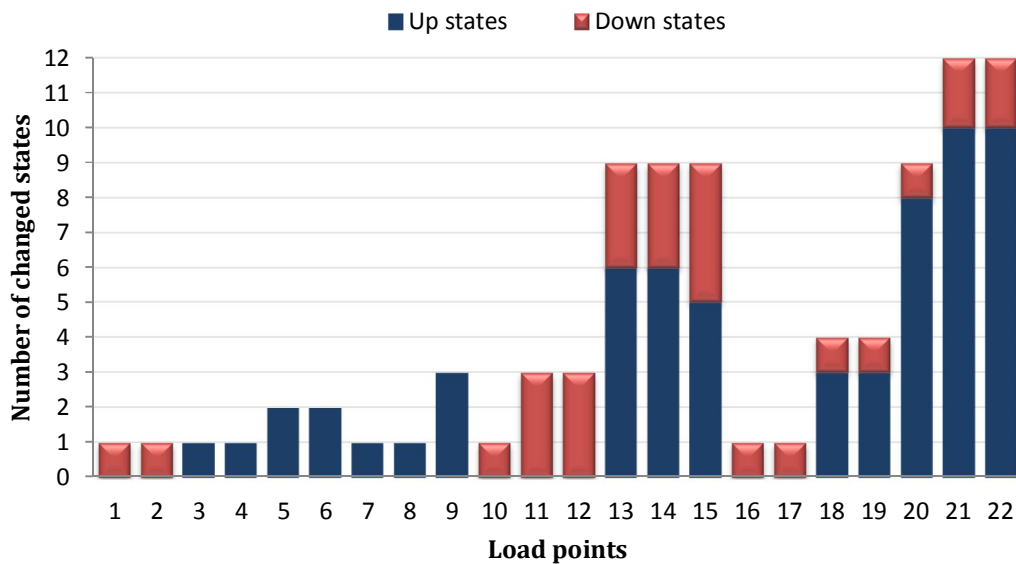

Figure 4.28 Changed states from down to up after DGs – case study 3

4.7.2 Reliability calculation using MM

After updating the states of the system, the load point and reliability system indices are calculated as shown in table 4.16 and 4.17.

Table 4.16 Load point reliability indices for all load points – case study 3

Load Points	A	U	MTTF (y)	AIF (f/y)	AID (h/y)	FD (h/f)	ENS (MWh/y)
1	0.999608	0.000392	9.732646	0.102710	3.437556	33.468668	1.839093
2	0.999600	0.000400	8.639594	0.115704	3.502529	30.271531	1.873853
3	0.999628	0.000372	14.919815	0.066995	3.258925	48.644594	1.743525
4	0.999635	0.000365	18.510256	0.054000	3.193951	59.147416	1.807776
5	0.999628	0.000372	14.919868	0.066996	3.258929	48.643473	1.844554
6	0.999630	0.000370	15.680222	0.063748	3.242686	50.867610	1.472179
7	0.999628	0.000372	14.920780	0.066994	3.258923	48.645267	1.479551
8	0.999970	0.000030	19.225907	0.052011	0.260023	4.999400	0.260023
9	0.999970	0.000030	19.223234	0.052017	0.260039	4.999108	0.299044
10	0.999608	0.000392	9.732646	0.102710	3.437556	33.468668	1.839093
11	0.999572	0.000428	6.079313	0.164430	3.746174	22.782840	2.004203
12	0.999571	0.000429	5.961537	0.167678	3.762417	22.438353	1.693088
13	0.999572	0.000428	3.039301	0.164440	3.746190	22.781470	2.120343
14	0.999570	0.000430	2.980426	0.167689	3.762432	22.437031	2.129537
15	0.999548	0.000452	2.418440	0.206670	3.957318	19.147978	1.796622
16	0.999600	0.000400	8.639594	0.115703	3.502529	30.271531	1.590148
17	0.999606	0.000394	9.434248	0.105958	3.453799	32.595864	1.554210
18	0.999606	0.000394	9.432682	0.105974	3.453830	32.591432	1.554224
19	0.999598	0.000402	8.402379	0.118968	3.518803	29.577835	1.583461
20	0.999598	0.000402	8.401494	0.118978	3.518821	29.575511	1.991652
21	0.999572	0.000428	3.039276	0.164451	3.746189	22.779915	2.120343
22	0.999570	0.000430	2.980404	0.167700	3.762432	22.435529	1.708144

Table 4.17 System reliability indices – case study 3

SAIFI	SAIDI	CAIDI	ASAI	ASUI	ENS (MWh/y)	AENS (MWh/y)
0.116771	3.504786	30.014170	0.999600	0.000400	36.304666	0.019028

In this case, the reliability get improved due to the DGs. However, the improvement is more at the end of the system. The reason for that, is the capacity and the location of the DGs. They are located at the end of the feeders, and the power capacity is not large enough to affect the entire system. Therefore, most of the impact occurs at the end of the lines. Figure 4.29 shows the Availability and Unavailability. The AID and FD are shown in figure 4.30. The AIF and MTTF are shown in figure 4.31. Figure 4.32 shows the ENS.
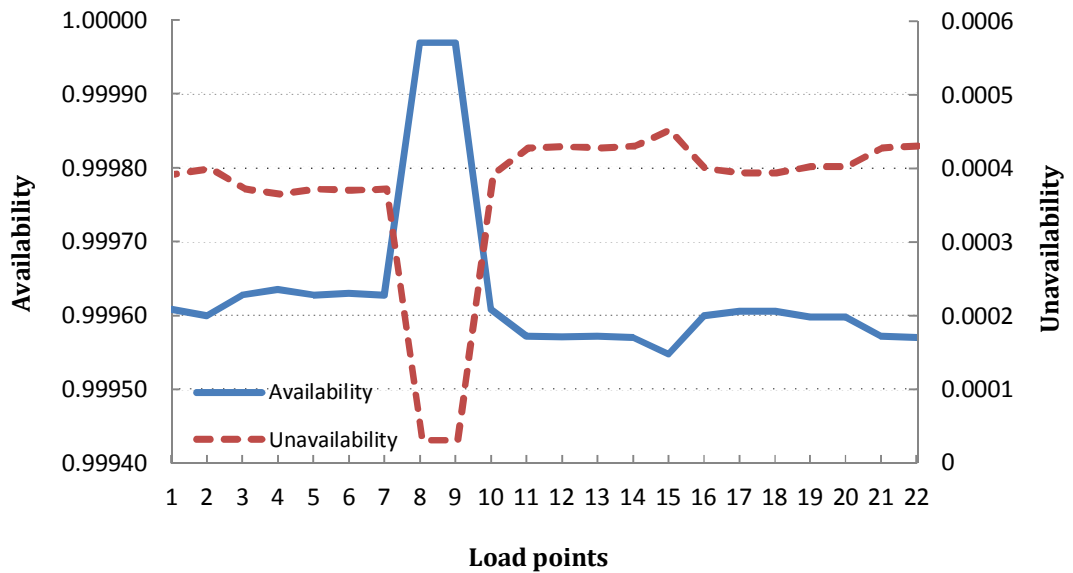

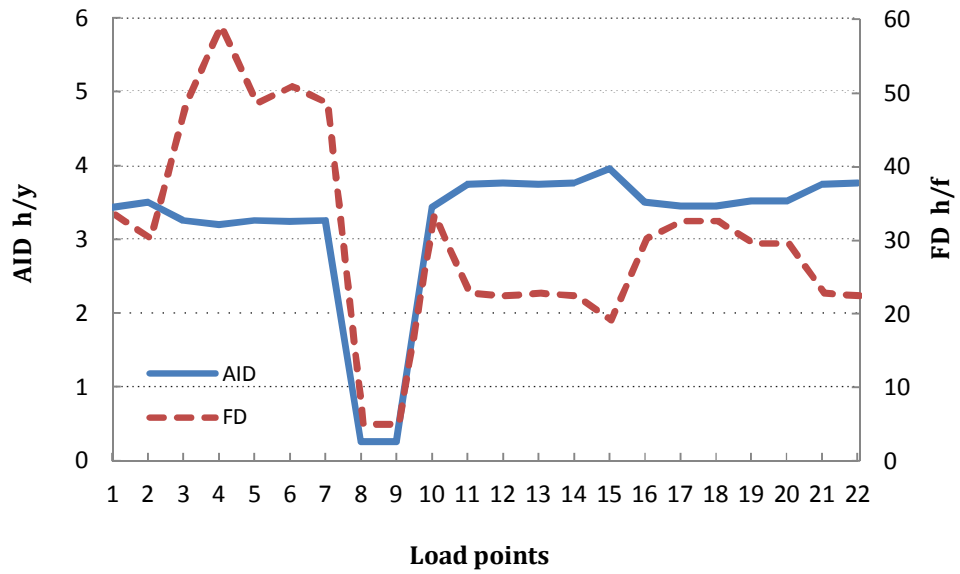**Figure 4.29 Availability and unavailability - case study 3**
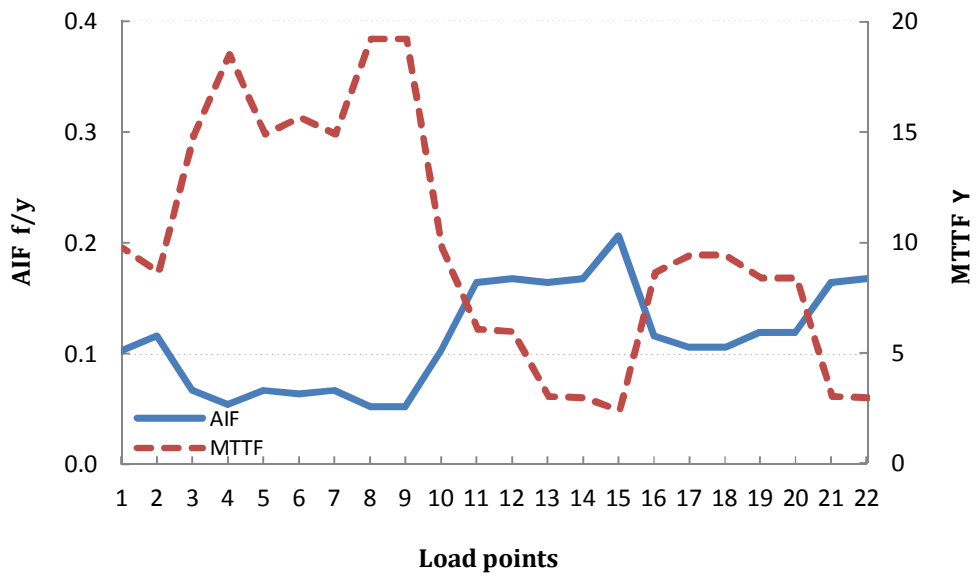
Figure 4.30 AID and FD - case study 3

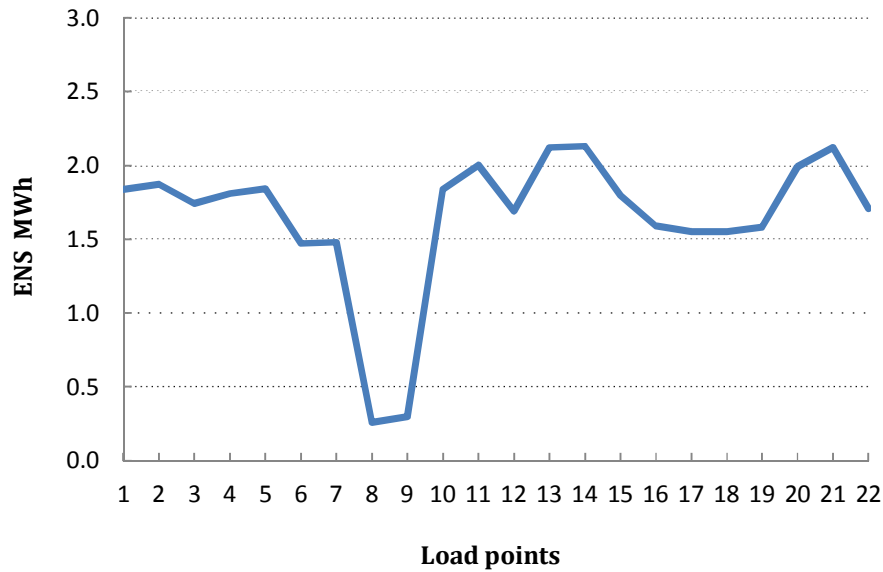**Figure 4.31 AIF and MTTF - case study 3**

87

Figure 4.32 ENS - case study 3

4.8 Case Study 4: RBTS-Bus2 with PV-DG at Bus 3 and 9

In case study 2 and 3, the DGs generate a constant power of 200 KW and 150 Kvar to enhance the power performance of the system. The factor of location was studied by installing the DGs in different buses. Size of DG is another essential factor that could affect the performance of the DG and power system. At this case, two DGs are included and modeled as a PV bus. One DG is installed at bus 3, and the other at bus 9 as shown in figure 4.33. The voltage at these buses is set to 1 pu, and the maximum generated active power is 800 kW to maintain the voltage at the desired value.
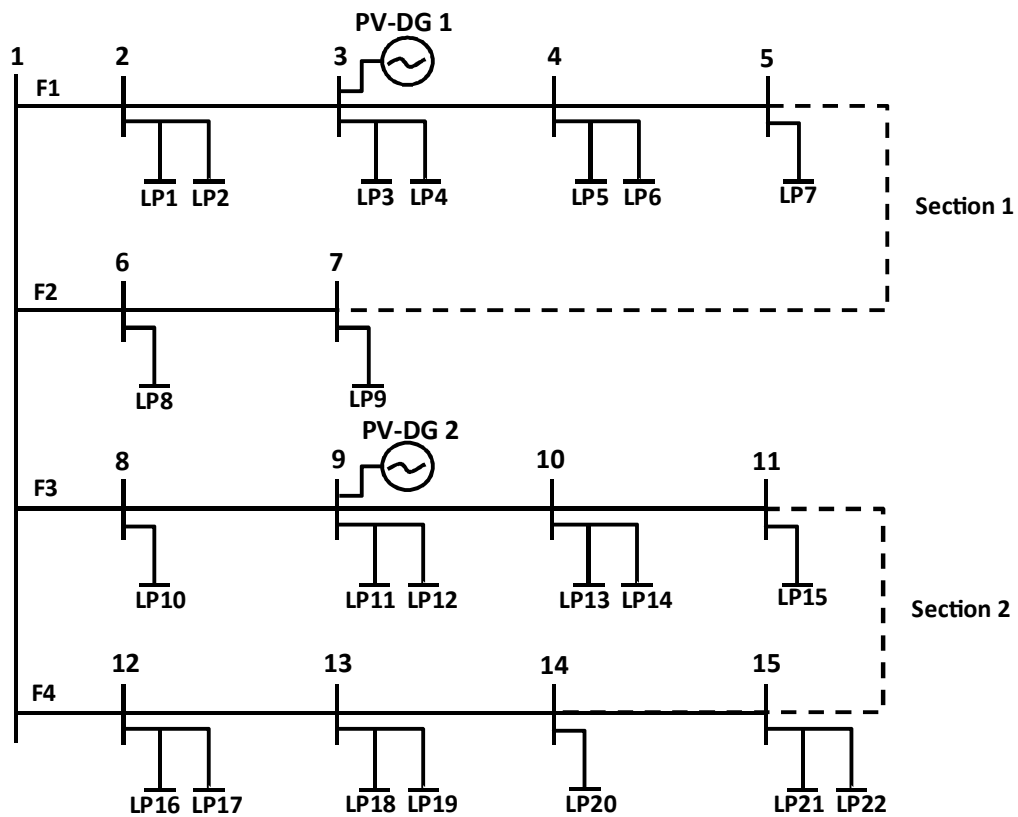
Figure 4.33 One line diagram RBTS-bus 2 with two DGs - case study 4

4.8.1 Reclassifying Process Based on Transfer Capability

In case study 4, two DGs are installed at buses 3 and 9 with controlling the voltage at these buses. To maintain the voltage of bus 3 and 9 at 1 pu, DGs must provide more power than the preceding cases. Generated active power is in the range of 800-400 kW based on the size of the system after isolation, while reactive power is changeable. Table 4.18 shows the results of DPF for LP1 at case study 4.

Number of states for LP1 that get improved is increased due to the enlarging the capacity of DGs. States 7 and 19-29 get raised above 0.99 pu as shown in table 4.18. The voltage of LP1 bus for all states is either 0.9947 pu or 0.9965 pu. That is because bus 2 is always connected to a bus with fixed voltage of 1 pu (either bus 1 or bus 3).

Table 4.18 DPF results for LP1 – case study 4

| State number	State classification	Voltage at LP1 before DG	Voltage at LP1 after DG	State after PF
7	MTS	0.9302	0.9947 ↑	UP ↑
14	TS	0.9947	0.9947	Up
15	TS	0.9947	0.9947	Up
16	TS	0.9947	0.9947	Up
17	TS	0.9947	0.9947	Up
18	TS	0.9947	0.9947	Up
19	TS	0.9908	0.9965↑	Up
20	TS	0.9908	0.9965↑	Up
21	TS	0.9908	0.9965↑	Up
22	TS	0.9908	0.9965↑	Up
23	TS	0.9871	0.9965↑	Up
24	TS	0.9871	0.9965↑	Up
25	TS	0.9871	0.9965↑	Up
26	TS	0.9808	0.9965↑	Up
27	TS	0.9766	0.9965↑	Up
28	TS	0.9808	0.9965↑	Up
29	TS	0.9883	0.9965↑	Up
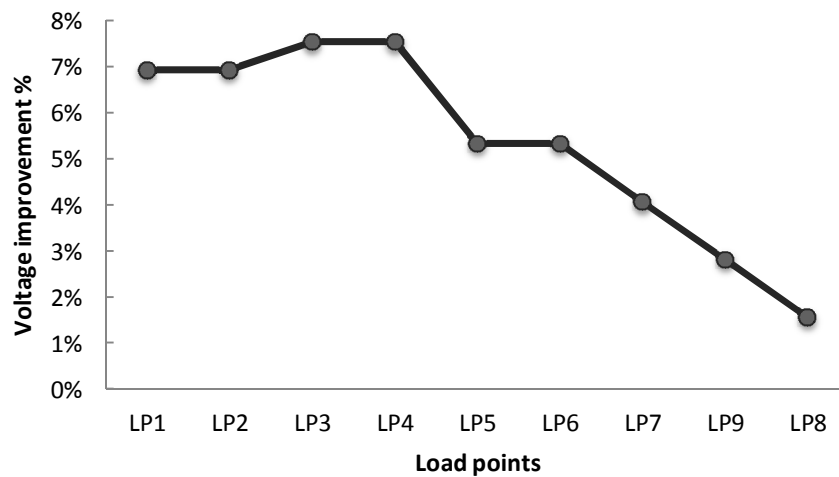
Figure 4.34 Voltage improvement at state 7 due to DGs – case study 4

Figure 4.34 shows the improvement of the voltage for all load points at state 7 due to the

PV-DGs. The improvement is greater than the previous cases since the DGs provide more

power (800 kW). Maximum voltage enhancement occurs at LP3 and LP4 by 7.55 %, whereas 1.56 % is the minimum improvement at LP8.

Numbers of states that change from down to up at this case are more than case 2 and 3, due to the contribution of the PV-DGs. Figure 4.33 shows that only LP16 and LP17 at bus 6 have no changed state as a result of weak voltage improvement at this particular bus. The remained buses have enough improvement to affect the states positively.
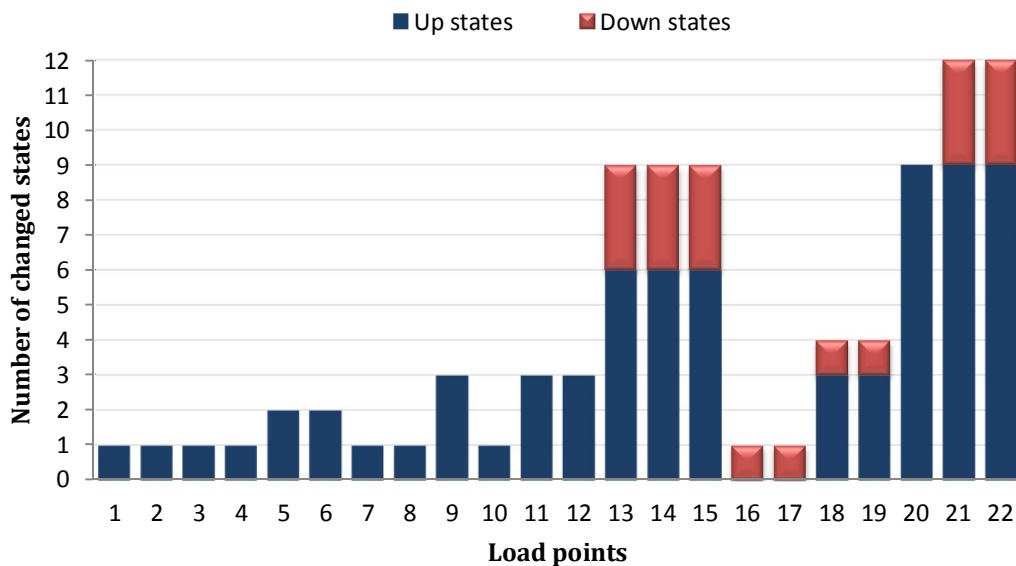

Figure 4.35 Changed states from down to up after DGs – case study 4

4.8.2 Reliability calculation using MM

All states of the system are updated in order to compute the reliability indices. MM with the updated states are used to find the load point and reliability system indices. The results of reliability calculation are given in table 4.19 and 4.20.

Table 4.19 Load point reliability indices for all load points – case study 4

Load Points	A	U	MTTF (y)	AIF (f/y)	AID (h/y)	FD (h/f)	ENS (MWh/y)
1	0.999635	0.000365	18.511872	0.053993	3.193933	59.154812	1.708754
2	0.999628	0.000372	14.920685	0.066988	3.258907	48.649451	1.743515
3	0.999628	0.000372	14.919815	0.066995	3.258925	48.644594	1.743525
4	0.999635	0.000365	18.510256	0.054000	3.193951	59.147416	1.807776
5	0.999627	0.000372	14.919868	0.066996	3.258929	48.643473	1.844554
6	0.999630	0.000370	15.680222	0.063748	3.242686	50.867610	1.472179
7	0.999628	0.000372	14.920780	0.066994	3.258923	48.645267	1.479551
8	0.999970	0.000030	19.225907	0.052011	0.260023	4.999400	0.260023
9	0.999970	0.000030	19.223234	0.052017	0.260039	4.999108	0.299044
10	0.999635	0.000365	18.508791	0.053999	3.193947	59.148744	1.708762
11	0.999630	0.000370	15.676278	0.063758	3.242712	50.859566	1.734851
12	0.999628	0.000372	14.916235	0.067007	3.258956	48.636172	1.466530
13	0.999608	0.000392	9.728745	0.102737	3.437624	33.460449	1.945695
14	0.999606	0.000394	9.430544	0.105985	3.453867	32.588119	1.954889
15	0.999613	0.000387	10.748163	0.092996	3.388901	36.441299	1.538561
16	0.999600	0.000400	8.639594	0.115704	3.502529	30.271532	1.590148
17	0.999606	0.000394	9.434248	0.105958	3.453799	32.595863	1.554210
18	0.999606	0.000394	9.432682	0.105974	3.453830	32.591431	1.554224
19	0.999598	0.000402	8.402379	0.118968	3.518803	29.577835	1.583461
20	0.999628	0.000372	14.915746	0.067014	3.258973	48.631317	1.844579
21	0.999608	0.000392	9.728605	0.102742	3.437631	33.458923	1.945699
22	0.999606	0.000394	9.430420	0.105990	3.453874	32.586685	1.568059

Table 4.20 System reliability indices – case study 4

SAIFI	SAIDI	CAIDI	ASAI	ASUI	ENS (MWh/y)	AENS (MWh/y)
0.078010	3.310942	42.442640	0.999622	0.000378	34.348590	0.018002

Figure 4.36 shows the availability and unavailability. Increasing the capacity of the DGs leads to better improvement in voltage profile and reliability of the system. Figure 4.37 shows the AID and FD. AIF and MTTF are shown in figure 4.38. The ENS is shown in figure 4.39.
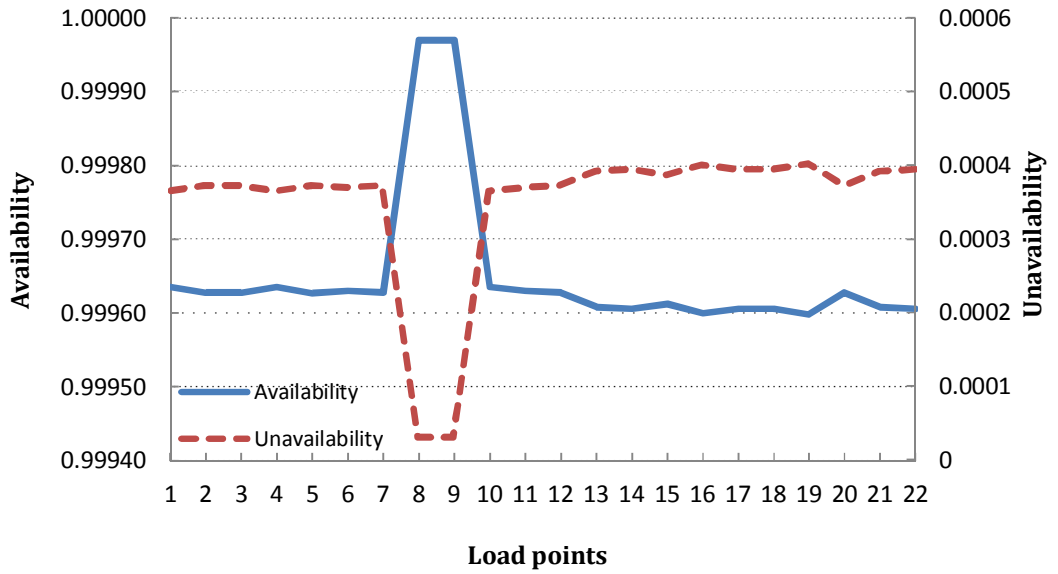
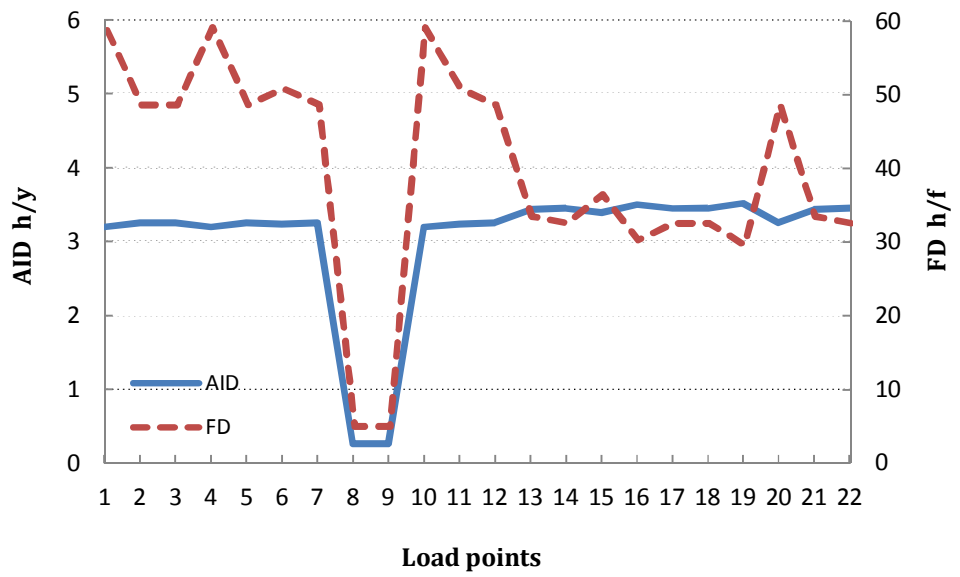**Figure 4.36 Availability and unavailability - case study 4**
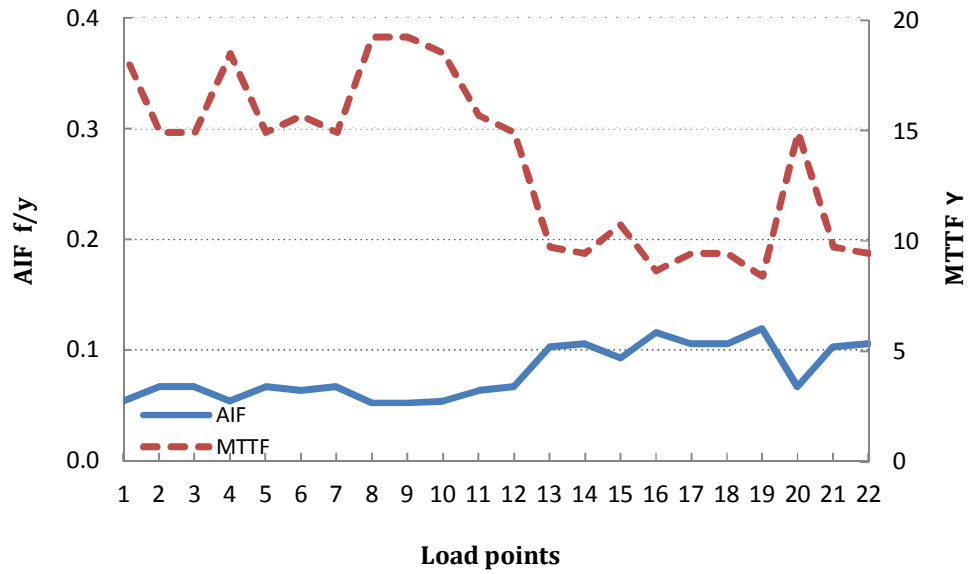

Figure 4.37 AID and FD - case study 4

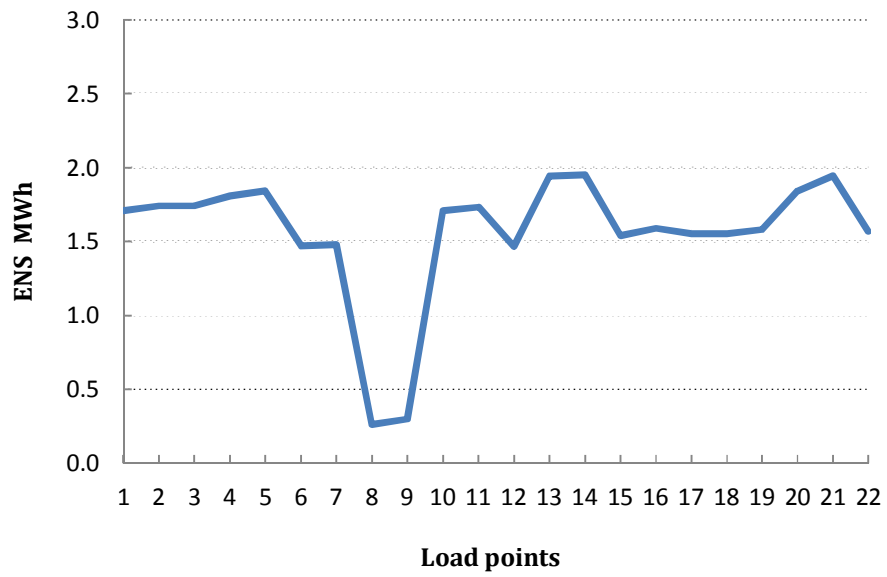**Figure 4.38 AIF and MTTF - case study 4**

Figure 4.39 ENS - case study 4

4.9 Case Study 5: RBTS-Bus2 With PV-DGs at Bus 5 and 15

Two PV-DGs are integrated with the system as the previous case. However, they are installed at bus 5 and bus 15 to investigate the impact of location and size of DGs. Figure 4.40 shows the RBTS-bus2 including the two DGs.
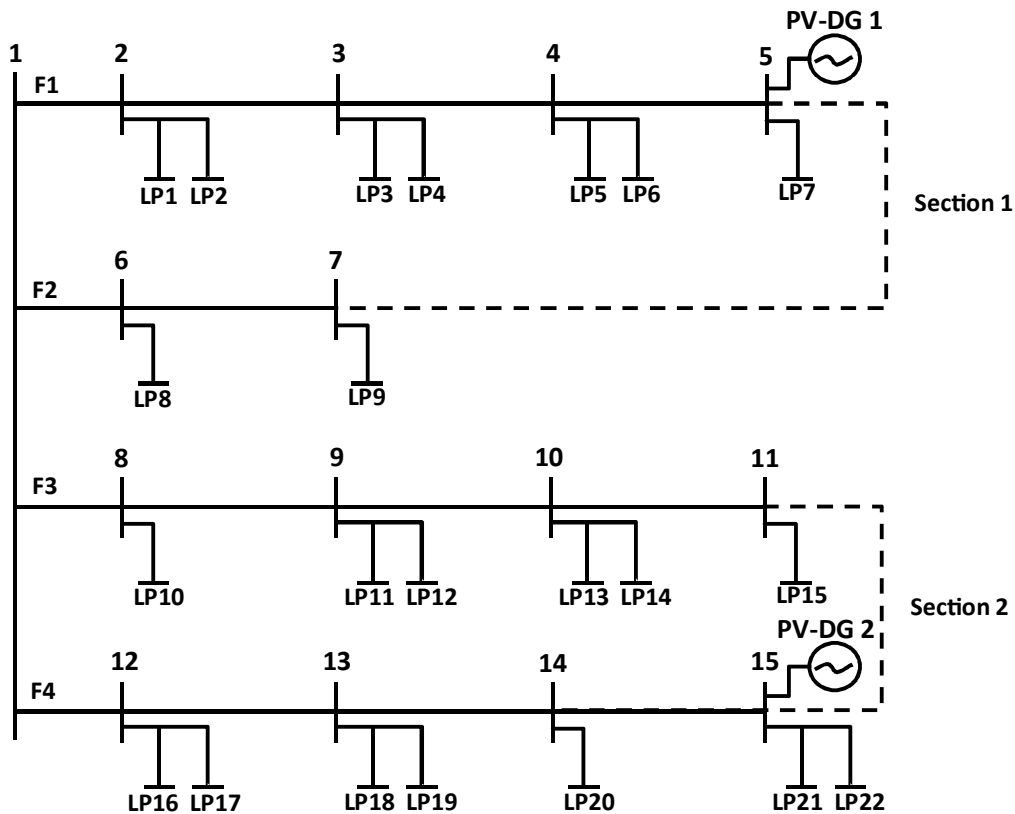

Figure 4.40 One line diagram RBTS-bus 2 with two DGs – case study 5

4.9.1 Reclassifying Process Based on Transfer Capability

The two DGs are modelled as P-V units with producing active power of 800 KW. The voltage at bus 5 and 15 are set to 1 pu. The DPF is applied to the RBTS-bus 2 for all load points. Result of DPF for LP1 is shown in table 4.21. Voltage at LP1 in states 7 and 26-

29 is improved and as a result, all the states in table 4.21 are up. The improvement of the voltages at LP1 at this case is less than case 4 as shown in figure 4.41. That is because the DGs at this case are installed at the end of the lines, which makes the voltage improvement is more at the end of feeders, and less at the beginning. Improvement of voltage profile at LP1 extends from 1.88% to 6.82% as given in figure 4.41.

Table 4.21 DPF results for LP1 – case study 5

State number	State classification	Voltage at LP1 before DG	Voltage at LP1 after DG	State after PF
7	MTS	0.9302	0.9781 ↑	UP ↑
14	TS	0.9947	0.9947	Up
15	TS	0.9947	0.9947	Up
16	TS	0.9947	0.9947	Up
17	TS	0.9947	0.9947	Up
18	TS	0.9947	0.9947	Up
19	TS	0.9908	0.9908	Up
20	TS	0.9908	0.9908	Up
21	TS	0.9908	0.9908	Up
22	TS	0.9908	0.9908	Up
23	TS	0.9871	0.9871	Up
24	TS	0.9871	0.9871	Up
25	TS	0.9871	0.9871	Up
26	TS	0.9808	0.9931 ↑	Up
27	TS	0.9766	0.9930 ↑	Up
28	TS	0.9808	0.9931 ↑	Up
29	TS	0.9883	0.9931 ↑	Up

After applying the DPF to all load points, All the states that were down as a result of weak voltage are found to be changed to up states as given in figure 4.42. The DGs manage to eliminate all the voltage violations at the end of the lines since they located at bus 5 and 15. Furthermore, the generated power is high enough to improve the voltages at

the beginning of the lines. Therefore, all voltage violations at the system are fixed in this case, and all down states change to up states.
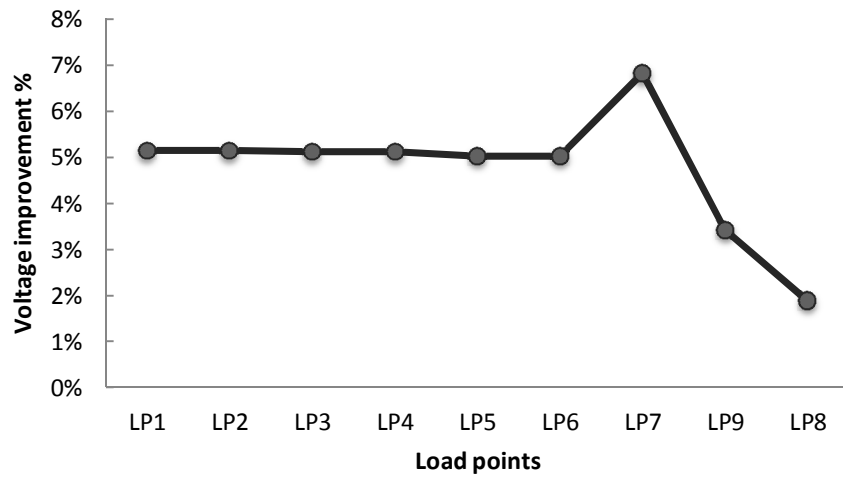

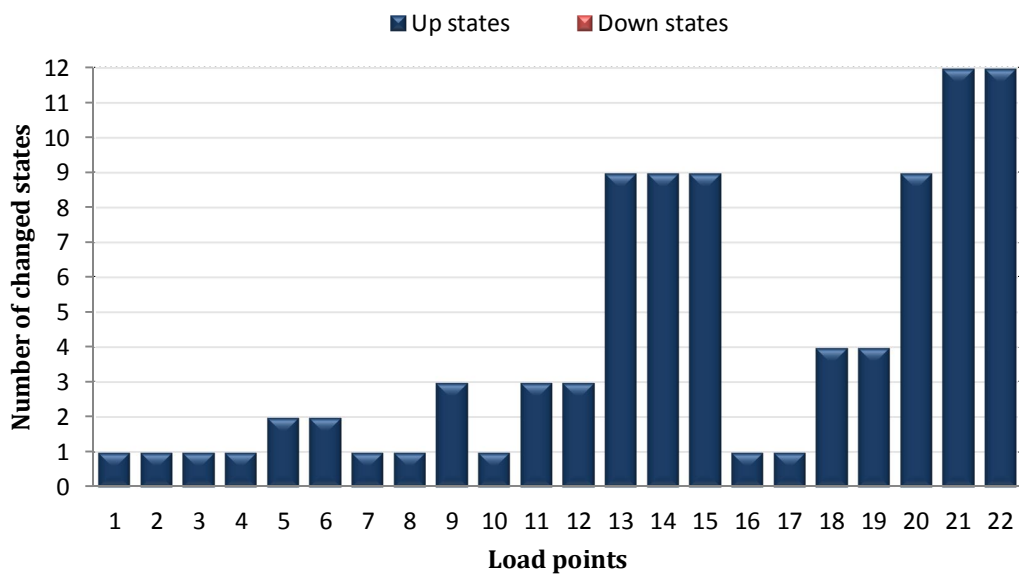**Figure 4.41 Voltage improvement at state 7 due to DGs – case study 5**

Figure 4.42 Changed states from down to up after DGs – case study 5

4.9.2 Reliability calculation using MM

After updating the states of the system, the load point and reliability system indices are calculated as shown in table 4.22 and 4.23.

Table 4.22 Load point reliability indices for all load points – case study 5

Load Points	A	U	MTTF (y)	AIF (f/y)	AID (h/y)	FD (h/f)	ENS (MWh/y)
1	0.999635	0.000365	18.511872	0.053993	3.193933	59.154812	1.708754
2	0.999628	0.000372	14.920685	0.066988	3.258907	48.649451	1.743515
3	0.999628	0.000372	14.919815	0.066995	3.258925	48.644594	1.743525
4	0.999635	0.000365	18.510256	0.054000	3.193951	59.147416	1.807776
5	0.999628	0.000372	14.919868	0.066996	3.258929	48.643473	1.844554
6	0.999630	0.000370	15.680222	0.063748	3.242686	50.867610	1.472179
7	0.999628	0.000372	14.920780	0.066994	3.258923	48.645267	1.479551
8	0.999970	0.000030	19.225907	0.052011	0.260023	4.999400	0.260023
9	0.999970	0.000030	19.223234	0.052017	0.260039	4.999108	0.299044
10	0.999635	0.000365	18.508791	0.053999	3.193947	59.148744	1.708762
11	0.999630	0.000370	15.676278	0.063758	3.242712	50.859566	1.734851
12	0.999628	0.000372	14.916235	0.067007	3.258956	48.636172	1.466530
13	0.999630	0.000370	15.675134	0.063764	3.242727	50.854960	1.835384
14	0.999628	0.000372	14.915216	0.067013	3.258971	48.631991	1.844577
15	0.999635	0.000365	18.502919	0.054021	3.194003	59.125379	1.450077
16	0.999630	0.000370	15.681351	0.063746	3.242681	50.869028	1.472177
17	0.999635	0.000365	18.511643	0.054000	3.193950	59.147670	1.437277
18	0.999635	0.000365	18.506855	0.054012	3.193981	59.134589	1.437292
19	0.999628	0.000372	14.917729	0.067007	3.258956	48.636172	1.466530
20	0.999628	0.000372	14.915745	0.067014	3.258973	48.631319	1.844579
21	0.999630	0.000370	15.674903	0.063767	3.242734	50.852904	1.835387
22	0.999628	0.000372	14.915027	0.067016	3.258978	48.630124	1.479576

Table 4.23 System reliability indices – case study 5

SAIFI	SAIDI	CAIDI	ASAI	ASUI	ENS (MWh/y)	AENS (MWh/y)
0.060928	3.225517	52.939862	0.999632	0.000368	33.371922	0.017491

In case study 4, the DGs are located at the middle of the lines with higher power capacity. The enhancement of voltage and reliability is better than other cases. However, not all down states changed to up states, especially in the load points at the end of the feeders. There are still some voltage violations since those load points are located far from the main source. In case study 5, this issue is solved by installing the DGs at the end of the lines, with producing enough power to improve the voltage at all nodes and load points. The availability and unavailability are shown in Figure 4.43. The AID and FD are shown in Figure 4.44. Figure 4.45 shows the AIF and MTTF. Figure 4.46 shows the ENS.
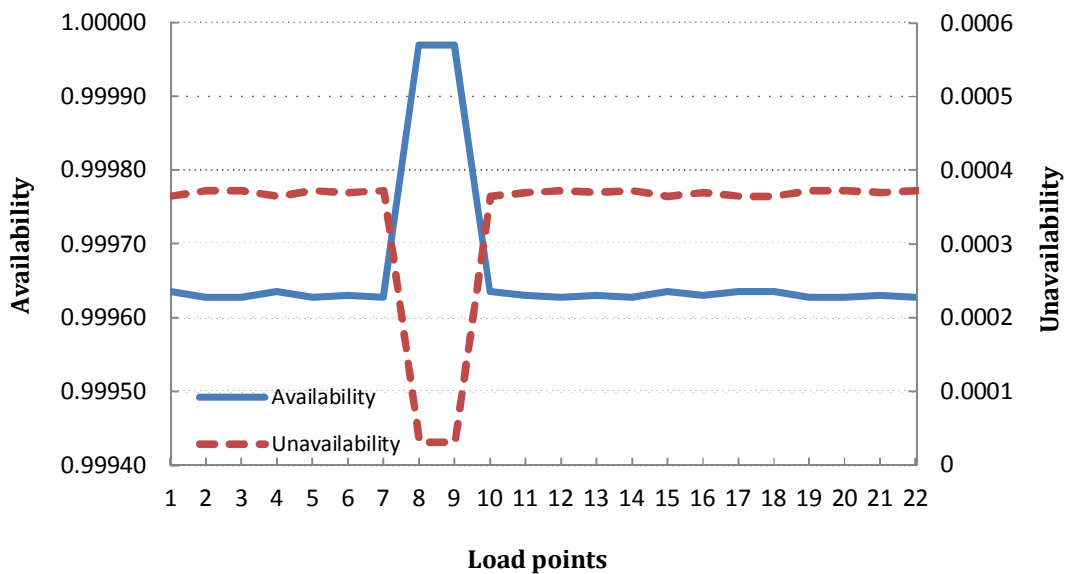

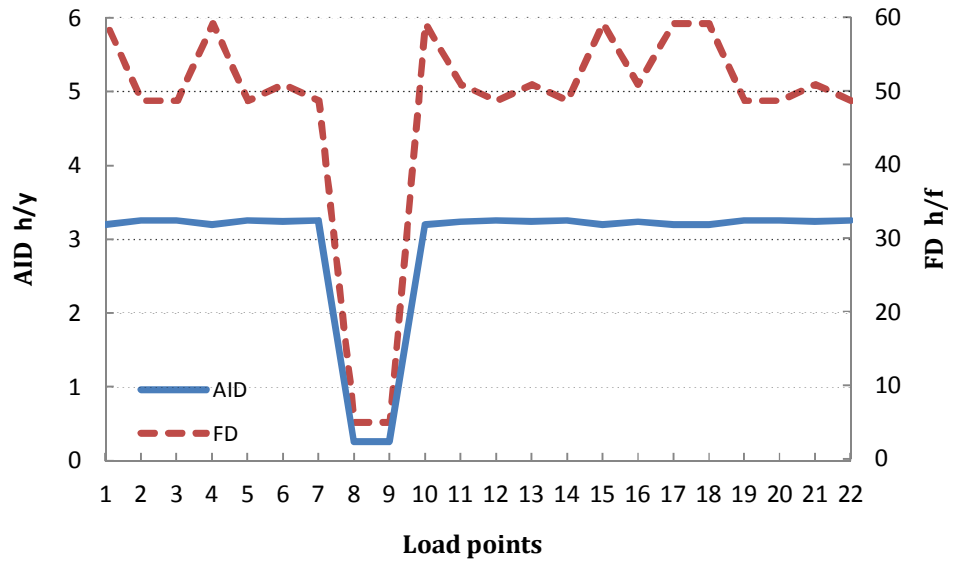**Figure 4.43 Availability and unavailability - case study 5**
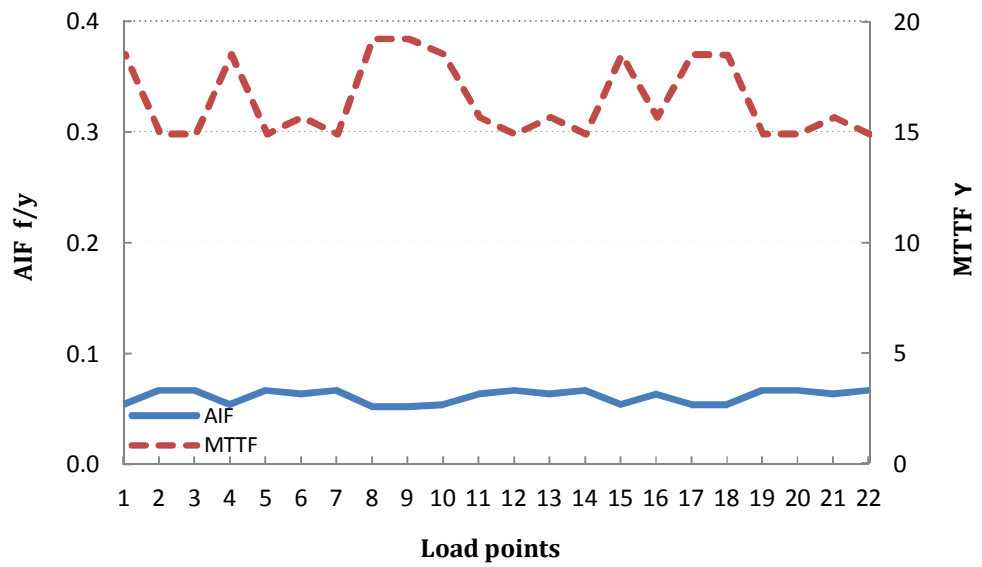
Figure 4.44 AID and FD - case study 5

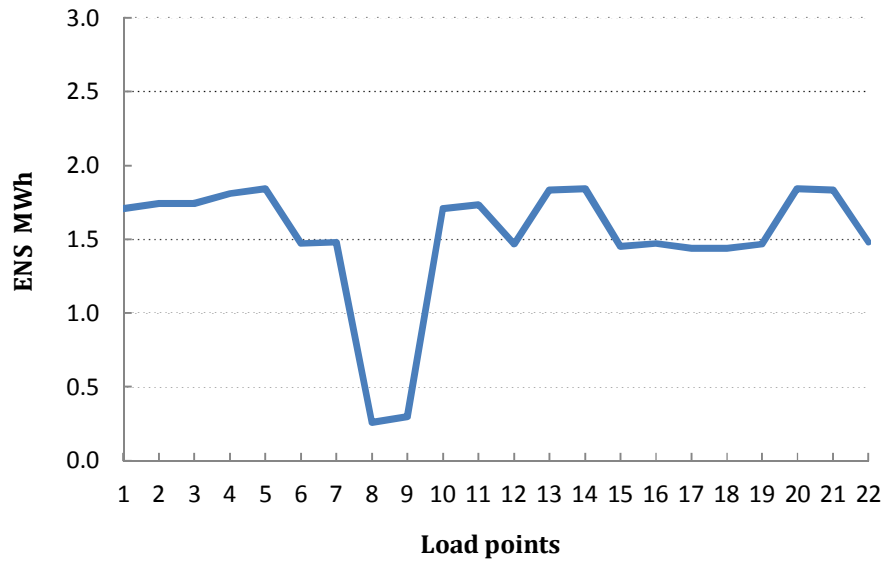**Figure 4.45 AIF and MTTF - case study 5**

Figure 4.46 ENS case study 5

4.10 Comparison Among The Case Studies

Five case studies are conducted in this chapter. First case is the weakly meshed system without DGs. After that, two PQ-DGs are used at two different locations for each one. Firs location is bus 3 and 9. Second location, is bus 5 and 15. Then, two PV-DGs with higher power capacity are installed at the same locations as PQ-DGs. Comparisons are performed based on voltage profile, number of undervoltage states, load point reliability indices, and system reliability indices.

Figures 4.47 and 4.48 show the voltage profile of RBTS-bus2 section 1 and 2 at state 7 respectively for all cases. In case study 1, the system is fed only by the main substation of 11 KV. This is why many voltage violations occur, especially at the end of the lines where the voltage is weaker. Installing the DGs of 200 KW at case 2 and 3 improves the

101

voltage profile up to certain limit, and eliminates some of the voltage violations. The voltage enhancement at case 2 is slightly better than case 3 at this particular scenario since the last has the DGs at the end of the lines 1 and 3 with no enough power to affect the entire system. At case 4 and 5, the capacity of DGs is increased to 800 kW and this improves the voltage much further. Case study 4 has better voltage at the beginning of the feeders than case 5, whereas the voltage at the end of the lines in case 5 is better.
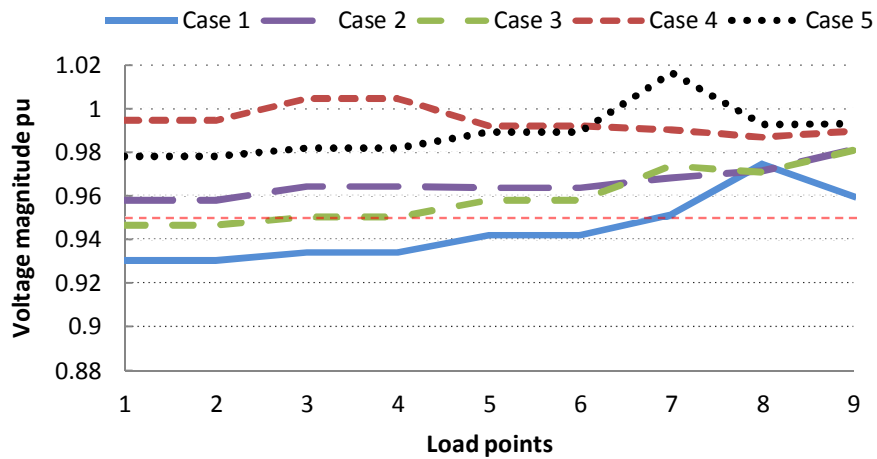

Figure 4.47 Voltage profile for all cases at state 7 section 1
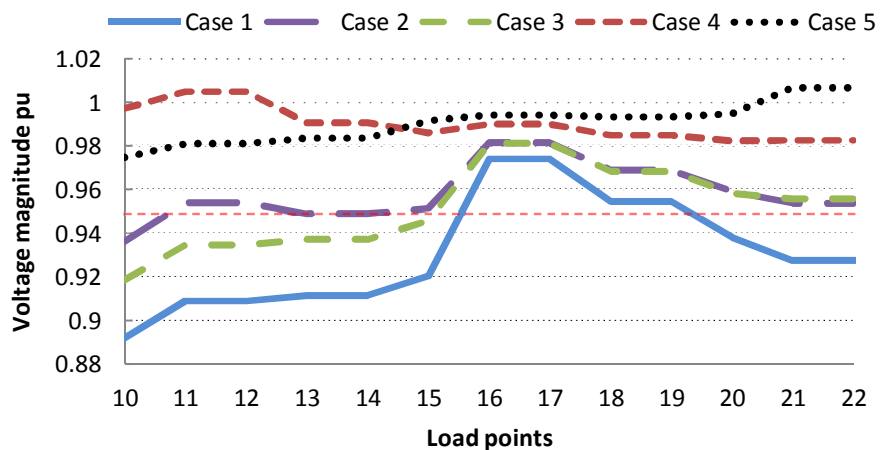

Figure 4.48 Voltage profile for all cases at state 7 section 2

Number of down states due to the transfer capability is directly related to the voltage violations. Figure 4.12 shows that largest number of down states are at the end of the feeders 3 and 4. Improving the system's voltage leads to eliminating those violations. Case study 1 has the maximum number of down states since there is no any DG integrated to the system. Therefore, down states in case 1 are considered as a percentage reference in figure 4.49 that shows the percentage of down states in all cases.
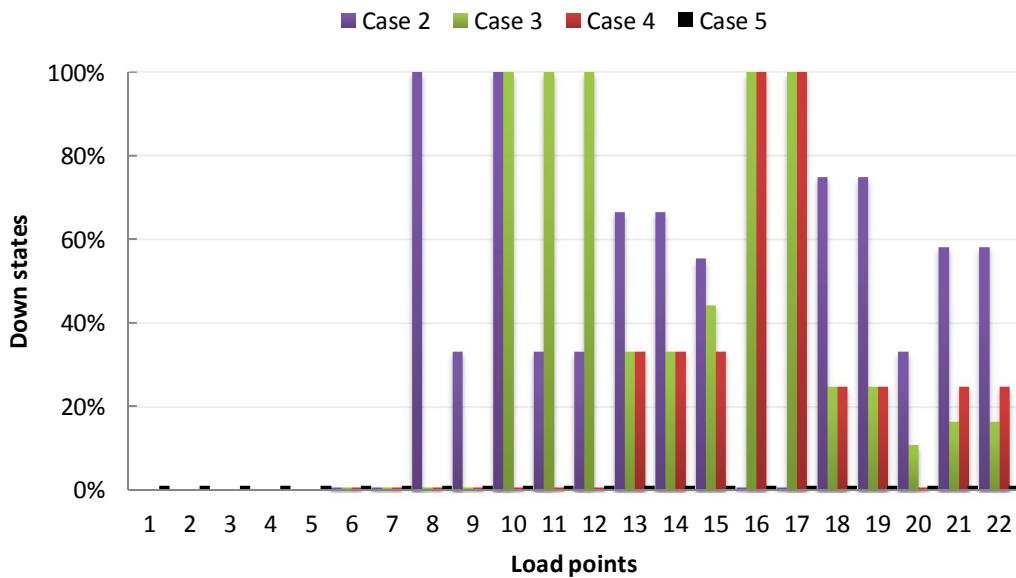
Figure 4.49 Percentage of down states for all cases

As voltage profile gets improved due to the DGs contribution, number of down states also get reduced. In case study 2, all down states of load points at the beginning of feeder 1 , and some of others, change to up state since DGs are installed at the middle. In case study 4, all down states at section 1, and some of others in section 2, change to up satates due to high power generated by DGs at middle of the line. In cases 3 and 5, the DGs are

installed at the end of feeders 1 and 3. All down states in section 1, and some at the end of feeder 3, change to up state in case 3. However, all voltage violations are eliminated, and all down states of all load points change to up states in case 5 due to the proper location of DGs and the high power capacity.

Figure 4.50 shows the availability of all load points for all the cases. In case study 1, the availability at all load points is below 0.99996, except for LP8 and LP9, due to the maximum number of the down states. In case study 2, availability gets enhanced at the beginning of the lines. On the contrary, the availability at case study 3 is improved more at the end of the feeders. With enlarging the capacity of the DGs in case 4, the availability gets enhanced further. The availability reaches the best case scenario (maximum value) at case 5 when all voltage violations are eliminated.
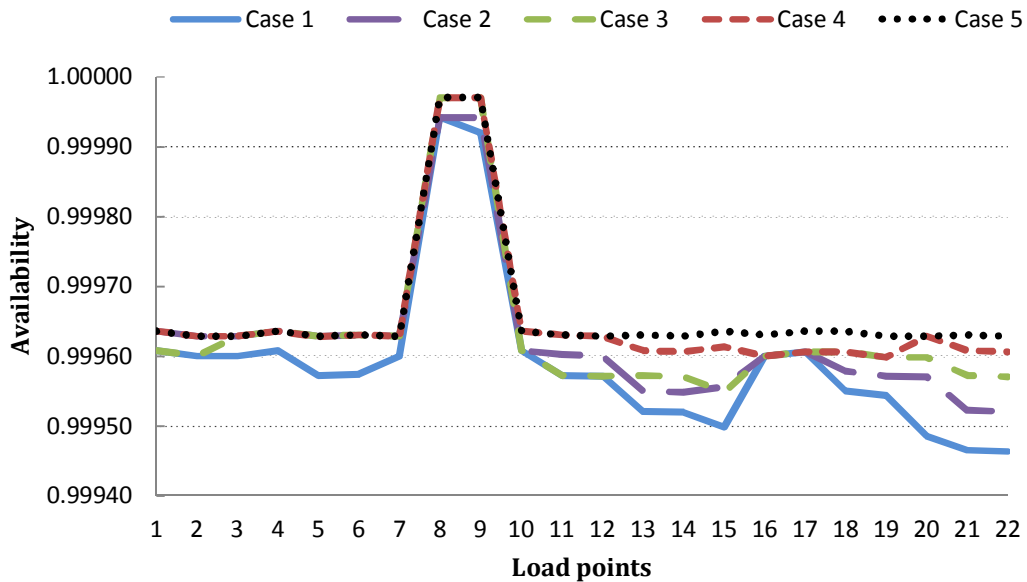

Figure 4.50 Availability of all case studies

AID for all case studies is shown in figure 4.51. Since it is directly proportional to the unavailability, higher values of AID indicate lower level of reliability. Case study 1 has the highest values of AID, while case study 5 has the lowest values of AID.
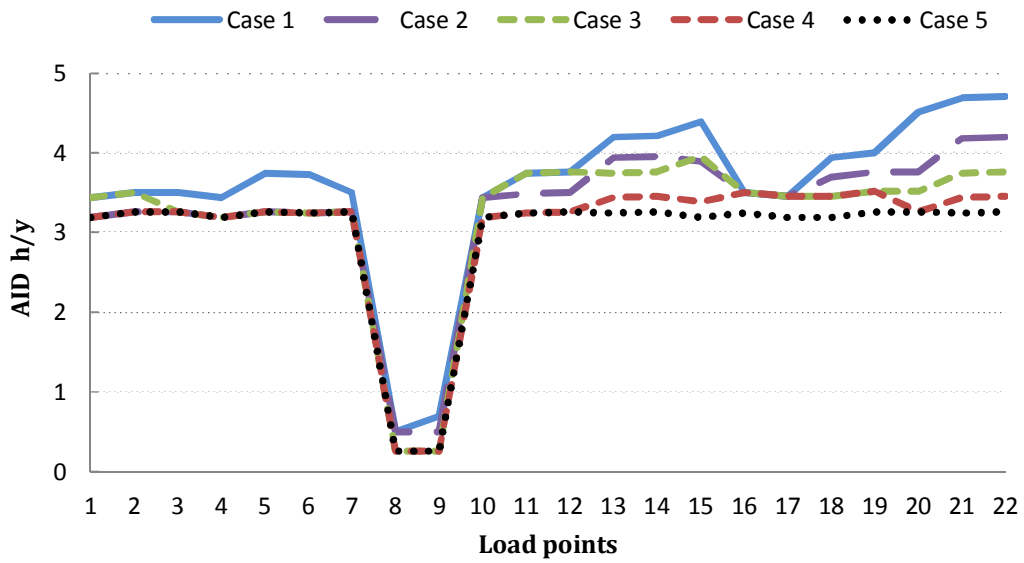
Figure 4.51 AID of all case studies

AIF of all load points for all cases is shown in figure 4.52. AIF is related to the number of down states of the system. Therefore, case study 1 has higher value of AIF due to the large number of down states. AIF decreases gradually with improving the voltage profile due to the DGs. AIF reaches the minimum value with the minimum number of down states in case study 5. Lower values of AIF in case study 5 indicate better reliability.

Figure 4.52 AIF of all case studies

Figure 4.53 and 4.54 show SAIFI and SAIDI respectively for all case studies. SAIFI provides the probability that an average customer experiences an interruption during a year, whereas SAIDI measures the total duration of interruption for average customer during a year. Therefore, SAIFI is related to the AIF, and SAIDI is related to the AID.
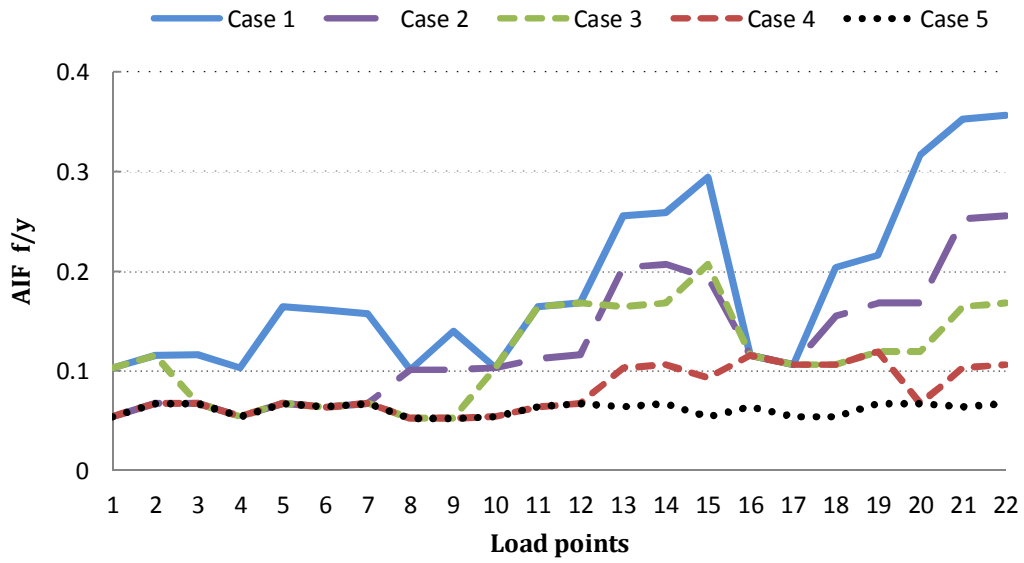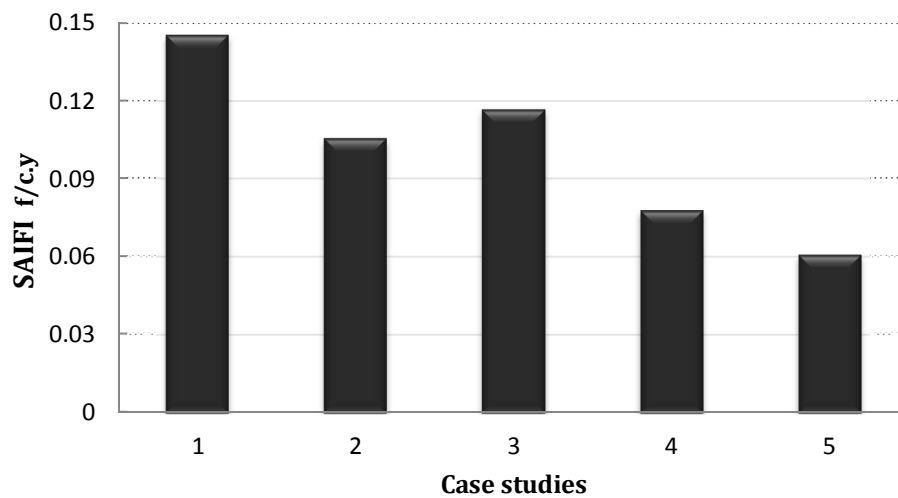

Figure 4.53 SAIFI for all cases

106
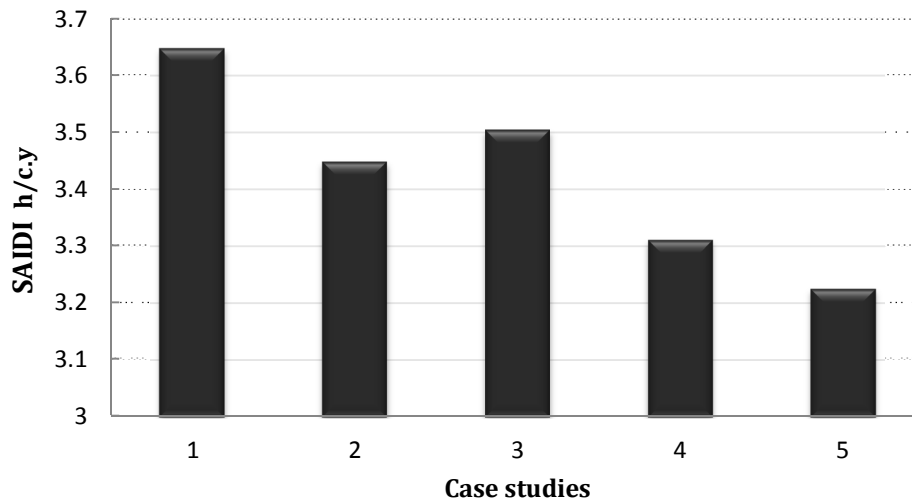
Figure 4.54 SAIDI for all cases

The lower SAIFI and SAIDI, the better the reliability. The values of SAIFI and SAIDI decrease as the number and duration of interruptions are reduced. Best SAIFI and SAIDI are at case study 5 as shown in figure 4.53 and 4.54 The system in case study 3 has higher SAIFI and SAIDI than case study 2. This is because the values of AIF and AID in case study 3 is higher at load points 1-2 and 11-12 than case study 2. These load points represent residential areas with large number of customers as shown in table 4.3.

CAIDI determines the average time to restore the service after an interruption, and it equals to the total interruption durations divided by total number of interruptions. Since case study 5 has the least number of interruptions (AIF), the value of CAIDI is the highest among the other cases. Higher CAIDI does not necessary mean worse reliability, it implies that the number of interruptions is very low comparing with the duration of these interruptions. CAIDI can be reduced by increasing the number of interruption. Figure 4.55 shows CAIDI for all case studies.

107
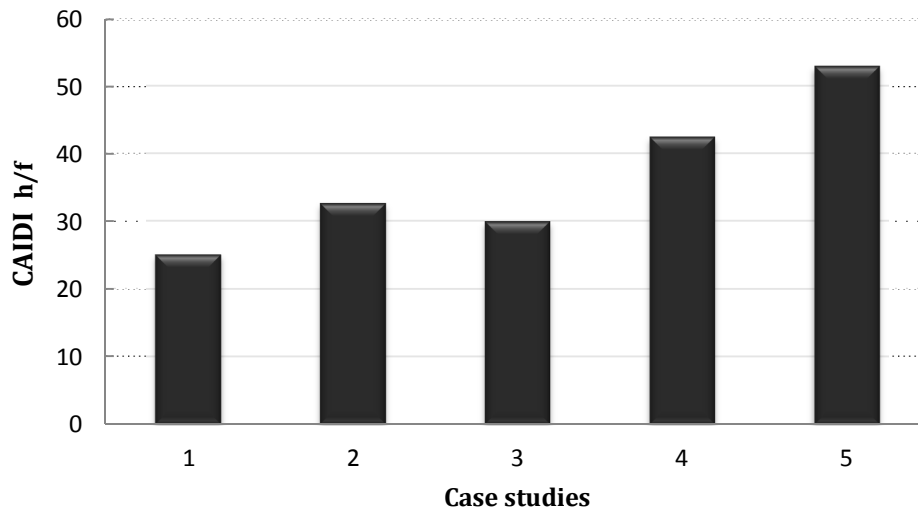
Figure 4.55 CAIDI for all cases

ASAI is shown in figure 4.56. ASAI provides the percent of time that average customer have a service during a year. Higher value of ASAI reflects better system reliability. Case study 3 has lower ASAI than case study 2 for the same reason that mentioned with SAIFI and SAIDI. Best ASAI is in case study 5, which represents best system reliability. On the other hand, case study 1 has the lowest ASAI and lowest level of reliability.
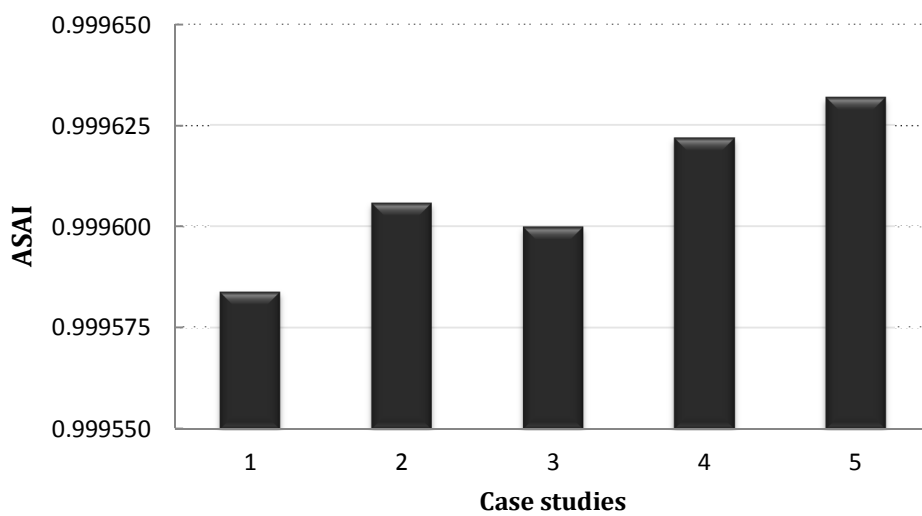
Figure 4.56 ASAI for all cases

108

Figure 4.57 shows the ENS for all cases. ENS measures the energy that does not supply to the load points during the interruption duration. The ENS to the system is equal to the summation of ENS to each load point. When the system has high level of reliability and low AID, the ENS is reduced, and vice versa.
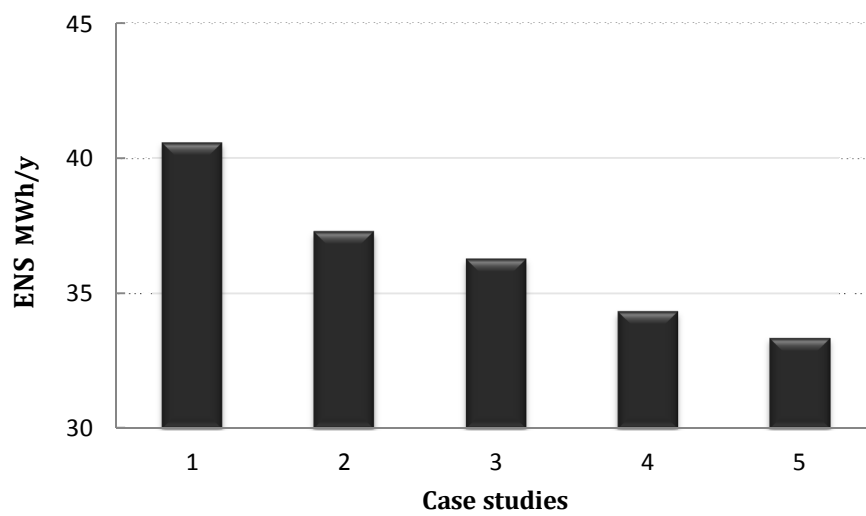
Figure 4.57 ENS for all cases

CHAPTER 5

CONCLUSIONS

5.1 Conclusions

In this research, Markov Model (MM) and Distribution Power Flow (DPF) are utilized to evaluate the power reliability of a Microgrid power system. Different methods of DPF are presented and tested to be used in the reliability assessment process. These methods are DLF method, ENR method, and RD method. DLF technique is the one used in reliability evaluation due to its simplicity, computational speed, and flexibility. The DPF analysis is included in order to provide more practical and accurate reliability indices by validating the voltage profile of the system in each state of the system. Markov process is used to model and evaluate the reliability of the distribution system. The states of the MM are classified based on connectivity between the source and the load points. The DPF is used to reclassify the states based on transfer capability of system from the source to the loads. The study is implemented on RBTS-bus2 system where five case studies are considered in this research.

In case study 1, the reliability of the weakly meshed RBTS-bus 2 system is assessed without including any distributed generations. Two PQ-DGs with a power of 200 kW and 0.8 PF are integrated to the system at bus 3 and bus 9 in case study 2. In case study 3, the locations of the PQ-DGs are connected to different locations to study the impact of the

110

DG's location on the reliability indices. Two PV-DGs are installed instead of the PQ-DGs at the same locations as case 2 with a power of 800 kW in case study 4. In case study 5, the two PV-DGs are integrated at bus 5 and 15 at the end of the feeders 1 and 4.

The conclusions that can be drawn from the case studies are as follows,

- The DPF provides more accurate analysis to the reliability by computing the voltage profile of the system. Voltage violations are considered as failures or down states in MM and they affect the reliability of the power system negatively. The comparison between the reliability calculations in case study 1 and [31] shows that considering the transfer capability provides additional accuracy to the reliability evaluation.

- In case study 1, the voltage becomes gradually weaker as moving toward the end of feeders due to the large number of nodes and load points. Therefore, large number of down states due to the under-voltage conditions occurs and this results in lower level of reliability. Number of under-voltage states in case study 1 is 90 states.

- Integrating DGs to the power system with proper location and capacity improves the voltage profile of the system, which in turn reduces the number of down states due to the under-voltage conditions. In case studies 2-5, DGs are installed to the system and they improve the voltage profile. Number of down states due to the under-voltage conditions is reduced from 90 to 45 states in case 2, 28 states in case 3, 19 states in case 4, and zero states in case 5.

- Installing PV-DGs with an active power of 800 kW at bus 5 and 15 in RBTS-bus2 system eliminates all the voltage violations in case study 5, and maintain the power reliability at best case scenario.

- Optimal location for the DG, in order to enhance the voltage profile, is at the node with the largest number of voltage violations. Which in our system bus 15 that have 24 under-voltage states. The DG also must generate enough power to improve the voltage of the entire system.

- The power reliability of the system is improved as the voltage profile raised and number of down states reduced. Therefore, the system has the highest level of reliability in case study 5 with ASAI of 0.99963 and ASUI of 0.00037, and the lowest value of reliability in case study 1 with ASAI of 0.99958 and ASUI of 0.00042.

- Low values of SAIFI and SAIDI reflects high level of reliability. A reduction in number and duration of interruptions results in a reduction in SAIFI and SAIDI. The system in case study 1 has SAIFI of 0.1452, and SAIDI of 3.6740. While in case study 5, the system has better SAIFI and SAIFI with 0.0609 and 3.2255 respectively.

- Low values of AIF, AID, FD, ENS and AENS indicate good reliability. They are lower in case 5, and higher in case 1 than any other case.

5.2 Future Work

The following are recommendations for future work:

- More complicated topologies of the RBTS-bus2 can be studied by connecting more than two tie links between the feeders. This will improve the connectivity between the source and the loads and therefore, improve the reliability further.

- Modelling different types of renewable DG, such as Photovoltaic system and wind turbine, can be taken into consideration. The behavior of the natural resources can affect the output of the DGs, the voltage profile, and the reliability of the system.

- The power distribution system can be presented in unbalanced system. Unbalanced power flow can be used to investigate the transfer capability of the unbalanced system. When a voltage violation or an outage occurs at only one or double phase, it may still be a connection to other loads with an acceptable voltage. This outage will affect the voltage profile and reliability differently than it does in balanced system.

- The study can be implementing on the RBTS-bus4. It has 38 load points and 67 components in addition to the transformers. Since it is larger system than RBTS-bus2, the results can provide wider vision about the power reliability.

APPENDIX

33-Bus system data

Table 1 Load data and line data for 33-Bus system

Node No.	P (KW)	Q (Kvar)	Line No.	Sending Node	Receiving Node	R (ohm Ω)	X (ohm Ω)
1	0	0	1	1	2	0.0922	0.0470
2	100	60	2	2	3	0.4930	0.2511
3	90	40	3	3	4	0.3660	0.1864
4	120	80	4	4	5	0.3811	0.1941
5	60	30	5	5	6	0.8190	0.7070
6	60	20	6	6	7	0.1872	0.6188
7	200	100	7	7	8	0.7114	0.2351
8	200	100	8	8	9	1.0300	0.7400
9	60	20	9	9	10	1.0440	0.7400
10	60	20	10	10	11	0.1966	0.0650
11	45	30	11	11	12	0.3744	0.1238
12	60	35	12	12	13	1.4680	1.1550
13	60	35	13	13	14	0.5416	0.7129
14	120	80	14	14	15	0.5910	0.5260
15	60	10	15	15	16	0.7463	0.5450
16	60	20	16	16	17	1.2890	1.7210
17	60	20	17	17	18	0.7320	0.5740
18	90	40	18	2	19	0.1640	0.1565
19	90	40	19	19	20	1.5042	1.3554
20	90	40	20	20	21	0.4095	0.4784
21	90	40	21	21	22	0.7089	0.9373
22	90	40	22	3	23	0.4512	0.3083
23	90	50	23	23	24	0.8980	0.7091
24	420	200	24	24	25	0.8960	0.7011
25	420	200	25	6	26	0.2030	0.1034
26	60	25	26	26	27	0.2842	0.1447
27	60	25	27	27	28	1.0590	0.9337
28	60	20	28	28	29	0.8042	0.7006
29	120	70	29	29	30	0.5075	0.2585
30	200	600	30	30	31	0.9744	0.9630
31	150	70	31	31	32	0.3105	0.3619
32	210	100	32	32	33	0.3410	0.5302
33	60	40	33				

Table 2 Tie lines data for 33-Bus system

Line No.	Sending node	Receiving node	R (ohm Ω)	X (ohm Ω)
33	8	21	2	2
34	9	15	2	2
35	12	22	2	2
36	18	33	0.5	0.5
37	25	29	0.5	0.5

REFERENCES

[1]   Richard E. Brown, Electric Power Distribution Reliability. CRC Press, USA: Taylor & Francis Group, 2009.

[2]   Ali Chowdhury, Don Koval, Power Distribution System Reliability: Practical Methods and Applications. John Wiley, IEEE press, 2009.

[3]   Allan, R. N., Billnton, R., Sjanef, I., Goel, L., and So, K. S., "A Reliability Test System for Educational proposes - Basic Distribution System Data and Results". *IEEE Trans Power System*, Vol. 6, No. 2, pp. 813-820, May 1991.

[4]   Billinton, R. and Allan, R. N., Reliability Evaluation of Power Systems.   Pitman Books, New York and London, 1984.

[5]   S. Chowdhury, S. P. Chowdhury and P. Crossley, Microgrids and Active Distribution Networks. IET Renewable Energy series 6, The Institution of Engineering and Technology, 2009.

[6]   R. Billinton and R. N. Allan, Reliability Evaluation of Engineering Systems. Plenum Press, New York, 1984.

[7]   Fishman, G. S, Monte Carlo: Concepts, Algorithms, and Applications. New York: Springer. 1995.

[8]   R. Billinton, M.S. Grover, "Reliability evaluation in distribution and transmission Systems," *PROC. IEEE,* vol. 122,no. 5, MAY 1975.

[9]   R. Billinton, S. Jonnavithula, "A test system for teaching overall power system reliability assessment," *IEEE Winter Power Meeting*, Paper No. 96 WM 056-2. 1996.

[10]   Huijia Liu, Hanmei Hu, Jingguang Huang, A Method of Reliability Evaluation for Complex Medium-voltage Distribution System Based on Simplified Network Model and Network-equivalent, development planning of distribution, technical session 5*, CICED* 2008.

[11]   Y. Wang, X. Han and Y. Ding, 'Power system operational reliability equivalent modeling and analysis based on the Markov chain', in *Power System Technology (POWERCON), 2012 IEEE International Conference*, Auckland, October 2012.

[12]   M. Al-Muhaini and G. Heydt, "Customized Reduction Techniques for Power Distribution System Reliability Analysis," *IEEE Power and Energy Society General Meeting,* July 2013.

[13]   M. Al-Muhaini, G. T. Heydt, "A Novel Method For Evaluating Future Power Distribution System Reliability," *IEEE Transactions on Power Systems*, Vol. 28, No. 3, August 2013.

[14]   Primen, The Cost of Power Disturbances to Industrial and Digital Economy Companies. Consortium for Electric Infrastructure to Support a Digital Society. Madison: EPRI, 2001.

[15]   Ramakumar, R, Engineering reliability: fundamentals and   applications. Englewood Cliffs, NJ: Prentice-Hall, 1993.

[16]   Hadi Saadat, Power System Analysis, McGraw Hill book, New York, 2004.

[17]   M S Srinjvas, "Distribution load flows : A brief review," IEEE 2000.

[18] D. Shirmohammadi, H. W. Hong, A. Semlyen, and G. X. Luo, "A compensation based power flow method for weakly meshed distribution and transmission networks," *IEEE Trans. Power Syst.*, vol. 3, no. 2, pp. 753–762, May 1988.

[19] Whei-Min Lin, Jen-Hao Teng, Three-phase distribution network fast-decoupled power flow solutions, International Journal of Electrical Power and Energy Systems, Vol. 22, No.5, pp. 375-380, 2000.

[20] P. Aravindhababu, S. Ganapathy and K.R. Nayar, A novel technique for the analysis of radial distribution systems, International Journal of Electrical   Power and Energy Systems, Vol. 23, No. 3, pp. 167-171, 2001.

[21] P. Aravindhababu and R. Ashokkumar, An Improved Power flow Technique for Distribution Systems, computer science, informatics and electrical engineering, Vo1.3, No.1, 2009.

[22] A. Alsaadi, and B. Gholami, An Effective Approach for Distribution System Power Flow Solution. World Academy of Science, Engineering and Technology, 28, 2009.

[23] P. Aravindhababu, R. Ashokkumar, A robust decoupled power flow for distribution systems. Energy Conversion and Management, 52,1930–1933, 2011.

[24] Alsaadi A, Gholami G. An effective approach for distribution system for power flow solution. Proc WASET 2009;37:220–4.

[25] K. Prakash and M. Sydulu, Topological and Primitive Impedance based Load Flow Method for Radial and Weakly Meshed Distribution Systems, Iranian

journal of electrical and computer engineering, vol. 10, no. 1, winter-spring 2011.

[26]   H. Shateri, M. Ghorbani, N. Eskandari and A.H. Mohammad-Khani, "Load Flow Method for Unbalanced Distribution Networks with Dispersed Generation Units", 47th Universities Power Engineering Conference, UPEC'2012, 4-7 Sept 2012, Brunel University, London, UK.

[27]   M. E. Baran and F. F. Wu, "Network reconfiguration in distribution systems for loss reduction and load balancing," *IEEE Trans. on Power Delivery*, vol. 4, no. 2, pp. 1401-1407, Apr. 1989.

[28]   J. Z. Zhu, "Optimal reconfiguration of electrical distribution network using refined genetic algorithm," *Electric Power Systems Research*, n.62, pp.37- 42, 2002.

[29]   M.P.Selvan, K.S.Swarup, "Distribution system load flow using object oriented methodology," November 2004.

[30]   M. Al-Muhaini and G. Heydt, "Minimal cut sets, Petri nets, and prime number encoding in distribution system reliability evaluation," in *Proc. 2012 IEEE Power and Energy Society T&D Conf.*, May 2012.

[31]   M. Almuhaini, 'An Innovative Method for Evaluating Power Distribution System Reliability', Ph.D, ASU, 2012.

VITAE

Name: Abdulrahman Mohammed Safi AL-Sakkaf

Nationality: Yemeni

Date of Birth: 4/22/1985

 Email: ams.saggaf@gmail.com

Address: Dammam, Saudi Arabia

Academic Background:

1) Bachelor of Science, Electronic and Communication Engineering, Hadramout University of Science and Technology (HUST), Mukalla, Yemen, (2010).

2) Master of Science, Electrical Engineering, King Fahd University of Petroleum & Minerals (KFUPM), Dhahran, Saudi Arabia, (2014).

Publications:

1) Al-Sakkaf and M. Al-Muhaini, "Power Flow Analysis of Weakly Meshed Distribution Network Including DG*," International Journal of Electrical Power and Energy Systems,* October 2014. (Submitted)

2) M. Al-Owaifeer, M. Al-Muhaini and A. Al-Sakkaf , "The Impact of Load Management and Hybrid Renewable DG Integration on the Reliability and Restoration Process of the Load," *IEEE PES General Meeting*, 2015. (Submitted)

3) Al-Sakkaf and M. Al-Muhaini, "Reliability Evaluation of Microgrids Based On Markov Model And Power Flow Analysis". (To be submitted)